RNA binding protein RBM3 modulates novel lncRNAs to increase colon cancer tumor progression

By

Afreen Asif Ali Sayed

Submitted to the graduate degree program in Cancer Biology and the Graduate Faculty of the University of Kansas in partial fulfillment of the requirements for the degree of Doctor of Philosophy.

Co-chair Shrikant Anant, Ph.D.

_____

Co-chair Sufi Mary Thomas, Ph.D.

_____

Roy Jensen, M.D.

_____

Shahid Umar, Ph.D.

_____

Tomoo Iwakuma, M.D., Ph.D.

_____

Outside Committee Member Udayan Apte, Ph.D.

_____

Date Defended: 16 April 2020

The Dissertation Committee for Afreen Asif Ali Sayed certifies that this is the approved version of the following dissertation:

RNA binding protein RBM3 modulates novel lncRNAs to increase colon cancer tumor progression

_____

Co-chair Shrikant Anant, Ph.D.

_____

Co-chair Sufi Mary Thomas, Ph.D.

_____

Graduate Director Joan Lewis Wambi, Ph.D.

Date Approved: 27 April 2020

Abstract

RNA binding proteins play a significant role in regulating gene expression, and dysregulation in their expression may skew cells to various pathophysiological conditions. In previous studies, the Anant laboratory has shown that RNA binding protein RBM3 may function as a protooncogene, with its expression increasing in colon cancers. To get a better understanding of how RBM3 works, we took an unbiased approach and performed total RNA-sequencing (RNAseq) and RNA-immunoprecipitation-coupled sequencing (RIPseq), to identify transcripts targeted by the protein. We identified several genes involved in cell movement and angiogenesis, including VEGF, ZEB1, TWIST1 and Slug mRNAs, which we validated by Real time RT-PCR analyses. Coupled with this, we observed that RBM3 overexpression increased stemness, migration and invasion *in vitro*. A second discovery from the RNA seq and RNA-IP studies was that RBM3 overexpression increased the levels of multiple long noncoding RNAs (lncRNAs), a class of regulatory RNAs that play important roles in tumorigenesis. Of these, we chose four lncRNAs, two known (HOTAIR, TUG1) and two novel ones (lnc-Flii-1 and lnc-LSAMP-3) based on their ability to interact with VEGF, ZEB1, TWIST1 and Slug mRNAs using the RNAfold program. Knocking down the lncRNAs using a combination of specific siRNAs and locked nucleic acid (LNA) oligonucleotides showed reduced levels of the four mRNAs, and their corresponding protein expression. The consequence of this was reduced cell migration and invasion in scratch plate and Boyden chamber assays. To determine the role of RBM3 *in vivo*, we performed three sets of experiments in various mouse models, including RBM3 overexpression, RBM3 knockout and a tumor xenograft model. For RBM3 overexpression, we developed a mouse where RBM3 is encoded in

the ROSA locus and driven by the cytomegalovirus immediate early gene promoter (RBM3tg). LncRNA (HOTAIR, TUG1, lnc-Flii-1 and lnc-LSAMP-3) levels were higher in the colons of the RBM3tg animals, when compared to matched controls. We also generated a mouse line where RBM3 is deleted specifically in the intestine (intRBM3ko mouse). Here, the four lncRNA levels were lower than wild type controls. To determine the effect of RBM3 loss on tumorigenesis, we treated the wild type and intRBM3ko mice with azoxymethane (AOM)-dextran sodium sulfate (DSS) to induce colitis-associated colorectal cancer. There was significantly lower number of tumors in colons of intRBM3ko mice, when compared to wild type controls. Moreover, there were lower levels of the four lncRNAs and mRNAs for VEGF, ZEB1, TWIST1 and Slug in the tumors from the intRBM3ko mice. Finally, we performed studies in a tumor xenograft model, where HCT116 and DLD1 cells overexpressing RBM3 (HR and DR, respectively) and compared them to vector controls (HG and DG, respectively). Overexpression of RBM3 in the two cell lines resulted in a significant increase tumor xenograft growth as compared to vector control cells. RBM3 overexpressing HR and DR xenograft tumors also showed higher levels of expression of lncRNAs as well as VEGF, ZEB1, TWIST1 and Slug mRNAs and proteins. Furthermore, intra-tumoral knockdown of the lncRNAs decreased the size and volume of HG and DG tumor xenografts along with a decrease in Slug and VEGF protein expression. We used the IntaRNA program to analyze lncRNA-mRNA interaction *in silico*. The lncRNAs formed a bridge between stem-loop structures in the 5' untranslated (5'UTR) and 3' untranslated (3'UTR) regions of the four mRNAs (VEGF, ZEB1, TWIST1 and Slug) resulting in formation of a closed circle. We confirmed the interaction of RBM3 with the lncRNAs using RIP-RT-PCR. The association results in the formation of the

kissing loop interaction between lncRNA and mRNA increasing translation. Based on these results, we conclude that RNA binding protein RBM3 enhances tumor progression by modulating novel lncRNAs.

Keywords: RNA binding protein, lncRNA, kissing-loop, stemness, translation control, colon cancer

Dedication

I dedicate this dissertation to my beloved family who means everything to me. My parents, Jabin Sayed and Asif Ali Sayed and, my sister Amreen Sayed. They have always been a source of inspiration, guidance and have been a constant support throughout my life. They have also always supported me and encouraged me in all my life endeavors. They especially taught me to be self-empowered and to chase my dreams. They have also pushed me to be a good human being. There are no words to describe my love and respect for my family.

Acknowledgements

First, I would like to express my heartfelt and sincere gratitude to my mentor Dr. Shrikant Anant. He is not only a good scientist but also a good mentor. He has always encouraged me to think and ask questions to look at future direction for the work. He not only mentored me but also encouraged me to become an independent thinker. I will treasure this valuable lesson in life. Dr. Anant always encouraged me to apply for awards and participate in different conferences and give talks at various platforms. This has helped me not only overcome my fear of public speaking but helped me become a better speaker. I don't know how to thank him for all the guidance and support in taking this project to greater heights. During my Ph.D. I have grown not only professionally but also as a person thanks to Dr. Anant. I will never forget all the parties we had at his house and am very thankful to Swati madam for being such an amazing host every time. I also want to thank her for her moral support and all the amazing food she has made when I was over there. I also want to thank my co-mentor Dr. Sufi Mary Thomas. Dr. Thomas has always guided me and pushed me to do better. She always knew my potential more than me. Dr. Thomas and Dr Anant have spent countless hours with me guiding me and helping me improve on my project. Thank to both of them for their guidance and support.

Second, I want to thank my committee members Dr. Roy Jensen, Dr. Shahid Umar, Dr. Tomoo Iwakuma, Dr. John Wood, and a special thanks to Dr. Udayan Apte. Their invaluable inputs and constructive evaluation of my work helped me shape my project and give it the right direction. All their support has not only made my project good but helped me improve as a scientist. I cannot thank them enough. Special thanks to Dr Jensen because he always made time for me no matter how busy he was. I did my

rotation in Dr, Tomoo's lab and I have learned a lot from him. He always guided and made sure I was on the right track. Dr Umar is always encouraging and helpful. I walk into his office so many times and he always helped me out with my queries. Dr. Wood was always so positive and encouraging. Dr. Apte was gracious and agreed to join my committee at a very crucial time. Thank you all so much. I would not be able to reach at this stage without their help.

I also want to thank the Anant lab members both current and previous. I have learned so much from each and every one of them. They all have not only helped me understand the experiments but also helped me learn valuable lessons in life. First Dr. Dharma and Priya, who were kind enough to open their house for me when I first came to the United States and helped me settle in. I have also learned so many techniques from both of them. I have known Dr. Prasad from before joining my Ph.D. program and he has been a constant support, and good friend. He always makes me laugh and gives me a tough time, but he is always there for me. I have learned so much about troubleshooting experiments, making figure and writing from Prasad. David has also been my friend since I joined the lab, and he has been there for me through all the ups and downs of my journey. He helped me in my experiments and whenever I need help around my house. Sonali is like a sister and has been very helpful with the RBM3 mice experiments. She is always smiling and encouraging me. Dr. Prabhu is always making jokes and makes people laugh but he is also very helpful in troubleshooting. There were so many people who also helped and contributed to my project who are no longer in the lab. Especially Dr. Gaurav Kaushik who helped me with troubleshooting my experiments. Dr. Pablo Angulo who was a big moral support. I also want to thank other members like Abeda Jamadar, Partha

Rangarajan, Pugazhendi Srinivasan, Balaji Krishnamurthy, Randi Ryan and Tamika Reed-Newman.

I want to thank Dr. Animesh Dhar who has always encouraged and guided me even before I joined my Ph.D. I also want to thank the members of Dr. Umar lab Dr. Ishfaq Ahmed and Dr. Badal Roy, and Dr. Thomas' lab members Levi Arnold and Dr. Jacob New. Dr. Sumedha Gunewardena helped me tremendously with my sequencing data and taught me how to use all the bioinformatics software. I am very thankful to him. I am also thankful to Dr. Osama Tawfik who was very patient with me and helped score my IHC slides.

I want to especially Dr. Joan Lewis-Wambi, who is the graduate director of the department. When she took over the position, she made excellent changes to the program, which really made feel like we belong. As a student, I do not have enough words to thank her for all she has done for me and the program. I want to thank all the faculty and staff of the Cancer Biology department. They have all been very encouraging and supportive. Ms. Valerie Freeman is so amazing at what she does and has helped me throughout my Ph.D. I remember going to her with all my administrative inquiries and she always helped me with a smile on her face. Also, Ms. Teresa Mota and Ms. Kerri Dean along with Valerie helped organize my online defense talk. They were instrumental in making sure that everything went smoothly. I would not have been able to do this without their support. Thank you so much.

I also want to thank my previous mentor Dr. Subhash Padhye. Dr. Padhye not only encouraged me to pursue my Ph.D., but he also helped and guided me in the right

direction. He still guides and encourages me, and he has been a constant support throughout my journey. He has been an emotional support both in academic and personal life. I want to take this opportunity to also thank all my teachers from school to the university who have made a great impact and helped shape my career. I also want to thank my previous colleagues from Abeda Inamdar Senior College. They all have always helped and supported my decision to pursue my Ph.D. I also want to thank all my friends back in India and in the US. I would not be able to go through this journey without their help and support. All my friends and lab members in Kansas City especially Abeda who helped make this a home away from home. The Indian Association of KUMC family have are always been there when I needed them.

Finally, I would not be able to do anything if it were not for the constant love and support from my family. My mother Jabin Sayed, father Asif Ali Sayed, and sister Amreen Asif Ali Sayed. They have always supported and stood by me through all the ups and downs in my life. They have helped and guided me to do the right thing in all my life choices. Whatever I am and have become in life is because of their guidance. It was not easy to come to a different country away from my family. But I could only do this because they were always supporting me and making sure I was doing well. There are no words to describe how much I love them and how grateful and blessed I feel. I also want to thank my extended family in includes all my cousins and relatives who have supported and prayed for me. Finally, I want to thank the almighty for blessing me with all these wonderful people.

Table of Contents

List of Tables

List of Figures

Chapter 1: Introduction

1.1 Overview of colorectal cancer (CRC)

Colorectal cancer (CRC) arises from benign, precancerous polyps in the colon or rectum that grows over time to form malignant tumors. The transition is a multistep process arising due to genetic and epigenetic changes (Jass et al., 2002). While almost 80% of CRC cases are sporadic, it can also be caused by inherited syndromes like Familial Adenomatous Polyposis (FAP), Lynch syndrome (also known as hereditary non-polyposis colon cancer), Peutz-Jeghers syndrome and MYH-associated polyposis (MAP) (Fishel et al., 1993, Rustgi, 1994, Jass et al., 2002). Nearly 55% of CRC in the US has been attributed to modifiable risk factors by The American Cancer Society (Siegel, 2019). These risk factors include long-term smoking, obesity, less physical activity, low calcium intake, high consumption of red or processed meat, low intake of fiber, fruits and vegetables and alcohol consumption (Siegel, 2019).

Vogelstein and Fearon proposed a multistep sequence of genetic mutations that contributed to the alteration of the normal epithelium of colon to adenocarcinoma (Fearon, 2011). Their model is based on genetic events leading to chromosomal instability, starting from early events such as loss of the tumor suppressor gene adenomatous polyposis coli (APC). Additional mutational activation of *KRAS* oncogene (12p12) leads to progression to large adenoma. Further, inactivation of tumor suppressor genes *TP53* (17p) and *DCC* (18q) contribute to the transition to adenocarcinoma. This is accompanied by supplementary genetic alterations including loss of heterozygosity (LOH) on chromosome 10q or gains of DNA sequences at chromosome locations 5p and 6p (Lengauer et al., 1997, Markowitz and Bertagnolli, 2009, Fearon, 2011). In 2018, there were about 1.8 million new cases of CRC diagnosed worldwide, making it the third most common cancer.

Moreover, by 2030, there is an expectation of an increase in the number of CRC cases to upwards of 2.2 million, with estimated deaths rising to over 1.1 million (Bray et al., 2018, Siegel et al., 2019). In the US, there will be an estimated 104,610 new cases of colon cancer in 2020 with no gender bias between males (52,340) and females (52,270). Along with this, there is an estimate of 53,200 deaths (males-28,630 and females- 24,570) due to colon cancer. This has also made colon cancer the third most commonly diagnosed and cancer-related deaths in the US. Though patients with localized disease have a 5-year survival of 90%, only 39% of patients are diagnosed early. Overall, colorectal cancer has a 5-year relative survival rate of 64%. Good screening and avoiding risk factors have helped decrease the incidence rates by 3.6% annually among adults over the age of 55 years, but there has been a rise in the cases of adults younger less than 55-year of age by 2% annually. (Cancer Facts & Figures 2020)

CRC can be classified into two distinct pathways depending on genetic instability status; chromosomal instability (CIN) found in nearly 85% of CRC, and microsatellite instability (MSI) found in 15% (Dunican et al., 2002). The CIN subgroup is characterized by abnormal chromosome number leading to aneuploidy and LOH (Pino and Chung, 2010). Faulty DNA damage response and atypical chromosomal segregation can lead to protooncogene activation while suppressor genes are inactivated (Rao and Yamada, 2013). CIN positive tumors commonly arise in the distal colon or left side of the colon. CIN is a prognostic marker for CRC and is also linked with poor outcomes (Walther et al., 2008, Hong, 2018).

Microsatellite instability (MSI) results from the loss of mismatch repair (MMR) proteins causing genome instability and increased frequency of alterations in microsatellite DNA

regions (Iino et al., 2000). MSI positive tumors constitutes 15% of colon cancer cases of which 12% are sporadic and 3% are due to Lynch syndrome (Fishel et al., 1993). While sporadic cases of MSI in CRC result from epigenetic silencing of the MMR gene *MLH1* due to promoter hypermethylation, Lynch syndrome is characterized by germline mutations in several MMR genes including *MLH1*, *MSH2*, *MSH6*, and *PMS2* (Boland et al., 1998, Lee et al., 2015). MSI positive tumors are commonly found in the proximal colon (right side). One key distinguishing feature between hereditary MSI positive tumors is *BRAF* gene mutation which is rare in Lynch syndrome CRC (Lee et al., 2015).

Apart from chromosomal instability, CRC is also associated with epigenetic instability, a situation referred to as CpG island methylator phenotype (CIMP) characterized by hypermethylation of numerous CpG islands. The CIMP phenotype was described by Toyota and colleagues and results from hypermethylation at gene promoters resulting in the inactivation of specific tumor suppressor genes (Jover et al., 2011). CIMP-high colon cancers usually associate with MSI and BRAF mutations, and less with KRAS and TP53 mutations, whereas CIMP-low colon cancer is accompanied by KRAS mutation. The CIMP+/MSI+/*BRAF*+ tumors show a gradual increase from the rectum to the ascending colon. The impact of CIMP status on survival after specific CRC therapies is unclear due to limited studies and improper CIMP classification. However, CIMP status along with microsatellite stable (MSS) status and *BRAF* mutation result in poor survival in colon cancer (Jia et al., 2016).

One common histological subtype of colon cancer is mucinous adenocarcinoma which is characterized by high mucin content compromising almost half of the tumor volume (Luo et al., 2019). Nearly 20% of patients with colon cancer showed this phenotype and

higher rates are found in western countries compared to Asia (Glasgow et al., 2005, Hugen et al., 2014, Luo et al., 2019). A distinct feature of mucinous adenocarcinoma is the upregulation of MUC2 protein. It is also associated with Lynch syndrome and inflammatory bowel disease (Hugen et al., 2014, Luo et al., 2019). Aside from epigenetic and genetic alterations post-transcriptional alterations also play an important role in tumorigenesis. RNA binding proteins (RBPs) are important regulators post-transcriptional control and several RBPs are involved in tumorigenesis. RBPs including LIN28A, LIN28B, MSI, RBM3, HuR, TTP, CELF1, CELF2, TIA1 are dysregulated in colon cancer. LIN28A/LIN28B influence tumor aggressiveness and metastasis by affecting miRNAs (Wang T. et al., 2015). Musashi protein is important for proliferation and invasion of colon cancer and acts by repressing the translation of Numb which is an inhibitor of the NOTCH pathway (Qiao and It is also associated with Lynch syndrome and inflammatory bowel disease (Hugen et al., 2014, Luo et al., 2019).

Aside from epigenetic and genetic alterations post-transcriptional alterations also play an important role in tumorigenesis. RNA binding proteins (RBPs) are important regulators of post-transcriptional control and several RBPs are involved in tumorigenesis. RBPs including LIN28A, LIN28B, MSI, RBM3, HuR, TTP, CELF1, CELF2, TIA1 are dysregulated in colon cancer. LIN28A/LIN28B influence tumor aggressiveness and metastasis by affecting miRNAs (Wang T. et al., 2015). Musashi protein is important for proliferation and invasion of colon cancer and acts by repressing the translation of Numb which is an inhibitor of the NOTCH pathway (Qiao and Wong, 2009; Lan et al., 2015; Wang S. et al., 2015; Voutsadakis, 2018). ELAVL1 or HuR can regulate mRNAs related

to cell cycle and proliferation (Lin et al., 2017). This makes it important to study the role of RBPs in colon cancer initiation and progression.

1.2 RNA binding proteins (RBPs)

RNA binding proteins (RBPs) belong to a class of factors that form ribonucleoprotein (RNP) complexes with RNA to regulate its fate and function (Glisovic et al., 2008b). They affect various aspects of RNA at the posttranscriptional level including methylation, polyadenylation, localization, splicing, stabilization, and mRNA translation by forming protein-RNA and protein-protein interactions (Glisovic et al., 2008b, Hogan et al., 2008). A mature messenger RNA (mRNA) encodes several distinct features that are important for its regulation and translation; these include the cap, 5' and 3' untranslated region (UTR), coding region (CDS) and polyadenine tail (Figure 1-1). Many *cis*-acting elements are spread through the mRNA and RBPs bind to these precise elements and affect their fate. Although the elements can be seen throughout the entire mRNA, they are frequently located in the 5′- or 3′-UTRs (Hogan et al., 2008, Gebauer et al., 2012). These elements contain AU-, CU-, U-rich or G-rich elements (Pullmann et al., 2007). Of these, a widely studied element is the adenylate/uridylate-rich elements (AREs) (Chen and Shyu, 1995b). Given their significant role in posttranscriptional gene expression, any dysregulation of the RBPs can affect gene expression, which in turn could have significant consequences in various diseases including cancer (Lukong et al., 2008, Kechavarzi and Janga, 2014).

1.2.1 Function of RNA binding proteins

RNA binding proteins are key to RNA processing and modification. Alternative splicing of the transcribed RNA is an important event and about 74% of the human genes generate

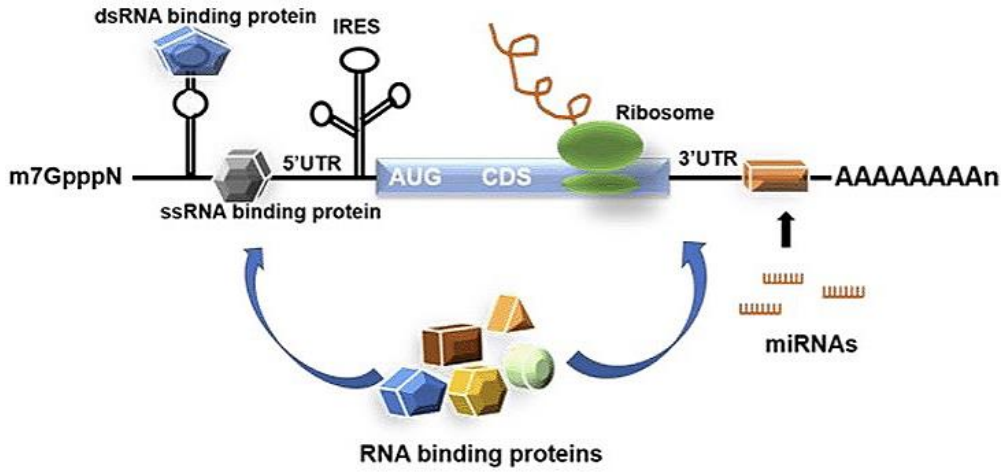

Figure 1-1 Schematic of mRNA structure
The mRNA has structural elements that can be bound by various regulatory proteins important for the translation. IRES is found in the 5' UTR and promote cap-independent translation. Both structural and non-structural RNA elements can be bound by RNA binding proteins (RBPs) on both 5’ and 3’ UTR for regulating translation of an mRNA by diverse mechanisms. RBPs can bind either double-stranded or single-stranded RNA elements. miRNA target sites are located in the 3' UTR. The canonical mRNA features of the cap (m7G) and poly(A) are targets of several regulatory interactions. m7GpppN: 7-methyl-guanosine; IRES: internal ribosome entry site; AUG: initiation codon; CDS: coding sequence; miRNA: microRNA; mRNA: messenger RNA

multiple transcripts through alternative splicing (Johnson et al., 2003). Alternative splicing is performed by many RBPs. One such example of an RBP is the Nova proteins, Nova-1 and Nova-2. Nova proteins encode three KH domains and recognize the intronic YCAY motif (Y= pyrimidine) on pre- mRNAs and recruit the spliceosome machinery to the target site. By this mechanism, they affect the splicing of several pre-mRNAs including gephyrins 1–2, JNK2, flamingo 1, neogenin (Allen et al., 2010). Polyadenylation is an event where multiple adenine residues are added at the 3’ end of an mRNA. Polyadenylation is important for the stability, transport and efficient translation of mRNA and is heavily dependent on RBPs. CPSF is an important protein complex involved in the polyadenylation process which binds to the canonical AAUAAA site. The CPSF-160 and CPSF-30 subunits of CPSF are important for RNA-binding (Ryan et al., 2004). Another

important posttranscriptional modification of mRNA is RNA editing, where an adenosine (A) is converted to inosine (I). This reaction is enzymatically catalyzed by the ADAR proteins (Valente and Nishikura, 2005).

Several RBPs have been studied for their role in stability and translation. RBPs like the ELAV/Hu family, RNA binding motif protein 3 (RBM3), TIA-1-related (TIAR), tristetraprolin (TTP), fragile X mental retardation protein (FMRP), polypyrimidine tract-binding protein (PTB), T-cell intracellular antigen 1 (TIA-1), CUG triple repeats RNA-binding protein (CUGBP), nucleolin, and heterogeneous nuclear ribonucleoproteins (hnRNP) A1, A2, and C1/C2 have been shown to influence the steady-state levels of mRNA (Barreau et al., 2005, De Rubeis and Bagni, 2010). RBPs can interact with specific sequences in the 3'UTR like AREs and either recruit degradation machinery to the transcript or stabilize the transcripts. One of the most widely studied proteins that influence mRNA turnover rate belongs to the ELAV/Hu family proteins (HuR, HuB, HuC, and HuD). They bind to the AREs in the 3'UTR of target mRNA to increase their stability (Simone and Keene, 2013).

Translation of most mRNAs' initiates from the 5′-end of the mRNA having the m^7GpppN cap. During this cap-dependent translation, first the small ribosomal subunit combines with the initiation factors eIF3 and eIF4F complex (eIF4A, eIF4E, eIF4G) to form the 43S particle. This 43S particle scans the mRNA for an AUG codon and then recruits the 60S subunit, to form the 80S ribosome conformation that is ready to initiate translation. At the 3'end, the poly (A)-binding protein (PABP) interacts with the poly (A) tail and with eIF4G, resulting in a closed-loop mRNA structure. This looping of the mRNA promotes recycling of ribosomes to begin another round of translation at the 5′end and hence, increasing the

efficiency of translation. This closed-loop structure of the mRNA provides a platform for the binding of 3′-UTR modulators, including RBPs that can then affect translation initiation (Chen and Shyu, 1995a, Wells et al., 1998, Szostak and Gebauer, 2013). Several RBPs such as AU-rich element binding proteins (AUBPs), HuR, RBM3, hnRNPK, interact within this closed-loop structure and regulate translation of mRNA. One example is hnRNPK that interacts with the 3'UTR of 15LOX (15-lipoxygenase) mRNA, which results in inhibition the 60S ribosomal subunit binding to the 40S thus decreasing 15LOX mRNA translation (Ostareck et al., 2001). Another mode for translation observed in virus is where the 5' end does not have the m^7G cap and the 5'UTR consists of highly structured sequences known as internal ribosome entry sites (IRES). These IRES are important for cap-independent translation under stress conditions and several mRNAs in mammalian like the cMyc, XIAP also have IRES for translation.

Localization of mRNA in the cell is also dependent on the binding of RBPs to the 3'UTR. A large number of hnRNPs like hnRNP A1, can interact with RNA for its cytoplasmic localization. Also,

Fragile X mental retardation protein (FMRP) interacts with G-quadruplex sequences in mRNAs such as MAP1B and CaMKIIa and affect their localization in dendritic cells (Dictenberg et al., 2008). Similarly, HuR protein also binds to ARE-containing mRNAs in the nucleus and accompanies them into the cytoplasm. This HuR mediated shuttling of mRNAs depends on the transcriptional activity of RNA polymerase II (Peng et al., 1998).

1.2.2 RNA binding domains

The RBPs contain RNA binding domains (RBDs) that help their recruitment to specific RNA targets. The RBD families consist of RNA recognition motif (RRM), KH domains,

zinc finger, RGG (Argenine-Glycine-Glycine) box, double-stranded RNA binding motif (dsRBM), Pumilio domain (PUF) and Piwi/Argonaute/Zwille domain (PAZ) (Castello et al., 2016). Other than the known structured domains, recent studies utilizing advanced sequencing technologies have revealed complex protein–RNA interactions that do not require canonical RBDs.

The RNA recognition motif (RRM) is the most common domain found in RNA binding proteins (Maris et al., 2005). The RRM domain consists of a primary sequence of 90 amino acids containing two conserved sequences called RNP1 (8 amino acids) and RNP2 (6 amino acids). Both RNP1 and RNP2 contain three conserved aromatic residues important for RNA interaction (Cléry et al., 2008). RRM can bind RNA and ssDNA. RBPs can contain multiple RRMs that can increase RNA binding affinity and sequence-specificity. HuR, RBM3, Sex-lethal, PABP, nucleolin, Hrp1 are a few examples of RBPs containing the RRM domain (Deo et al., 1999, Handa et al., 1999, Allain et al., 2000).

The hnRNP K homology (KH) domain is an important RNA binding domain comprising of nearly 70 amino acids. The domain is present in many proteins involved in splicing, transcription and mRNA translation. The motif is also found in various proteins present in archaea, bacteria and eukaryotes (Siomi et al., 1993a). Normally, KH domains are found in multiple copies; for example, the FMRP protein contains two while vigil protein has 14 copies of the KH domain (Siomi et al., 1993b). KH domains can be divided based on two types; type-I is found in eukaryotes while type-II is in prokaryotic proteins. The type-I KH domain has a conserved ‘GXXG loop’ motif (Grishin, 2001). Both KH motif folds are known for interacting with RNA or single-stranded DNA. (Valverde et al., 2008).

Zinc finger (ZnF) motifs also bind RNA and are found in RNA binding proteins. ZnFs can exist alone, repeated or in combination with other RBDs in proteins. A typical ZnF domain consists of 30 amino acids which form a ββα fold and are held together by a Zn^{2+} ion (Krishna et al., 2003). The protein domain can be further classified into CCHH, CCCH or CCCC based on the amino acids that interact with zinc ion. They were initially described as DNA binding motifs but subsequently also found to bind RNA (Chothia et al., 1981). The ZnF domain from Human Splicing Factor (ZRANB2) is an example of a zinc figure protein encoding two zinc finger domains (Loughlin et al., 2009).

Double-stranded RNA binding motif (dsRBMs) is a unique RNA binding domains that initially described as recognizing a specific RNA shape rather than a sequence (Stefl et al., 2005). These proteins have a conserved αββββα topology consisting approximately 70 amino acids. DsRRMs are often found in multiple copies; an example is the Staufen protein in *Drosophila melanogaster* that has five copies. DsRBMs are involved in RNA shuttling, processing, interference, editing and translational control (Chang and Ramos, 2005). An example of a dsRBMs is ADAR2 which is involved in editing of mRNA and converts Adenosine-to-Inosine (A-to-I) in its target mRNAs (Bass, 2002).

Pumilio domain containing RNA binding proteins usually interact with regulatory proteins and are involved in decay and translation of target mRNAs (Edwards, 2015). Pumillo family proteins contain the PUF domain (Pumilio and FBF), abd are highly conserved in eukaryotes. The domain recognizes target RNA using a multiple repeat element consisting of 35–39 amino acids (Abbasi et al., 2011) Another RNA binding domain is PAZ named after Piwi Argonaut and Zwille involved in RNA interference with DICER. The domain binds single-stranded RNA (Yan et al., 2003).

The Arginine-glycine rich (RGG) motif is an evolutionarily conserved sequence motif. The domain generally contains either repeats of glycine and arginine residues (RG) or serine, arginine and glycine (SAG), and also have aromatic residues in between them that can form hydrophobic interactions with RNA (Corley and Gready, 2008, Oliveira et al., 2017). The RBPs in this class are important in splicing, stability and translation (Haynes and Iakoucheva, 2006). These proteins also contain other RBDs like the RRMS. The RRMs can interact with proteins while the RG/SR domain is involved in protein interactions (Pérez-Cañadillas and Varani, 2001). An example is U2AF65 that is involved in 3' mRNA end processing (Zamore and Green, 1991).

1.2.3 RNA binding protein in Cancer

Aberrant expression of several RBPs is found in different cancer types. RPBs can act as tumor promoters, oncogenes or tumor suppressors in cancers. Examples of some RBPs upregulated in cancer include HuR, RBM3, RBM38, HuR, RBM3, RBM34, Lin28B, CEBP1, Musashi-1, Musashi-2 IMP1, IMP2, IMP3, AUF, hnRNPA1/A2 (Sureban et al., 2008, Masuda and Kuwano, 2019, Mohibi et al., 2019). RBPs that are downregulated in cancers include LRP7, PUM1, PUM2, TTP, CELF2, RBM9, etc. (Mohibi et al., 2019, New et al., 2019). RBPs are important modulators of post-transcriptional control and malfunction of RBPs can affect important cellular functions like proliferation, growth, death and invasion of cancer cells (Mohibi et al., 2019). (Mohibi et al., 2019). RBPs like HuR, SAM68, IGF2BP, are RBM3 are important for proliferation, while CELF1, CELF2, TIA, and hnRNPH are important for apoptosis. HuR, eIF4E, RBP2 are also involved in angiogenesis, while RBM47, hnRNPE-1, IGF2BP play a role in EMT and metastasis (Hong, 2017).

One of the widely studied RBPs in cancer is HuR, which belongs to the ELAV family of RNA binding proteins (Brody and Dixon, 2018). HuR has two RRM domains at the N-terminus that binds to the AREs in the 3'UTR and is important for shuttling, stability and translation of mRNAs (Brody and Dixon, 2018). HuR is upregulated in many cancers including brain, bladder, breast, colon, gastric, ovarian, prostrate. The Gorospe and Dixon laboratories were first to show the role of HuR in colon carcinogenesis by stabilizing mRNAs like COX-2 (de Silanes et al., 2003). HuR can also bind and stabilize VEGF, c-fos, TNF-α, and β-catenin mRNAs and contribute to colon carcinogenesis (Folkman, 1995; Jooss and Muller, 1995; Balkwill, 2002; Wong and Pignatelli, 2002). HuR can stabilize growth factor mRNAs important for medulloblastoma and high-grade brain tumor. HuR is correlated with higher grade and poor survival in hepatocellular carcinoma, brain tumor, breast cancer and gastric cancers (Zhu et al., 2015a). Several studies have targeted HuR for cancer therapy using small molecule inhibitors and nanoparticle delivery of siRNA (Blanco et al., 2016).

An example of a protein that acts as tumor suppressor is CELF2 which is downregulated in cancers and its reduced expression correlates with poor prognosis. CELF2 is the CUG binding ELAV like family-2 protein (CUGBP2). It is also involved in stability, shuttling, translation, editing and splicing (Hong, 2017). Our laboratory found that CELF2 expression is decreased in colon cancers and induces cell death thereby acting as a tumor suppressor. The laboratory has also demonstrated that expression of CELF2 can be modulated by the natural compound curcumin. In pancreatic cancers, curcumin can cause mitotic catastrophe by increasing CELF2 expression, which results in reduced expression of cyclooxygenase-2 (COX-2) and vascular endothelial growth factor (VEGF)

proteins (Subramaniam et al., 2011). The promoter of CELF2 also shows increased CpG methylation in several cancers including breast cancer (Piqué et al., 2019). CELF2 also inhibits proliferation and tumor growth in non-small cell lung carcinoma (Yeung et al., 2019). Another example of a RBP is RBM3 which is upregulated in bladder, prostrate, ovarian, breast, gastric and colorectal cancers. Our laboratory showed that RBM3 is a protooncogene and suppresses mitotic catastrophe in colon cancer cells (Sureban et al., 2008).

1.3 RNA binding motif protein 3 (RBM3)

Derry et al, identified RBM3 as a novel gene on the Xp11.2 region of the genome (Derry et al., 1995a). Using cDNA selection from the fetal brain with a YAC from the Xp11.2 region, they found RBM3. They also found that the encoded polypeptide from this region had high sequence similarity to a group of proteins that bind to RNA (Derry et al., 1995a). Later, Cok et al. identified that HuR and RBM3 bound to AU-rich sequences in COX-2 3′UTR using biotinylated RNA probes (Cok et al., 2004). Our lab also identified RBM3 as a HuR binding protein by yeast two-hybrid screening. It binds to the first 60 nucleotides within the 3'UTR of COX-2 mRNA and upon binding, increased its stability and translation (Sureban et al., 2008).

1.3.1 Structure and distribution of RBM3:

Structurally RBM3 has two domains, with an RNA recognition motif (RRM) domain in the N terminus and an Arginine-Glycine-rich (RGG) domain in the C terminus. The N terminal of RBM3 is highly conserved and has high sequence homology to other stress-responsive proteins including CIRP and HSPA4. The N terminal RRM domain of RBM3 contains two ribonucleoprotein motifs (RNP1 and RNP2) which are located at the end of the domain.

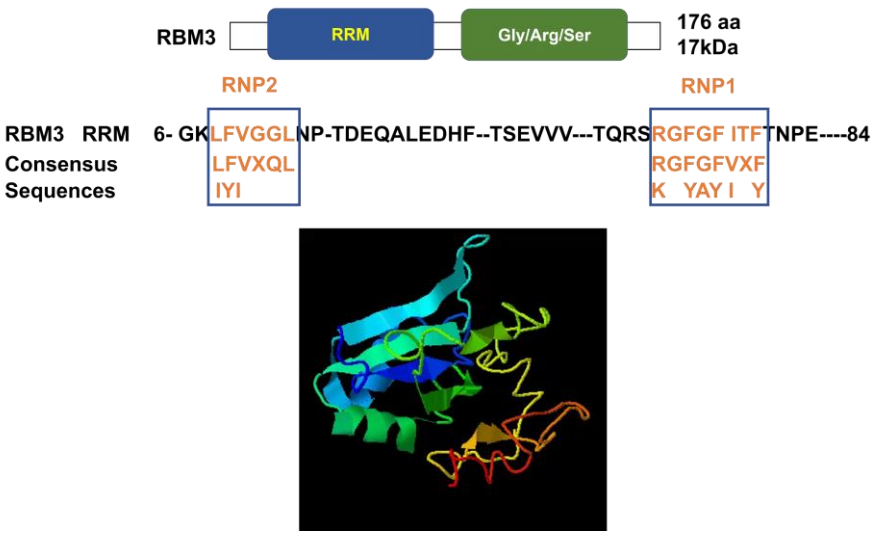

Figure 1-2 RBM3 structure
At the top is a representation of the two domains in RBM3 including the RNA recognition motif (RRM) domain at the N terminus, and an Arginine-Glycine-rich (RGG) domain at the C terminus. The N terminal RRM domain of RBM3 is represented below with the two ribonucleoprotein motifs (RNP1 and RNP2) highlighted, along with the consensus sequence. At the bottom is the homology model of the RRM domain derived using the iTasser software, showing the typical alpha-helix and beta-sheet sandwich.

The consensus sequence for the RNP1 is (K/R)G(F/Y)(G/A)FVX(FY) and RNP2 is (L/I)(F/Y)(V/I)(G/K)(G/N)L (Figure1-2). These RNPs have moderate sequence and functional identity to other RNA binding proteins especially belonging to cold shock proteins showing evolutionary conservation among the family (Ciuzan et al., 2015, Zhu et al., 2016b). RRMs are important for the post-transcriptional functions including pre-mRNA capping, splicing and polyadenylation (Streitner et al., 2012, Ciuzan et al., 2015). The C-terminal region encodes a less conserved Arginine-Glycine-rich (RGG) domain, suggesting that RBM3 belongs to the large family of glycine-rich proteins (GRP). As RBM3 has both an RRM and an RGG domain, it also considered to be a member of the IVa class of GPR proteins (Zhu et al., 2016b). The IVa class GRP subfamily is evolutionarily conserved in amino acid sequence and function across higher plants and vertebrates (Ciuzan et al., 2015). RBM3 is also evolutionarily conserved and has preservation of biological function across mammalians (Zhu et al., 2016b). Both the RRM

domain and the RGG domain are involved in associating with mRNA and have roles in their stability and translation. For example, CIRBP is a RBP that binds the 3'UTR of target mRNA thiodredoxin and independently promotes translation from both RRM and RGG domains (Yang et al., 2006). The RGG domain is important for mRNA export and the absence of single arginine residue can disrupt nuclear-cytoplasmic export (Smart et al., 2007b).

RBM3 is ubiquitously expressed in the body with a high expression seen in the brain and testis while it is low or absent in thyroid and heart. In the brain, RBM3 levels are high at postnatal period and gradually decreases in youth and adulthood in most regions of the brain. The levels of RBM3 remain high in the hippocampal sub-granular zone (SGZ) and sub-ventricular zone (SVZ) which have active proliferation. This shows an important role for RBM3 in stemness and proliferation of neural progenitor cell (Pilotte et al., 2009, Chip et al., 2011). In the testis, RBM3 expression was observed in the Sertoli cells as early as 8-day old neonatal mice and remains thereafter. Sertoli cells are important for providing physical and nutritional support for developing spermatocytes and spermatids (Danno et al., 2000). RBM3 is a cold inducible protein and usually high expression is found in hibernating animals. In black bears, RBM3 is upregulated in muscle, liver, and heart tissues during hibernation (Fedorov et al., 2011). RBM3 is also upregulated in human cells in response to cold stress. When cells are incubated at 32°C (moderate hypothermia) for 24 hours, there is an increase in RBM3 mRNA expression (Zhu et al., 2016b). Similarly, RBM3 levels are also affected by oxygen stress, with a mild to severe hypoxia resulting in increased RBM3 levels in non-neural cells (Rosenthal et al., 2017). At the sub-cellular level, RBM3 is predominantly present in the nucleus; the RGG domain

in RBM3 is thought to act as nuclear localization signal. Thus, it can shuttle between nucleus and cytoplasm. RBM3 is also associated with translation machinery and may interact with 60S ribosomes (Dresios et al., 2005, Smart et al., 2007b). RBM3 protein has also been found to shuttle to the endoplasmic reticulum (ER) upon ER stress where it regulates the activity of phospho-ERK (Zhu et al., 2015b). Two transcript variants of RBM3 have been seen in the brain, the difference between the two transcript lies in a single arginine residue in the RGG domain that promotes RBM3 to localize in dendrites instead of the nucleus of the neurons (Smart et al., 2007a).

1.3.2 Function of RBM3

Like other cold shock proteins, RBM3 also plays important role in regulating RNA translation, stability and splicing of several proteins including COX-2. COX-2 is a rate-limiting enzyme in the conversion of arachidonic acid into prostaglandins, prostacyclins and thromboxanes. COX-2 mRNA stability and translation is highly regulated by RNA binding proteins that bind to the 3'UTR (Newton, 1997). Cok et al. used the first 60 nucleotides of the 3'UTR of COX-2 mRNA to identify proteins regulating its expression. They *in vitro* transcribed and biotin labeled the first 60 nucleotides of 3'UTR which encodes ARE elements. Analyses of proteins by mass spectrometry that bound to this region identified RBM3 as one of the proteins. Further studies revealed that RBM3 is involved in stabilizing the COX-2 mRNA by increasing its half-life (Cok, 2004). Since then RBM3 has been shown to interact and stabilize mRNAs containing AU rich elements like IL-6 and VEGF (Sureban et al., 2008). RBM3 was also found to enhance global protein translation by interacting with the 60S ribosomal subunit. It also increases the formation of active polysomes (Pilotte et al., 2011). RBM3 overexpression enhances

phosphorylation of translation initiation factors eIF4E and 4EBP1. 4EBP1 is a translation inhibitor that interacts with eIF4E. However, phosphorylated 4EBP1 cannot interact with eIF4E, thereby releasing eIF4E to enhance mRNA translation (Smart et al., 2007a). Study of RBM3 circadian genes shows that RBM3 is involved in controlling alternative polyadenylation of these mRNAs by binding near the polyadenylation sites (PAS) and increasing translation (Cok et al., 2004). RBM3 is involved in splicing and can associate with the spliceosome machinery (Barbosa-Morais et al., 2006). Specifically, RBM3 can repress the splicing of variant v8–v10 of CD44 mRNA while enhancing the standard spliced CD44 transcript as seen in prostate cancer cells (Zeng et al., 2013).

RBM3 can also regulate miRNA expression. Pillote et al. found that RBM3 can bind directly to the pre-miRNA (~70 nt) intermediates and thus promote or repress their ability to associate with the active dicer complexes (Pilotte et al., 2011). On the other hand, Dresios et al. found that miRNAs associated with the 40S subunit were less abundant in RBM3 overexpressing conditions such as hypothermia (Dresios et al., 2005). Another study showed that reduced RBM3 levels promotes the expression of temperature-sensitive miRNAs such as miR-142-5p and miR-143, which target immune genes important to regulation of immune cell function during fever (Wong et al., 2016). However, the role of RBM3 in regulating non-coding RNAs is limited. A recent study to determine the role of RBM3 on circular RNAs showed that knockdown of RBM3 in hepatocellular cancer caused down regulation of SCD-circRNA2. They demonstrated that RBM3 can increase expression of SCD-circRNA2 by binding to 3' UTR of SCD mRNA (Dong et al., 2019a). Other RBPs like Quaking and RNA-binding motif protein 20 (RBM20) have also been shown to regulate circular RNA formation (Conn et al., 2015, Khan Mohsin et al.,

2016). The role of RBM3 in regulating other noncoding RNAs especially lncRNAs have not yet been evaluated.

1.3.3 Role of RBM3 in cancer

RBM3 is up-regulated in solid tumors including high stage colorectal cancer, poorly differentiated prostate cancer, malignant melanoma, ovarian cancer, breast cancer and high-grade astrocytoma (Sureban et al., 2008, Shaikhibrahim et al., 2013b, Zhang et al., 2013a). Our laboratory previously showed using tumor tissue microarray that RBM3 is overexpressed in breast, pancreas, colon, lung, ovary and prostate cancers. RBM3 levels are also upregulated in a stage-dependent manner in colon cancer. Overexpression of RBM3 results in the transformation of NIH-3T3 cells demonstrating the role of RBM3 as a proto-oncogene. However, overexpressing another RBP HuR in NIH-3T3 cells did not cause transformation. Overexpression in transformed cells such as SW480 results in increased proliferation and larger colonies. On the other hand, down-regulation of RBM3 caused cells to undergo mitotic catastrophe as seen by the increase in caspase-mediated apoptosis leading to nuclear cyclin B1 along with phosphorylation of chk1/2 and cdc25c. Knockdown of RBM3 also resulted in reducing tumor xenograft growth. Our lab further demonstrated the mechanism where RBM3 overexpression increases the stability and translation of COX-2, IL-8, and VEGF mRNAs that are important in tumorigenesis (Sureban et al., 2008).

Next, the laboratory studied the role of RBM3 in increasing stemness. Previous studies had shown that RNA binding proteins could affect the cancer stem cell population (Krausova and Korinek, 2014). Cancer stem cells (CSCs) belong to a subset of cells in the tumor population that have the capacity to regenerate survive stress and can resist

chemotherapeutics and radiation. In colon cancer RBM3 overexpression in colon cancer cells resulted in an increase in the side population along with resistance to chemotherapeutic drugs. Along with this, RBM3 also increased spheroid formation, further indicating its role in stemness. RBM3 overexpression also increased the levels of LGR5 and DCLK1 and the $CD44^{Hi}/CD24^{Low}$ population. Moreover, RBM3 overexpression increased nuclear β-catenin level, in part due to Ser9 phosphorylation-mediated inactivation of GSK3β (Venugopal et al., 2016b). These results demonstrate the role of RBM3 in increasing stemness in colon cancer cells.

Chen et al. demonstrated that elevated levels of RBM3 in patients with breast cancer was associated with reduced overall survival (OS) rates and worse post-operative relapse-free survival (RFS). They showed that RBM3 positively regulated the expression of actin-related protein 2/3 complex subunit 2 (ARPC2) and contributes to breast cancer progression (Chen et al., 2019). Though previously it was reported that nuclear expression of RBM3 showed improved the clinical outcome in breast cancer patients, this study was based on immunohistochemistry observation only and no mechanisms were studied (Jogi et al., 2009). Similarly, cohort studies involving immunohistochemical studies have shown that RBM3 expression correlates with good prognosis in breast cancer, cisplatin sensitivity in epithelial ovarian cancer, prostate cancer, and colorectal cancers (Jonsson et al., 2011a, Siesing et al., 2017a, Zhou et al., 2017b). These studies are mostly based on observation and focus on nuclear localization, and do not consider cytoplasmic levels of the protein.

Yang et al. evaluated the role of RBM3 in neuroprotection from nitric oxide (NO)-induced apoptosis and found that the protein protects human neuroblastoma cells.

Mechanistically, they determined that increased RBM3 inhibited the activation of p38 signaling which is also important for apoptosis. They also established that RBM3 overexpression along with mild hypothermia diminished the induction of miR-143 by NO (Yang et al., 2017).

Wellman et al. showed that RBM3 expression increased proliferation rates and rescued human embryonal kidney (HEK293) cells from serum starvation induced cell death. However, RBM3 modulation in HEK293 cells did not affect COX-2 expression demonstrating an alternate mechanism. They concluded that RBM3 is important for cell survival by reinstating translation efficacy in adverse conditions (Wellmann et al., 2004).

Zeng et al. showed that siRNA-mediated downregulation of RBM3 affected survival of prostate cancer by impeding DNA damage response induced by p53 and p21. They also showed that downregulating RBM3 expression increased chemotherapeutic susceptibility in prostate cancer cell lines (Zeng et al., 2013). Higher expression of RBM3 correlates with high grade astrocytoma as compared to lower grade or normal tissue (Zhang et al., 2013a).

Studies in breast cancer detected RBM3 among a set of RBPs in the invasive pseudopodia (de Hoog et al., 2004). Pillote et al. also detected RBM3 at the spreading initiation centers (SICs) of pseudopodia and blebs in migrating myoblast cells. They found that disruption of RBM3 expression dramatically affected cell polarity and migration in neuroblastoma cells. They inferred the loss of migration in RBM3 lacking cells to a combined effect of decreased global translation and increased Rho-A-ROCK signaling. These results further imply that RBM3 could affect epithelial-mesenchymal transition-induced metastasis and tissue repair (Pilotte et al., 2018). Nevertheless, the mechanistic

role of RBM3 in tumor progression remains contested. Dong et al performed ribosomal-depleted RNA sequencing of hepatocellular carcinoma (HCC) and examined the expression of circRNAs regulating HCC. They found a circular RNA SCD-circRNA-2 that was up-regulated and correlated with poor prognosis in HCC. They also found that RBM3 was important for biogenesis of SCD-circRNA-2 and increased the HCC cell proliferation via SCD-circRNA-2 (Dong et al., 2019a).

1.4 Long noncoding RNAs (lncRNAs)

Only two percent of the human genome is transcribed into protein-coding transcripts. The remaining part of the genome that does not code for protein and has been commonly termed as junk DNA (Djebali et al., 2012). Recent advances in high-throughput genomic technologies have helped discover transcripts called non-coding RNAs from this region of the genome. Of these, long noncoding RNAs (lncRNAs) are a major class with transcripts with lengths of more than 200 nucleotides (Iyer et al., 2015). They have little to no protein-coding potential due to the absence of an open reading frame (ORF). LncRNA transcripts are generally transcribed by RNA polymerase II and have features like mRNA including 5′ capping, 3′ polyadenylation and multiple exons. The exons in lncRNAs can undergo splicing through canonical genomic splice motifs (Wang and Chang, 2011). LncRNAs are classified based on their location on the genome; intergenic lncRNAs are located in the intergenic region of the genome, antisense lncRNA is transcribed from the antisense strand, bidirectional lncRNA is transcribed from near the gene promoter from complementary strand and sense-overlapping lncRNA are transcribed within protein-coding genes (Balas and Johnson, 2018). Various databases

are available for lncRNA and sequences are being added every day to the growing list of newly discovered lncRNAs.

There are nearly 30,000 transcripts of lncRNAs annotated in the reference human genome according to GENCODE database (Derrien et al., 2012). The LNCipedia database has a collection of 127,802 long noncoding transcripts from 56,946 genes in human, although they are not annotated (Volders et al., 2018). Similarly, there is a collection of 172,216 lncRNA transcripts in NONCODE database that are not annotated (Zhao et al., 2016).

1.4.1 Roles and Functions of lncRNAs

LncRNAs are regulatory molecules that can impact gene expression through interaction with DNA, RNA and proteins. They can act as guides, scaffolding molecules, decoys and sponges (Mongelli et al., 2019). Also, lncRNAs are known to regulate gene expression at epigenetic, chromatin remodeling, transcription, posttranscriptional, translation and posttranslational levels (Figure 1-3). LncRNAs acting as guides can bind to regulatory proteins and RNA to localize them to specific regions in the cell or the genome (Fernandes et al., 2019). LncRNA can affect the chromatin structure of a gene affecting its accessibility to transcription factors and polymerases (Li et al., 2016). The best studied example of lncRNAs acting as a guide is HOTAIR that binds to the Polycomb Repressive Complex 2 (PRC2) and directs it to the HOXD locus of the genome for chromatin modification (Rinn et al., 2007). The PRC2 is an epigenetic modifier that can methylate Histone H3 lysine 27. This leads to closed chromatin structure thus silencing the transcription from that region for metastasis suppressor genes. LncRNAs can also act as scaffolds, providing a transient docking site for the assembly of multiple protein

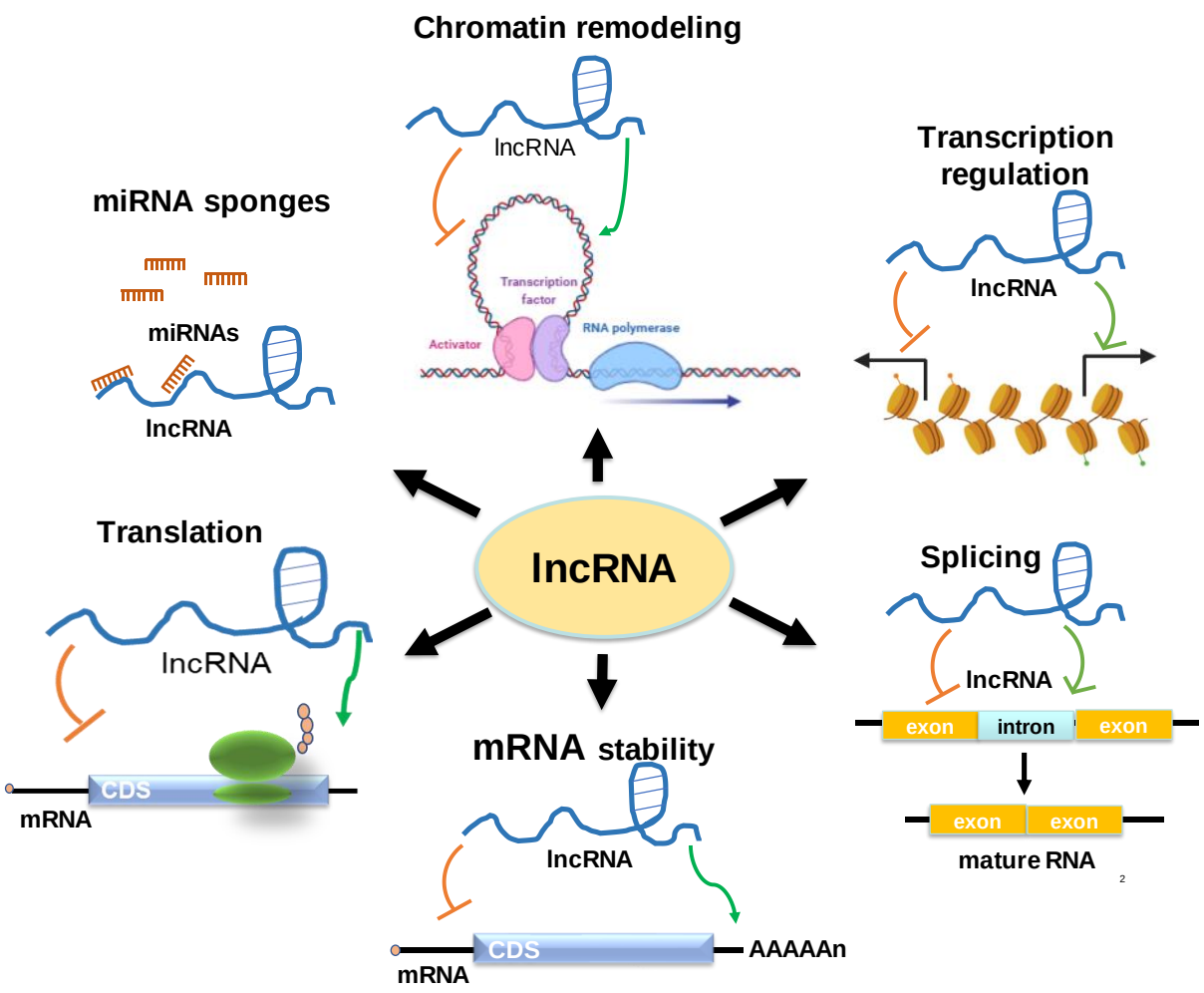

Figure 1-3 Functions of lncRNA

LncRNAs can regulate gene expression at various stages including epigenetic, chromatin remodeling, transcription, post transcription, translation and post translation. Some of their functions are highlighted above. LncRNA act as sponges for miRNA and sequester it away from its target mRNA. LncRNA can affect the chromatin structure through chromatin remodeling and regulate transcription by affecting promoter accessibility to transcription factors and polymerases. LncRNAs are also involved in different steps of post-transcriptional regulation starting from pre-mRNA capping, splicing, polyadenylation, stability, editing and transport. Figure made with biorender software.

complexes, RNA and cofactors. LncRNA scaffold can bring various proteins and other regulatory molecules together and provides a platform for their combined biological function (Schorderet and Duboule, 2011, Guttman and Rinn, 2012, Kung et al., 2013). The lncRNAs HOTAIR, TUG1, MALAT1 and ANRIL can act as scaffolds connecting

PRC2 and PRC1 complexes for chromatin modification (Kotake et al., 2011, Yang et al., 2011, Balas and Johnson, 2018).

One of the main functions of lncRNA is acting as a molecular sink where they can sequester transcription factors, catalytic proteins, protein complexes, miRNA and other RNAs. This decoy function of lncRNAs is very important as this can negatively regulate cellular functions by titrating away effector molecules (Rinn et al., 2007, Balas and Johnson, 2018). One example is PANDA, a lncRNA shown to bind the transcription factor NF-YA, sequestering it away from target sequences in the chromatin, resulting in decreased expression of senescence and apoptotic genes (Peng et al., 2017). They can also bind DNA to and interfere with the binding of polymerases and transcription factors to gene promoters. One example is lncRNA HIFCAR (HIF-1α co-activating RNA) which is upregulated in oral carcinoma. One example is lncRNA HIFCAR (HIF-1α co-activating RNA) which is upregulated in oral carcinoma. Shih et al. demonstrated that lnc-HIFCAR can form a complex with HIF-1α and facilitate its recruitment along with p300 cofactor to promoters of target genes (Shih et al., 2017).

LncRNAs also acts as sponges for miRNA where it can interact with the miRNA and sequester it away from its target mRNA. This results in stabilizing the target mRNA and its subsequent translation (Huarte, 2015). MALAT1 lncRNA can bind to miR-320a and thus inhibit miR-320a's suppressive function, thereby upregulating the expression of miR-320a target gene FOXM1 (Sun et al., 2017a). Zhou et al. also showed a sponging role for lncRNA H19, wherein it sequesters miR-200b/c and let-7b thereby resulting in increased expression of EMT genes in breast cancer (Zhou et al., 2017c). Other lncRNAs like MEG3

and TUG1 also sequester miRNAs from their mRNA targets resulting in dysregulated protein expression (Thomson and Dinger, 2016, Yang et al., 2019).

LncRNAs are also involved in different steps of post-transcriptional regulation starting from pre-mRNA capping, splicing, polyadenylation, stability, editing and transport (Dykes and Emanueli, 2017, He et al., 2019b). All these roles are similar to those of RNA binding proteins and also, there is evidence that lncRNA may work with RBPs for post-transcriptional regulation. LncRNA MALAT1 was shown to interact with splicing factor proteins and be involved in alternative splicing (Tripathi et al., 2010). Matsui et al. found that lncRNA iNOS generated from the antisense strand interacts with RNA binding protein HuR and stabilized iNOS mRNA (Matsui et al., 2008). LncRNA can stabilize proteins by interacting and inhibiting ubiquitination. One such example is lncRNA p21 that binds to HIF-1α and inhibits VHL facilitated ubiquitination and degradation of HIF-1α (Yang et al., 2014). LncRNAs also regulate protein translation by interaction with mRNA, ribosomes and eukaryotic elongation initiation factors. Tran et al. showed that lncRNA AS-RBM15 has overlapping sequences within RBM15 5'UTR and helps protein translation by recruiting polyribosomes to RBM15 mRNA in a CAP dependent manner (Tran et al., 2016). LncRNAs not only affect gene expression, but are also involved in enzymatic reactions affecting cellular pathways contributing to disease. Zhou et al. demonstrated that lnc-H19 binds and decreases the activity of S-adenosyl-L-homocysteine hydrolase (AdoHcyase) which is the only mammalian enzyme for the breakdown of S-adenosyl-homocysteine to homocysteine and adenosine. AdoHcyase plays a role in gene expression and cell growth (Zhou et al., 2015). All these examples show that lncRNAs can interact with diverse molecules and regulate cellular function at various levels.

1.4.2 LncRNAs in cancer

Cancer is a disease caused in a significant part by genetic and epigenetic alterations resulting in abnormal gene expression. Recent advances in sequencing techniques and genome-wide association studies have discovered that almost 80% of single nucleotide polymorphisms (SNPs) are associated with noncoding regions of the genome. These SNPs also occur in regions where lncRNAs are transcribed (Schmitt and Chang, 2016, Bolha et al., 2017, Tornesello et al., 2020, Zhang et al., 2020). LncRNAs can regulate and influence several important cellular functions such as survival, mobility, cell cycle, pluripotency and immune response all of which also contribute to cancer (Bartonicek et al., 2016). They can act as tumor suppressors or tumor promoters, based on their expression and role in tumorigenesis. Studies have shown that lncRNAs in cancers can be associated with tumor initiation, metastasis, progression, stemness, and patient survival (Bhan et al., 2017, Bolha et al., 2017, He et al., 2019b). Some examples of tumor promoting lncRNAs are HOTAIR, H19, HOTTIP, MALAT1, NEAT1, TUG1, XIST, PCAT1. Examples for tumor suppressor lncRNAs include MEG3, GAS5, PTENP1, BGL3 and others (Niland et al., 2012, Balas and Johnson, 2018).

LncRNAs can affect cell transformation through epigenetic modification causing changes in gene expression (Guttman and Rinn, 2012). As such, several lncRNAs associate with the polycomb repressive complex 2 (PRC2), resulting in silencing of genes that affect cell proliferation (Zhang et al., 2013b). Another important target for lncRNAs is the transcription factor p53 which acts as a tumor suppressor and is important for cellular homeostasis. The lncRNA Trp53cor1, PANDAR and lincPINT can regulate apoptosis and

cell cycle arrest through a p53 dependent mechanisms (Huarte et al., 2010, Sánchez et al., 2014).

LncRNAs also affects signaling pathways involved in cancer stemness. LncRNAs can directly regulate stemness of cells. For example, lncBRM can stimulate YAP1 to regulate liver stem cell self-renewal (Zhu et al., 2016a). Moreover, lncRNA SOX4 regulates self-renewal of cells by regulating the STAT3 pathway (Chen et al., 2016). Similarly, lncRNA TCF7 activates Wnt signaling to promote stemness of cancer cells. This occurs in part by lncTCF7 recruiting the SWI/SNF complex to the TCF7 promoter (Wang et al., 2015b, Zhou et al., 2017a).

LncRNAs have also been shown to play important roles in tumor progression especially in the epithelial to mesenchymal transition (EMT) of cells. ZEB1, ZEB2, SNAIL1, SNAIL2, TWIST1 and TWIST2 are transcriptional repressors of E-cadherin and important for EMT (Zhou et al., 2017a). It was seen that overexpression of lncRNA p21 in HCC decreases the expression of N-cadherin and SNAIL1 leading to inhibition of EMT. HOTAIR has been shown to enhance EMT through several mechanisms. It acts as a scaffold and recruits EZH2 and SNAIL1 to the promoter of E-cadherin. This repressive complex suppresses E-cadherin and promotes EMT in hepatocytes. This is also true in HCC, where EZH2, HOTAIR and SNAIL1 are upregulated and correlate with tumor aggression and progression (Battistelli et al., 2017). In esophageal and epithelial cancers, HOTAIR negatively regulates miR-148a. MiR-148 is involved in suppression of SNAIL2 which is also a key factor of EMT in cancer (Xu et al., 2013, Xu and Zhang, 2017). MALAT1 lncRNA affects EMT and metastasis in esophageal cancer through an EZH2-Notch signaling mechanism.

LncRNAs have been shown to regulate angiogenesis directly or indirectly through modulation of VEGF (Yu and Wang, 2018). VEGFA is a key regulator of tumor angiogenesis affecting cancer growth, invasion and metastasis (Hanahan and Weinberg, 2011). The lncRNA HOTAIR can promote angiogenesis by directly activating the transcription of VEGFA (Fu et al., 2016). It can also upregulate VEGFA and ANG2 expression (Fu et al., 2016). The lncRNA TUG1 can affect endothelial cell proliferation, migration and tube formation. TUG1 can directly bind to and repress the miRNA miR-299 that targets VEGFA mRNA and increase angiogenesis in glioblastoma (Liu et al., 2017b). LncRNA PVT1 is upregulated in gastric cancer and promotes angiogenesis by inducing the STAT3/VEGFA axis. PVT1 forms a complex with STAT3 and protects it from ubiquitin mediated degradation and in turn STAT3 can increase PVT1 levels through transcriptional regulation. This sustained STAT3 can then bind the VEGFA promoter and increase its expression inducing angiogenesis (Zhao et al., 2018).

1.4.3 LncRNAs and RNA binding proteins

RNA binding proteins are critical for the post-transcriptional modifications and translation of RNA (Hentze et al., 2018). Recent studies have found important interactions between RBPs and lncRNAs (Bierhoff, 2018, Chu and Chang, 2018). Liu et al. performed binding activity assay for 13 lncRNA on human proteome arrays to identify novel lncRNA-RBP interactions. They identified 671 RBPs, out of which 525 had unconventional RNA binding domains (Liu et al., 2019). Huang et al, used a click chemistry-assisted RNA interactome capture (CARIC) method for identifying RBPs binding to mRNA and noncoding RNAs. They found 572 RBPs including 170 previously unknown RBPs that interacted with mRNA and noncoding RNAs (Huang et al., 2018).

Many RBPs have been evaluated for their interactions with lncRNAs. The RBP hnRNPK plays important roles in cancer cell proliferation, differentiation and apoptosis by regulating target mRNAs including c-Myc, c-Src, eIF4E, p21, r15-LOX. Moreover, in several cancers, hnRNPK can also interact with lncRNAs including lnc-p21, NEAT1, PTOV1-ASI, Xist, lnc91H, TUNA, CASC11, MYCLo-2 (Sun et al., 2017b). Through interactions with these lncRNAs, hnRNPK has been shown to increase transcription of genes involved in tumorigenesis (Xu et al., 2019). Dimitrova et al., confirmed that lncRNA-p21 can interact with hnRNPK to increase p53 mediated gene expression (Bao et al., 2015). LncRNA TUNA (Tcl1 upstream neuron associated) can interact with hnRNPK to form a multiprotein complex and directly activate pluripotency genes like SOX2, Fgf4 and Nanog (Xu et al., 2019). HnRNPK also affect the stability of CDK6 mRNA and affect cell cycle, by interacting with lncRNA MYU in human colon cancer cells (Kawasaki et al., 2016).

HuR can interact with various lncRNAs like NEAT1, HGBC, lincBRN1a, RMST, OIP5-ASI, OCC1. HuR can bind and stabilize lncRNA NEAT1 in ovarian cancer cells contribution to tumor progression (Chai et al., 2016). LncRNA OCC-1 (overexpressed in colon carcinoma-1) is a tumor suppressor lncRNA that enhances the ubiquitination and degradation of HuR thereby decreasing HuR protein levels and its target mRNAs (Lan et al., 2018). LncRNA-HGBC (lncRNA highly expressed in gallbladder cancer) has increased expression in gallbladder cancer, where it binds to HuR, thereby contributing to increased cell proliferation and invasion (Hu et al., 2019).

LncRNA HOTAIR was also shown to interact with several RBPs. HnRNP A2/B1 binds to HOTAIR and HOTAIR's target transcript JAM2 increasing RNA-RNA interactions. hnRNP

A2/B1 also increases HOTAIR-mediated cellular invasion and methylation of H3K27 of gene promoters in breast cancer (Meredith et al., 2016). Ding et al showed that RNAi mediated suppression of HOTAIR reduced the expression of RBM38 and increased invasion and migration in HCC cells (Ding et al., 2014). Xue et al, showed that HOTAIR can interact with Runx3 and induce its degradation through the RNA binding protein Mex3b (Xue et al., 2018).

RBP-lncRNA interaction and its role in cancer is still vastly understudied. Studies have shown that several lncRNAs are associated with colon cancer, few examples being H19, DANCR, BLACAT1, HOTAIR, Xist, CCAT1, UCA, PCAT1, GAS5 (He et al., 2019a, Kalmár et al., 2019, Siddiqui et al., 2019). These lncRNAs are important for colon cancer cell migration, proliferation and act as biomarkers for prognosis (Siddiqui et al., 2019). However, there remain a large number of lncRNAs whose role in colon cancer is unknown. As mentioned previously, RBM3 is a proto-oncogene that is upregulated in colon cancer and is important for stemness and cell survival. A recent study in triple-negative breast cancer (TNBC) evaluated the role of lncRNAs in tumor invasion and proliferation. They found that lncRNA LINC00096 increased the proliferation and invasion of TNBC cells by regulating expression of miR-383-5p and in turn RBM3 (Tian et al., 2019). However, the role of RBM3 in lncRNA interactions and regulation has not been evaluated. In this study, we have used an unbiased approach to analyze the lncRNAs regulated by RBM3 and its role in colon cancer progression.

Chapter 2 : Overexpression of RBM3 increases tumor progression in colon cancer cells

2.1 Introduction

RNA binding motif protein 3 (RBM3) was first discovered within the Xp11.23 region of the X chromosome (Derry et al., 1995b). It is a cold shock protein which is 157 amino acid protein with a molecular mass of 17 KDa. It belongs to the glycine-rich RNA binding protein family (Danno et al., 1997). It was also shown to be induced by stress conditions like cold, low nutrient and hypoxia (Wellmann et al., 2004). RBM3 binds to the 3'UTR of its client mRNA and affects the stability and translation of the mRNA. RBM3 also regulates the posttranscriptional biogenesis of a majority of miRNAs at the Dicer step (Pilotte et al., 2011). In addition to its effect on protein synthesis, RBM3 also plays an important role in cell survival (Sureban et al., 2008).

RBM3 is up-regulated in many cancers including bladder, ovarian, prostate, gastric, high stage colorectal cancers, poorly differentiated prostate cancers and high-grade astrocytoma (Ehlén et al., 2010, Shaikhibrahim et al., 2013a, Zhang et al., 2013a, Siesing et al., 2017b, Zhou et al., 2017b). It is an independent prognostic marker associated with tumor recurrence in prostate cancer and downregulating RBM3 expression increased chemotherapeutic susceptibility in prostate cancer cell lines (Jonsson et al., 2011b). Our laboratory previously demonstrated that RBM3 acts as a protooncogene, because overexpression of protein results in the transformation of NIH-3T3 cells (Sureban et al., 2008). RBM3 increases proliferation, stemness, motility and chemoresistance in cancer cells. Moreover, RBM3 is indispensable for cell cycle and cell survival as knockdown of RBM3 induces apoptosis and mitotic catastrophe (Sureban et al., 2008). Subsequent studies also established that RBM3 enhances stemness (Venugopal et al., 2016b).

A limited number of studies have evaluated the role of RBM3 in pathways involved in tumorigenesis. RBM3 binds and increases the stability and translation of COX-2, IL-8, and VEGF mRNAs (Sureban et al., 2008). RBM3 can also modulate G2/M transition promoting cell cycle progression in cancer, because knockdown of RBM3 results in increased G2-phase cells cycle arrest (Sureban et al., 2008, Matsuda et al., 2011). RBM3 also inhibits caspase-mediated and staurosporine-induced apoptosis by repressing PARP cleavage [34]. In addition, RBM3 protects neurons from ER stress-induced apoptosis (Yang et al., 2017). RBM3 can repress the phosphorylation of eIF2α and PERK, thereby decreasing CHOP and ultimately rescuing cells from apoptosis. RBM3 also regulated DNA damage response by modulating the expression of Chk1, Chk2, and MCM3. For its role in stemness, RBM3 was involved in CD44 variant splicing along with the activation of ERK and depletion of PTEN (Ehlén et al., 2011).

Cancer development is a complex process involving dysregulation of genetic, epigenetic and regulatory factors. It is known that RBPs can modulate the expression of mRNA through splicing, stability, translation and localization (Glisovic et al., 2008a). The regulation of oncogenic and tumor suppressor mRNAs by RBPs can play an important role in tumorigenesis (Masuda and Kuwano, 2019). Hence it is important to study the RBPs and the fate of their interacting transcripts in the context of cancer. To date, very few targets for RBM3 have been studied and especially as it relates to tumor progression and metastasis.

2.2 Materials and Methods

Cells and reagents

Human colon cancer cells HCT116, DLD1, RKO and endothelial cell line HUVEC were obtained from American Type Culture Collection (ATCC). The cell lines were grown in DMEM with 4.5 g/L glucose, L-glutamine and Sodium Pyruvate (Corning, Tewksbury, MA) containing 10% heat-inactivated fetal bovine serum (Sigma-Aldrich, St. Louis, MO) and 1% antibiotic-antimycotic solution (Corning, Tewksbury, MA) at 37°C in a humidified atmosphere of 5% CO_2. The cells were transfected with empty vector and Human RBM3 ORF cDNA expression plasmid and were cultured in media mentioned above with an additional 1mg/mL G-418 (Santa Cruz Biotechnology) and 1µg/mL puromycin (Life Technologies). For this study, we only used cells with less than 20 passages after receipt or reviving.

The Cancer Genome Atlas Data Analysis

Colon adenocarcinoma (COAD) cohort gene expression RNAseq data from The Cancer genome atlas (TCGA) was downloaded using UALCAN Browser (Chandrashekar et al., 2017) (http://ualcan.path.uab.edu/). The UALCAN browser uses TCGA level 3 RNA-seq and clinical data from 31 cancer types. We used the UALCAN browser to analyze the relative expression of RBM3 gene across colon tumor and normal samples. In addition, we analyzed the expression of the gene in various tumor sub-groups based on individual cancer stages, tumor grade, race, body weight or other clinicopathologic features. All these features were analyzed, and data downloaded for RBM3 gene. Expression levels of RBM3 were designated as transcripts per million in colon adenocarcinoma compared to normal.

Real-time reverse-transcription PCR analysis

To analyze mRNA the expression of RBM3 in patient samples, we purchased a colon

cancer cDNA panel with matched adjacent tissue controls from Origene (Rockville, MD). The cDNA panel was utilized to analyze the abundance of RBM3 in the samples by real-time PCR analysis. The real-time PCR analysis was performed using specific primers for RBM3, JumpStart Taq DNA polymerase (Sigma-Aldrich, St. Louis, MO) and SYBR green nucleic acid stain (Molecular Probes, Eugene, OR). Crossing threshold (Ct) values for individual genes were normalized to GAPDH as an internal standard (ΔCt). Changes in mRNA expression were expressed as fold change relative to control ($\Delta\Delta$Ct).

For gene expression analysis of lncRNA (lnc-HOTAIR, lnc-TUG1, lnc-LSAMP-3 and lnc-Flii-1) and mRNA (VEGFA, ZEB1, SNAI2 AND TWIST1) between vector control and RBM3 overexpressing cells, we first isolated total RNA from cell lines (HCT116, DLD1 and RKO) having both vector control and RBM3 overexpression using TRIzol reagent (Invitrogen, Carlsbad, CA) following manufacturer's instructions. Two µg RNA was used to synthesize complementary DNA using Superscript II reverse transcriptase and random hexanucleotide primers (Invitrogen, Carlsbad, CA). The gene expression for individual genes and lncRNA was quantified by PCR analysis with complementary DNAs by using a premix containing *Taq* DNA Polymerase (Takara, Shiga Prefecture, Japan). The PCR products were resolved on 2% agarose gel and imaged on BioRad ChemiDoc--XRS+ instrument and analyzed by ImageJ software.

We also used quantitative PCR to analyze individual gene expression for VEGFA, ZEB1, SNAI2 AND TWIST1 between the vector control and RBM3 overexpressing cell lines (HCT116, DLD1 and RKO). We used JumpStart Taq DNA polymerase (Sigma-Aldrich, St. Louis, MO) and SYBR green nucleic acid stain (Molecular Probes, Eugene, OR) to perform quantitative PCR analysis. The threshold values for individual genes were

normalized to GAPDH as an internal standard. Changes in mRNA expression were expressed as fold change relative to vector control.

Primers used for the PCR include RBM3, VEGFA, ZEB1, Snai2, TWIST, lnc-HOTAIR, lnc-TUG1, lnc-Flii-1, lnc-LSAMP-3 (Table 2-1).

Western blot analysis

We used the vector control and RBM3 overexpressing cell lines (HCT116, DLD1 and RKO) for western blot analysis. Cells were washed with PBS 3 times and lysed in protein lysis buffer (ThermoFisher Waltham, MA) containing protease inhibitor (Roche, Basel, Switzerland) and sonicated. The resultant lysates were then centrifuged at 6000 rpm for 10 mins. Protein (30–75 µg) was loaded into gels. Cell lysates were subjected to polyacrylamide gel electrophoresis and transferred onto Immobilion polyvinylidene difluoride membranes (Millipore, Bedford, MA). The membranes were then blocked with 5% milk or 5% BSA and probed with antibodies specific to RBM3 (Abcam Cambridge, United Kingdom), VEGFA (Santacruz Dallas, TX), ZEB-1 (Cell Signaling Technology Denver, MA), SNAI2 (Cell Signaling Technology Denver, MA), TWIST (Cell Signaling Technology Denver, MA) and E Cadherin (Cell signaling Denver, MA). The specific proteins were detected by the enhanced chemiluminescence system (GE Health Care, Piscataway, NJ). The protein expression was captured by Bio-Rad ChemiDoc-XRS+ instrument and densitometric analysis was carried out with Image lab software.

Scratch Plate assay

The migration of colon cancer cells was measured using an "*in vitro* wound-healing assay" (or scratch plate assay). We used the vector control and RBM3 overexpressing cell lines (HCT116, DLD1 and RKO) to analyze the effect of RBM3 on cell migration. The

experiment was performed in a 6-well plate (Becton Dickinson). Briefly, the cell lines were seeded at a density of 5 –10 × 10^4 cells per well, grown to near confluent monolayers in DMEM medium with 10% serum-supplemented and then starved overnight in serum-free medium. Perpendicular wounds were scratched through the cell monolayer using a sterile 10 µL pipette tip. The cells were then washed twice very gently using PBS and treated with 10% serum supplemented DMEM. The scratched areas were photographed at 4X or 10X magnification taken every three hours for up to 12 hours on the Cytation3 imaging reader (BioTek) instrument. We measured the area of the scratch at zero hour and 12 hour using ImageJ and the difference in cell movement was calculated. The data was calculated as percent migration for RBM3 overexpressing cells compared to vector control and statistically analyzed. The experiment was repeated three times.

Trans-well migration and invasion assay

Another method to analyze the migration of cancer cell using chemotaxis is the trans-well migration assay. For this assay, we used cell culture insert with an 8-µm pore polyethylene terephthalate membrane (EMD Millipore, Burlington, MA), seated in each well of a 24-well companion plate. We seeded 5 x 10^4 HCT116, 1 x 10^5 DLD1 or 2 x 10^5 RKO cells having vector control or RBM3 overexpression in the upper chamber of an insert in serum-free media and positioned in a 24-well plate containing 10% serum containing media. These plates were placed in a humidified incubator at 37ºC with 5% CO2 for 18 h. After 18h the nonmigratory cells on the upper surface of the insert were removed with a cotton swab. Migrated cells at the bottom of the insert were fixed with formalin and stained with Hoechst dye. For quantification, we randomly selected three fields on the lower side of the insert then these were photographed and quantified using

ImageJ software. The data was calculated as percent migration of RBM3 overexpressing cells compared to vector control and statistically analyzed. The experiment was repeated three times.

To analyze the role of RBM3 in cell invasion we performed Trans-well invasion assay. Matrigel was thawed on ice and diluted in serum-free DMEM in a 1:1 ratio. 50 µl of Matrigel was added to a 24-well transwell insert and kept in a 37ºC incubator for 15-30 minutes to form a thin gel layer. The insert with Matrigel was placed in a 24 well companion plate. We seeded 5 x 10^4 HCT116, 1 x 10^5 DLD1 or 2 x 10^5 RKO cells having vector control or RBM3 overexpression in the upper chamber of an insert in serum-free media and positioned them in a 24-well plate containing 10% serum containing media. These plates were placed in a humidified incubator at 37ºC with 5% CO2 for 18 h. After 18h the noninvasive cells on the upper surface of the insert along with Matrigel were removed with a cotton swab. The cells that invaded through the matrigel at the bottom of the insert were fixed with formalin and stained with Hoechst dye. For quantification, we randomly selected three fields on the lower side of the insert then they were photographed and quantified using ImageJ software. The data was calculated as percent invasion for RBM3 overexpressing cells compared to vector control and statistically analyzed. The experiment was repeated three times.

Tube formation assay

To analyze the ability of RBM3 to contribute towards angiogenesis, we performed a Tube formation assay. We first collected condition media from HCT116, DLD1 and RKO cells having vector control or RBM3 overexpression. For the assay 15,000 HUVEC cells were seeded per well in a 96 well plate on a layer of matrigel (BD Biosciences, Bedford, MA).

The cells were treated with condition media from HCT116 or DLD1, empty vector or RBM3 overexpressing cells. The plates were then incubated in a humidified incubator at 37ºC with 5% CO2 for 6 h. We then imaged each the well under an inverted light microscope. HUVEC cells form a mesh-like network of vessel-like tubules. We then analyzed the images and the tube length was calculated using the angiogenesis counter in ImageJ software. The experiment was repeated three times and measurements were statistically analyzed and plotted as fold change in tube length.

Spheroid assay

The effect of RBM3 on stemness was analyzed using the spheroid formation assay. The HCT116 and DLD1 vector control and RBM3 overexpressing cells were cultured in DMEM supplemented with 20 ng/ml bFGF, 10 mL per 500 mL of 50X B27 supplement and EGF 20 ng/ml (all from Life Technologies), at low densities (HCT116 50 cells/well or DLD1 100 cells/well) in 96 well low adhesion plates. After 5-7 days, the wells were imaged and the number of spheroids per well was determined. The results were plotted as number of spheroids per well between vector control and RBM3 overexpressing cells along with statistics. The experiment was repeated three times.

To assess the propensity of cells to migrate from spheroids, spheroids were transferred to a 96 well attachment plate having serum containing DMEM media. Images of each well were taken on Cytation 3 imaging reader (Biotek) from zero to 24 h, at 4 h intervals. The area of spheroid was calculated at hour zero and 24 h using ImageJ software. The difference in the area between the 24 and zero h time points were calculated and the percent migration relative to empty vector cells was determined. The percent migration of RBM3 overexpressing cells relative to the empty vector was calculated and plotted. The

experiment was repeated three times and cumulative data are was plotted on a bar graph with ± SEM. Make sure to include somewhere how many replicate wells were used per experiment.

Colon cancer xenograft model

Athymic *Foxn1nu* mice were injected with 1×10^6 cells subcutaneously in the flank. Either empty vector or RBM3 overexpressing cells (DLD1 or HCT1), or HCT116 cells stably expressing scramble or RBM3 shRNA were used. The tumors were allowed to grow for three weeks. Tumor volume were measured with calipers weekly and the volume calculated [(length × width^2) × 0.5]. At the end of three weeks, the animals were euthanized, and the tumors were weighed and photographed. For lncRNA knockdown siRNA+LNA gapmer were incorporated into DOPC (1,2-Dioleoyl-*sn*-Glycero-3-Phosphocholine) (Mangala et al., 2009). Xenograft tumors were generated by injecting HCT116 and DLD1 cells (1×10^6 cells) subcutaneously into the flanks of male athymic Foxn1nu mice and housed under specific pathogen-free conditions. Tumors were measured with calipers and the volume calculated [(length × width^2) × 0.5.

Immunohistochemistry

Colon cancer tissue microarray, including primary, metastasis and normal tissue, with associated TNM and clinical stage, and pathology grade was purchased from Biomax (Cat. No. CO702b, 69 cases/69 cores). Paraffin-embedded tumor xenografts were subjected to immunohistochemical analysis. Paraffin-embedded tissues were cut to 4µm sections and deparaffinized followed by antigen retrieval. The tissue sections were blocked with the UltraVision Hydrogen Peroxide block for 10 mins (Thermo Scientific). The slides were incubated with primary antibodies for overnight at 4ºC. were RBM3

(Abcam Abcam Cambridge, United Kingdom), VEGFA (Santacruz), MMP2 (Santacruz Dallas, TX) and E Cadherin (Cell Signaling Technology, Denver, MA). The next day, the primary antibody was washed, and tissues were incubated with HRP Polymer Quanto for 10 mins then developed with a DAB Quanto Chromogen-Substrate mixture. Finally, the slides were counterstained with hematoxylin and eosin. The slides were examined in the Nikon Eclipse Ti microscope under a 20X objective. The TMA slides were scored by pathologist and composite score calculated as (intensity X percent positive cells) along with statistical analysis.

Table 2-1 Primer sequences

No	Name	Forwad primer	Reverse primer
1.	RBM3 (H)	ATGCTCTGGGTTGGTGAAG	TGGGAGGGCTCAACTTTAAC
2.	GAPDH (H)	GGAAGGTGAAGGTCGGAGTCA	GTCATTGATGGCACCAATATCCACT
3.	ZEB1 (H)	AAGAATTCACAGTGGAGAGAAG CCA	CGTTTCTTGCAGTTTGGGCATT
4.	TWIST (H)	GTCTGGAGGATGGAGGG	TCCTTCTCTGGAAACAATGAC
5.	SNAI2 (H)	AACTACAGCGAACTGGACAC	GAGGATCTCTGGTTGTGGTATG
6.	VEGFA (H)	AGCGCAAGAAATCCCGGTA	
7.	RBM3 (M)	GGTGGTGGAGACCAGGGATA	TCTCTAGACCGCAACTACCC
8.	GAPDH (M)	GACTTCAACAGCGACACCCAC	CTCTTCCTCTTGTGCTCTTGC
9.	VEGFA (M)	GTACCTCCACCATGCCAAGT	CACACAGGACGGCTTGAAGA

H: *Homo sapiens*; M: *Mus musculus*

Statistical analyses

Statistics calculations were performed using the GraphPad Prism Software (v. 8.1.2, GraphPad Software, San Diego, CA). Student *t* tests are used to calculate statistical

significance between groups, and data are reported as mean ± standard error of the mean (SEM), unless otherwise noted. Correlation analysis was done using Pearson correlation. Comparison of survival curves was done by Log-Rank (Mantel-cox) test. Non-parametric, Mann-Whitney test was used to assess the significance in tumor volumes and weights, and immunohistochemistry biomarker determinations. Statistical significance between test groups determined by p <0.05. All experiments were validated by two or more biological repeats.

2.3 Results

2.3.1 RBM3 is overexpressed in colon cancer

We evaluated the expression of RBM3 in relation to patients and tumor characteristics. We first analyzed RBM3 mRNA expression using The Cancer Genome Atlas (TCGA) database, which is an extensive database compromising thirty-three different cancers that includes patient tumor sequencing data from various sequencing studies on single platform. We specifically analyzed the database for expression of RBM3 mRNA between colon tumors and normal colon tissue. We observed that RBM3 mRNA levels are

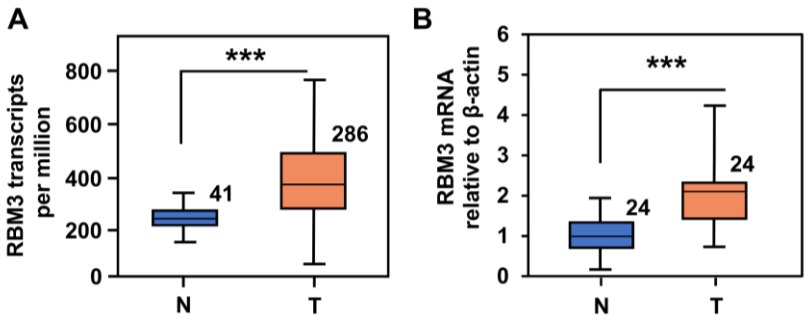

Figure 2-1 Increased RBM3 mRNA expression in colon cancer patient sample
A. The RBM3 mRNA levels in patient samples from The Cancer Genome Atlas (TCGA) database show significantly high expression in colon cancer (T) (n = 286) as compared to normal colon (N) (n = 41) (p<0.001). B. RBM3 mRNA expression of cDNA array consisting colon tumor (T) samples (n=24) normalized to matched adjacent normal colon tissue (N) (n=24) and found RBM3 expression was higher in in tumor tissue (p=0.023).

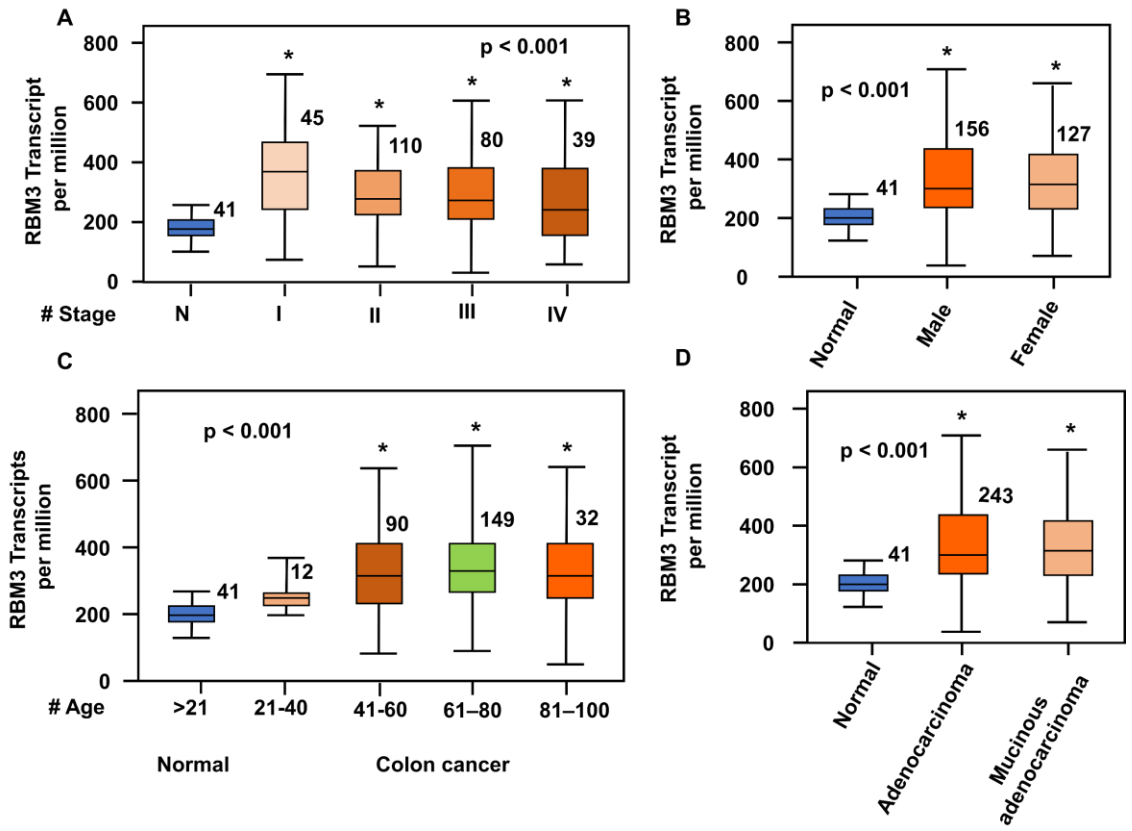

Figure 2-2 RBM3 expression in relation to patients and tumor characteristics
Distribution of RBM3 mRNA levels from TCGA database expressed as transcripts per million in as seen in colon cancer stage (A), gender (B), age (C) and histology (D) in colon cancer patients compared to normal. RBM3 shows no overall increase in the colon cancer tissues irrespective of age, gender, or histology

significantly higher in colon tumor samples (n=286) as compared to normal colon (n=41) ($p<0.001$) (Figure 2-1 A). Furthermore, RBM3 mRNA levels were higher in all stages of cancer compared to normal colon (Figure 2- 2 A). We then analyzed the expression of RBM3 for patient characteristics to find whether expression is affected by age, histology or gender. We found that RBM3 expression shows an overall increase in the colon cancer tissues irrespective of age, gender, or histology (Figure 2-2 A-D). To validate these findings, we also investigated the expression of RBM3 in colon cancer samples with matched adjacent normal colon tissue by performing RT-PCR using a cDNA array (Figure 2-1 B). We found that the RBM3 mRNA expression was higher in colon tumor samples

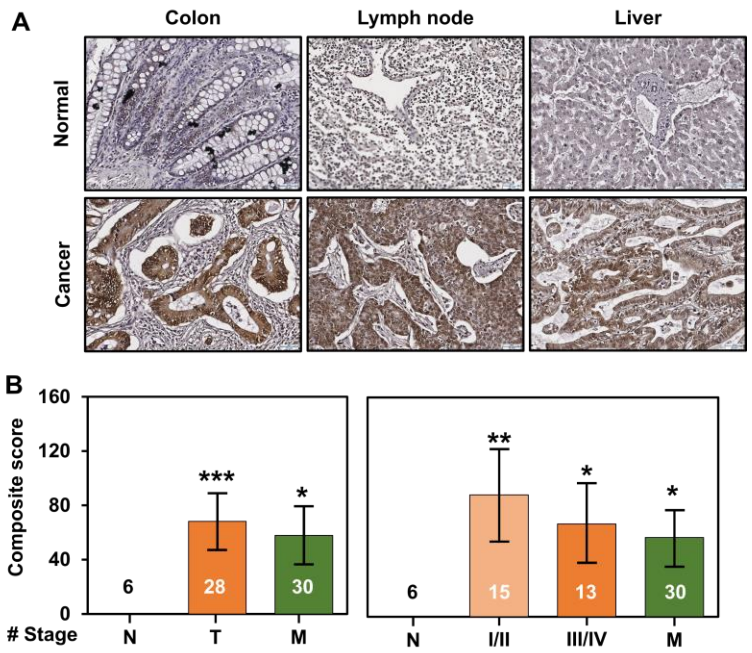

Figure 2-3 RBM3 protein levels is increased in colon cancer patient tissues
A. Immunohistochemistry (IHC) of a colon cancer tumor microarray (TMA) shows that RBM3 is upregulated in colon adenocarcinoma along with lymph node metastasis and liver metastasis as compared to normal colon, lymph node and liver.
B. Composite score of colon cancer TMA shows significantly higher expression of RBM3 in tumor (n=28) (p=0.002) and metastasis (n=30) (p=0.036) as compared to normal tissue. RBM3 expression is also increased in the different stages of colon cancer (Stage I (n = 3), Stage II (n = 12) (p=0.015), Stage III (n= 11) (p=0.07), Stage IV (n = 2) and metastasis (n=30) (p=0.036)) as compared to normal colon, liver and lymph node (n=3 each).

(n=24) compared to adjacent normal colon tissue (p=0.023) in the cDNA array. To characterize RBM3 protein levels, we utilized a tissue microarray (TMA) that included primary adenocarcinoma, metastatic tumor and normal tissue. We performed immunohistochemistry using RBM3 antibody and the expression across the tissues were scored by a board-certified pathologist (Figure 2-3 A). We then calculated the composite score for the tissues and found a significantly higher expression of RBM3 in the primary tumors (n=28, p=0.002) and metastasis (n=30, p=0.036) as compared to normal tissue (n=6). RBM3 expression was also increased in advanced stages of colon cancer, Stage II (n=12, p=0.015), Stage III (n=11, p=0.07) and metastasis (n=30, p=0.036) as compared

to normal (n=6) and Stage I (n=3) tumors (Figure 2-3 B). TMA immunohistochemistry also shows an overall increase in RBM3 levels irrespective of age, gender, or histology (Table 2-1). For *in vitro* studies, we utilized established colon cancer cell lines. We first analyzed the expression of RBM3 in seven colon cancer cell lines compared to a fetal human normal colon epithelial (FHC) cell line. We found by western blot analysis that there was an increased level of RBM3 protein in established colon cancer cell lines as compared to FHC (Figure 2-4 A). To study the role of RBM3, we overexpressed RBM3 in colon cancer cell lines with low to moderate expression of RBM3 (RKO, HCT116, and DLD1), and demonstrate increased RBM3 expression by western blot analyses (Figure 2-4 B). These data establish that RBM3 expression is upregulated in a stage- dependent manner in colon cancer.

2.3.2 RBM3 regulates expression of RNA involved in angiogenesis and EMT

Our laboratory along with others have previously shown than RBM3 is an RNA binding protein that binds to the AU rich element of the 3'UTR of COX-2 mRNA (Cok et al., 2004, Smart et al., 2007b). We have also shown that when overexpressed, RBM3 increases the stability and translation of rapidly degraded mRNAs such as COX-2, VEGFA and IL8(Cok et al., 2004, Smart et al., 2007b). However, comprehensive analyses of transcripts regulated by RBM3 are lacking. To get a better understanding of RBM3 regulation, we took an unbiased approach and performed total RNA-sequencing (RNAseq) and RNA-immunoprecipitation-coupled sequencing (RNA-IP Seq) to identify transcripts targeted by the RBM3.

We performed RNA-seq and RNA-IP Seq on RBM3 overexpressing or empty vector HCT116 and DLD1 cell lines. The differentially expressed RNA between RBM3

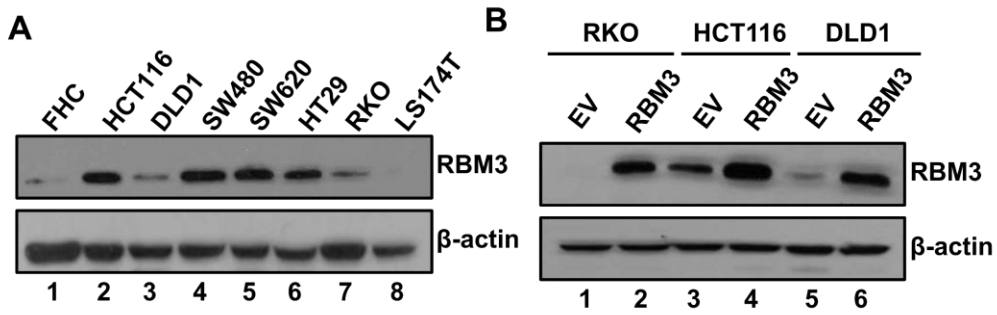

Figure 2-4 RBM3 protein levels are increased in colon cancer cell lines
A. Western blot demonstrates RBM3 expression is increased in established colon cancer cell lines HCT116, DLD1, SW480, SW620, HT29, RKO and LST17T as compared to normal colon epithelial cells (FHC cell line).
B. RBM3 was overexpressed in three colon cancer cell lines (RKO, HCT116 and DLD1) the increased RBM3 expression is demonstrated by western blot analysis.

Table 2-2 RBM3 characteristics from immunohistochemistry of patient tumor microarray

TMA Characteristic		Number (N=70)	P value
Sex	Male	51	0.730
	Female	19	
Age	range	Below 52	0.693
	median	Above 52	
Tumor grade	Normal	10	
	Moderately differentiated	12	0.041
	Well differentiated	22	0.051
	Poorly differentiated	21	0.018
Tumor stage	I	3	0.42
	II	12	0.015
	III	11	0.078
	IV	2	0.344
Metastatic		30	0.032
	liver	5	
	lymph node	25	

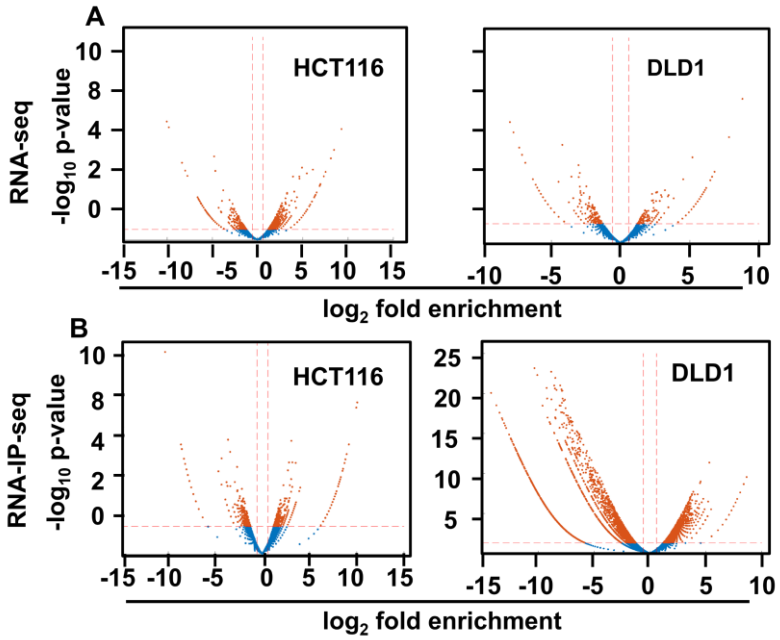

Figure 2-5 Volcano plots showing differential gene expression after RBM3 overexpression
The volcano plots for the differentially expressed mRNAs in both HCT116 and DLD1 RBM3 overexpressing cell lines compared to vector control cell lines are for RNA-sequencing (A) shows differential expression of mRNAs with RBM3 modulation. The volcano plots for RNA-immunoprecipitation-coupled sequencing (B) show that many transcripts were pulled down by RBM3.

overexpressing and empty vector cells were calculated and visualized by volcano plots. HCT116 RBM3 overexpressing cells have 718 upregulated and 715 downregulated lncRNA as compared to empty vector (Figure 2-5 A). The DLD1 RBM3 overexpressing cells showed 551 upregulated and 556 down-regulated RNA as compared to empty vector. The RNA-IP seq showed 368 upregulated and 746 downregulated RNA in HCT116 RBM3 overexpressing cells (Figure 2-5 B). In the DLD1 RBM3 overexpressing cells, there were 2882 upregulated and 1467 downregulated RNA compared to control. The heat plot for the gene body coverage of the RNA-seq across the genome also shows differential expression of RNA within RBM3 overexpressing and empty vector cells (Figure 2-6). We then subjected the RNA-seq and RNA-IP seq data to Ingenuity pathway analysis (IPA). IPA is a web-based bioinformatics application for analysis if high-

throughput experimental data like microarray and next generation sequencing. IPA can perform functional analysis, integration, and help understand data from gene expression experiments. IPA data analysis can help in understanding and interpreting sequencing data for significance, identify specific targets and biomarkers for biological system. We performed IPA analysis on our sequencing data to identify pathways and gene associated with disease that were differentially expressed between vector control and RBM3 overexpressing cells. We found 'Cancer' as the top dysregulated disease in both HCT116 and DLD1 cell line with RBM3 overexpression. We then generated heat plot for disease and function in the IPA for the sequencing data. We found that

We then distributed the upregulated genes according to the classical hallmarks of cancer and we found that RBM3 differentially regulated genes were involved in classical hallmarks of cancer like stemness, tissue invasion and metastasis, sustained angiogenesis, cell survival and viability and pluripotency (Figure 2-7). Therefore, we wanted to analyze the role of RBM3 in tumor progression. Our laboratory has previously shown that RBM3 is a protooncogene involved in cell survival pathway. We also established the role of RBM3 in stemness and showed that RBM3 overexpression causes increase in side-population and spheroid formation by enhancing β-catenin signaling in cells (Venugopal, 2016). Therefore, for this work we focused on cell movement and angiogenesis pathways. To identify which pathways were upregulated by RBM3, we analyzed the sequencing data using Gene Set Enrichment Analysis (GSEA). GSEA is bioinformatics tool used to identify classes of genes or protein from sequencing or other datasets that may be associated with disease phenotype. GSEA analysis helped us find out pathways that were differentially regulated in the sequencing data from RBM3

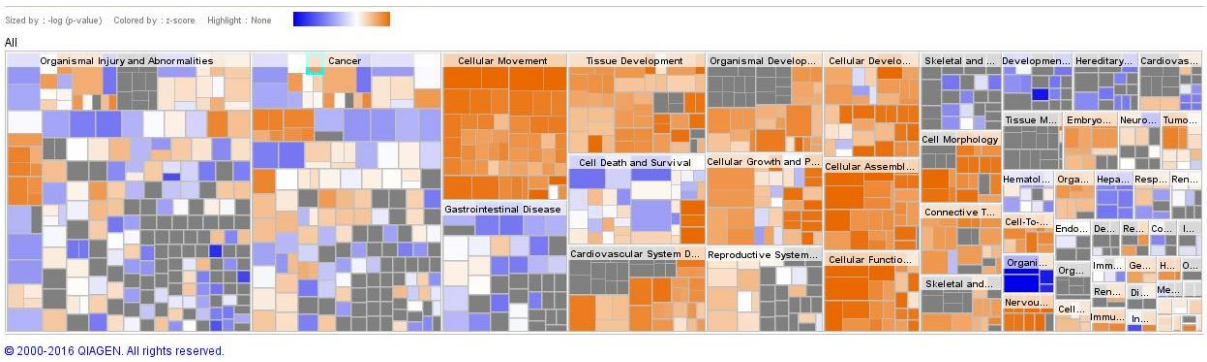

Figure 2-6 Heat plots showing differential gene expression after RBM3 overexpression
The heat plots for the differentially expressed mRNAs involved in cellular processes was generated using the sequencing data in IPA. The size is according to -log(pvalue) and color is according to z-score. Cellular processes like cellular movement, tissue development, cellular assembly and cancer were upregulated with RBM3 overexpression.

overexpressing cells. We focused on the pathways for cell movement and found that the epithelial to mesenchymal transition (EMT) was upregulated (Figure 2-8). We then identified the mRNAs for VEGFA, ZEB1, TWIST1 and SNAI2 (Snail Family Transcriptional Repressor 2) also known as Slug protein involved in cell movement and angiogenesis that were upregulated in RBM3 overexpressing cells. Previous studies have shown that the process of transition to a mesenchymal phenotype from that of an epithelial one is dynamic and occurs during normal embryonic development, tissue regeneration, organ fibrosis, and wound healing (Nieto, 2016). Similarly, EMT plays a significant role during tumor progression especially in metastasis (Moustakas, 2017). We validated the mRNA expression of VEGFA, ZEB1, SNAI2 and TWIST mRNA in HCT116, DLD1 and RKO RBM3 overexpressing cell lines by quantitative PCR. We found increased mRNA expression for VEGFA, ZEB1, SNAI2, and TWIST in RBM3 overexpressing cell lines compared to empty vector (Figure 2-9).

2.3.3 RBM3 induces angiogenesis, growth, migration and invasion in colon cancer cells

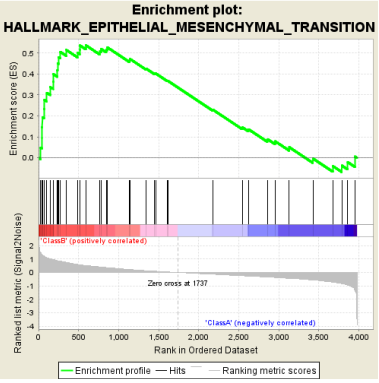

Figure 2-7 Gene Set Enrichment Analysis (GSEA) for RNA sequencing data
GSEA analysis was used to find out pathways that were differentially regulated in the sequencing data from RBM3 overexpressing cells. We found that the epithelial to mesenchymal transition (EMT) pathway was upregulated with RBM3 overexpression.

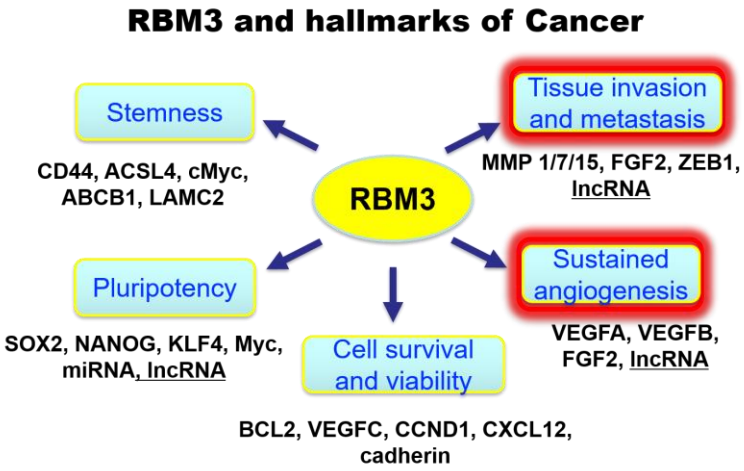

Figure 2-8 RBM3 and hallmarks of cancer.
The genes upregulated in the sequencing analysis were distributed according to the classical hallmarks of cancer and the figure was made. We found that RBM3 differentially regulated genes were involved in all the classical hallmarks of cancer like stemness, tissue invasion and metastasis, sustained angiogenesis, cell survival and viability and pluripotency.

Our laboratory previously reported that RBM3 regulates cancer stem cells but its impact on other hallmarks of cancer remain unknown (Venugopal et al., 2016b). Our sequencing data indicated a role of RBM3 in cell movement and angiogenesis. Therefore, we performed *in vitro* assays to validate the phenotype associated with tumor progression. We first confirmed the effect of RBM3 on stemness by performing spheroid assays for

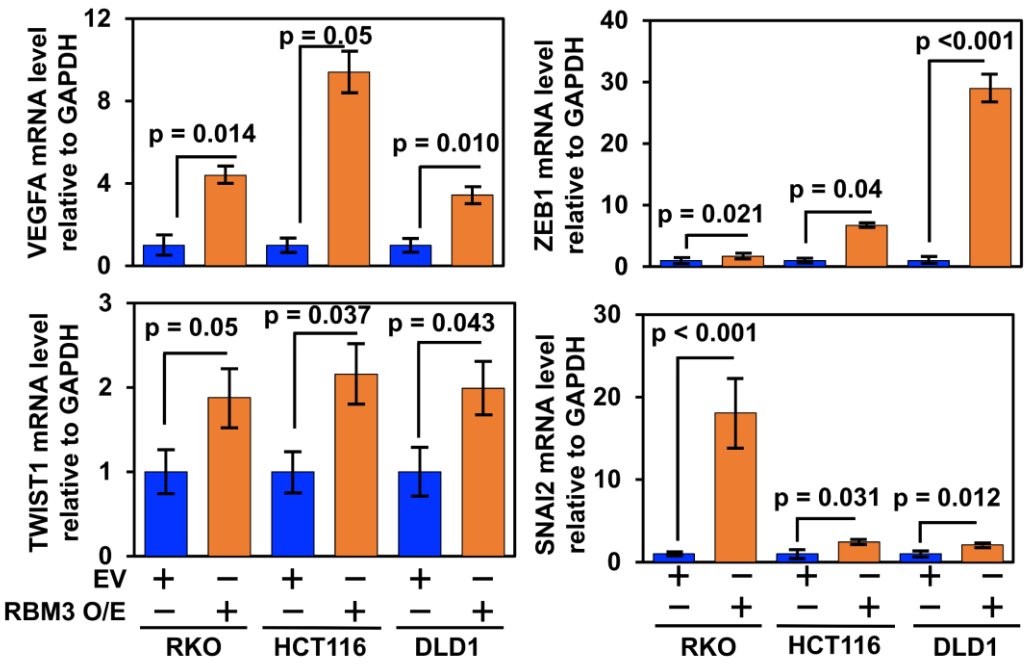

Figure 2-9 RBM3 increases expression of EMT marker genes and VEGFA
Quantitative polymerase chain reaction was for performed for VEGFA, ZEB1, TWIST and SNAI2 in HCT116, DLD1 and RKO RBM3 overexpressing cell lines (orange) compared to vector control (blue). We found that RBM3 overexpression increases expression of EMT marker genes ZEB1, SNAI2, TWIST along with VEGFA.

both HCT116 and DLD1 cell lines overexpressing RBM3. As expected, overexpression of RBM3 induced a significant increase in the number of the spheroids in HCT116 ($p=0.047$) and DLD1 cells ($p<0.01$) (Figure 2-10 A and B).To determine if RBM3 facilitates cell migration in addition to three-dimensional growth, we subjected the spheroids from RBM3 overexpressing or empty vector expressing cells to 2D culture conditions. We found that RBM3 increased the migration of the cells from 3D spheroids (HCT116 $p=0.01$, DLD1 $p=0.02$) (Figure 2.10 C and D).

We also performed two other *in vitro* assays analyzing the effect of RBM3 on cell migration. First, we performed a wound healing assay and found that RBM3 overexpression increased cell migration, as compared to empty vector in RKO ($p=0.001$), HCT116 ($p=0.023$) and DLD1 ($p=0.04$) cell lines (Figure 2.11 A). We then determined the

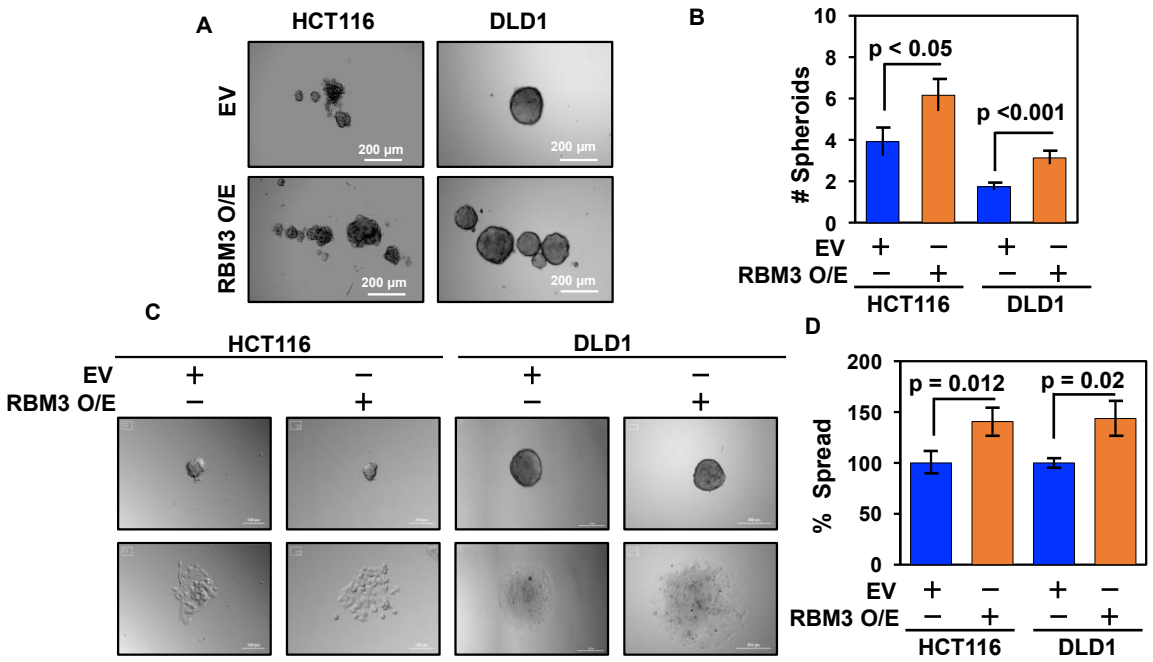

Figure 2-10 RBM3 increases number of spheroid and migration of colon cancer cell lines
A. Representative image of the number of spheroids formed in HCT116 and DLD1 RBM3 overexpressing cells compared to vector control.
B. Plot of the spheroid number shows a significant increase was seen in the of number of spheroids in HCT116 ($p=0.047$) and DLD1 ($p<0.01$) when RBM3 is overexpressed.
C. The spread of migratory cells from the spheroid was assayed. Representative images for HCT116 and DLD1 RBM3 overexpressing cells compared to vector control.
D. Plot for percent spread shows that RBM3 overexpression increases migration from 3D spheroids (HCT116 $p=0.01$, DLD1 $p=0.02$)

effects of RBM3 on migration through a transwell assay using the Boyden transwell chamber. RBM3 increased the migration of cell through transwell chambers in all three cell lines compared to vector control, RKO ($p=0.006$), HCT116 ($p=0.002$) and DLD1 ($p=0.006$) (Figure 2.11 B). We also evaluated the ability of RBM3 overexpressing cells to invade through Matrigel. For this, we used Boyden transwell chambers coated with Matrigel. We found that RBM3 overexpression increased cell invasion through Matrigel compared to vector control in all three cell lines (Figure 2-11 C). These data demonstrate that RBM3 increases colon cancer cell migration and invasion *in vitro*.

To evaluate the role of RBM3 in angiogenesis, we performed the endothelial cell tubule

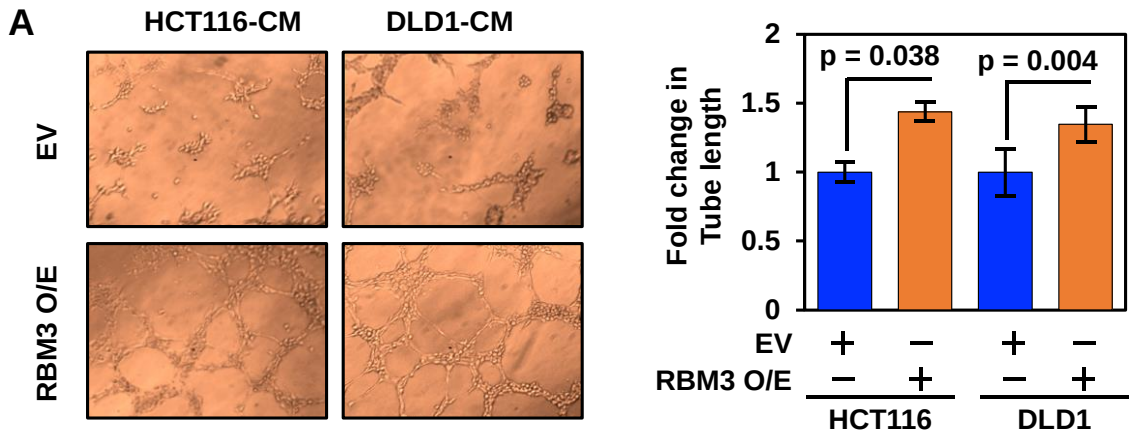

Figure 2-11 RBM3 conditioned media increases tube formation in HUVEC cell line
A. Representative image of the tube formation in HUVEC cell line treated with conditioned media from HCT116 and DLD1 RBM3 overexpressing cells compared to vector control.
B. Plot of the fold change in tube formation shows increase in the tube length in HUVEC cells treated with conditioned media from RBM3 overexpressing (orange) HCT116 (p=0.038) and DLD1 (p=0.004) cell lines compared to vector control (blue), indicating that RBM3 facilitates angiogenic tubule formation.

formation assay. HUVEC cells in Matrigel were incubated with conditioned media from HCT116 or DLD1 RBM3 overexpressing or empty vector cells. The tube mesh network formed by HUVEC cells was imaged after 6 hours. The images were analyzed by ImageJ software to calculate the tube length for HUVEC cells treated with condition media from either vector control or RBM3 overexpressing cells. We observed an increase in the tube length in HUVEC cells treated with conditioned media from RBM3 overexpressing HCT116 (p=0.038) and DLD1 (p=0.004) cell lines, indicating that RBM3 facilitates angiogenic tubule formation (Figure 2.12 A and B). Thus, RBM3 regulates several hallmarks of cancer including anchorage-independent growth, migration, invasion and angiogenesis.

2.3.4 RBM3 overexpression increases tumor growth in the xenograft model

Given the promising results observed *in vitro*, we sought to assess the role of RBM3 on tumor growth in a xenograft model. We inoculated HCT116 and DLD1 cells having vector

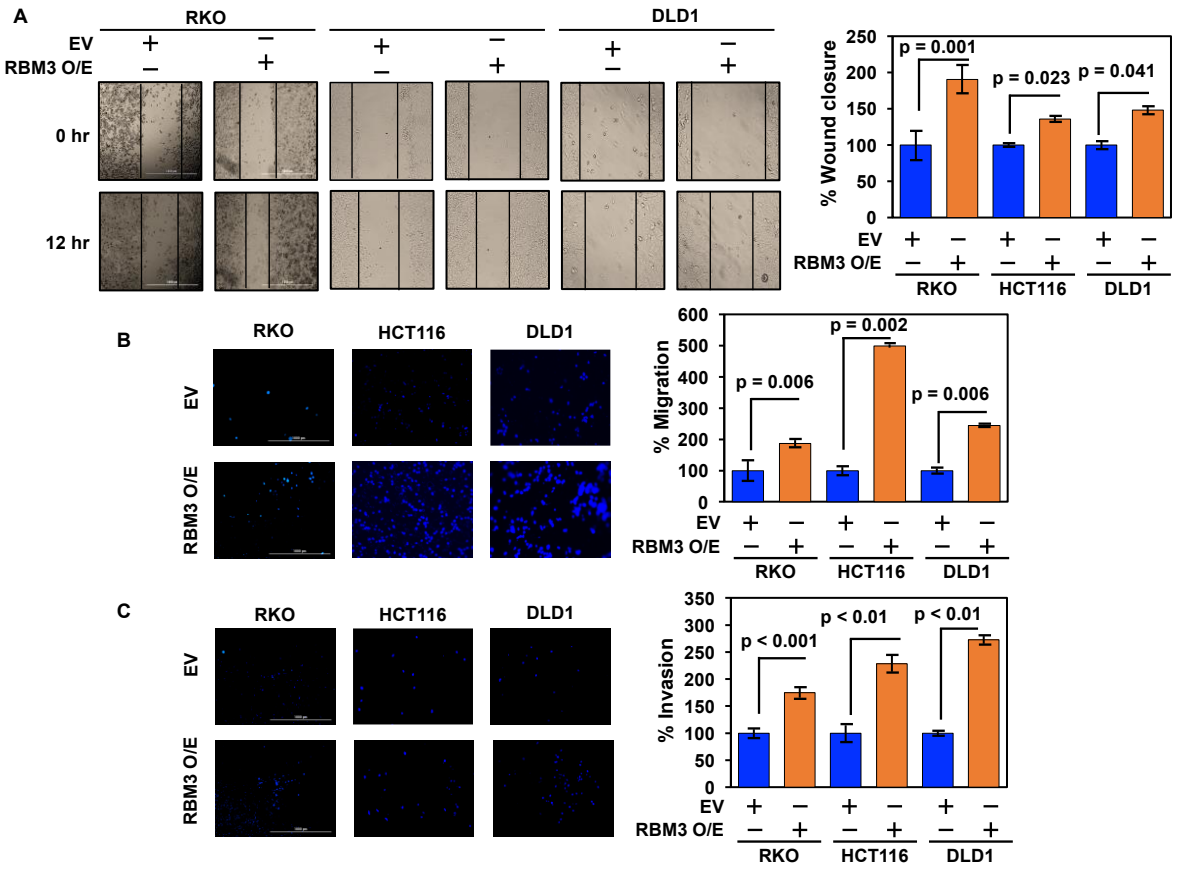

Figure 2-12 RBM3 increases invasion and migration of colon cancer cell lines
A. Representative image of the wound healing assay in HCT116 and DLD1 RBM3 overexpressing cells compared to vector control. On right the plot shows that RBM3 overexpression (orange) increased the migration of cells across the wound in the assay, as compared to empty vector (blue) in RKO (p=0.001), HCT116 (p=0.023) and DLD1 (p=0.04)
B. Representative image of the transwell migration assay in HCT116 and DLD1 RBM3 overexpressing cells compared to vector control. Plot on right shows that RBM3 overexpression increased the migration of cells through Boyden transwell chambers in all three cell lines compared to vector control, RKO (p=0.006), HCT116 (p=0.002) and DLD1 (p=0.006)
C. Representative image of the transwell invasion assay in HCT116 and DLD1 RBM3 overexpressing cells compared to vector control. Plot on right shows that RBM3 overexpression increased the invasion of cells through Matrigel in the transwell chambers, in all three cell lines compared to vector control, RKO (p<0.001), HCT116 (p<0.001) and DLD1 (p<0.01)

control or RBM3 overexpression subcutaneously in athymic nude mice. The xenograft tumors were then monitored for three weeks (Figure 2-13 A). We found that RBM3 overexpression increased the weight and volume of HCT116 (weight p=0.023 and volume p<0.05) and DLD1 (weight p<0.001 and volume p<0.01) xenograft tumors, as compared to empty vector tumors (n=10 per group) (Figure 2-13 B and C). We next

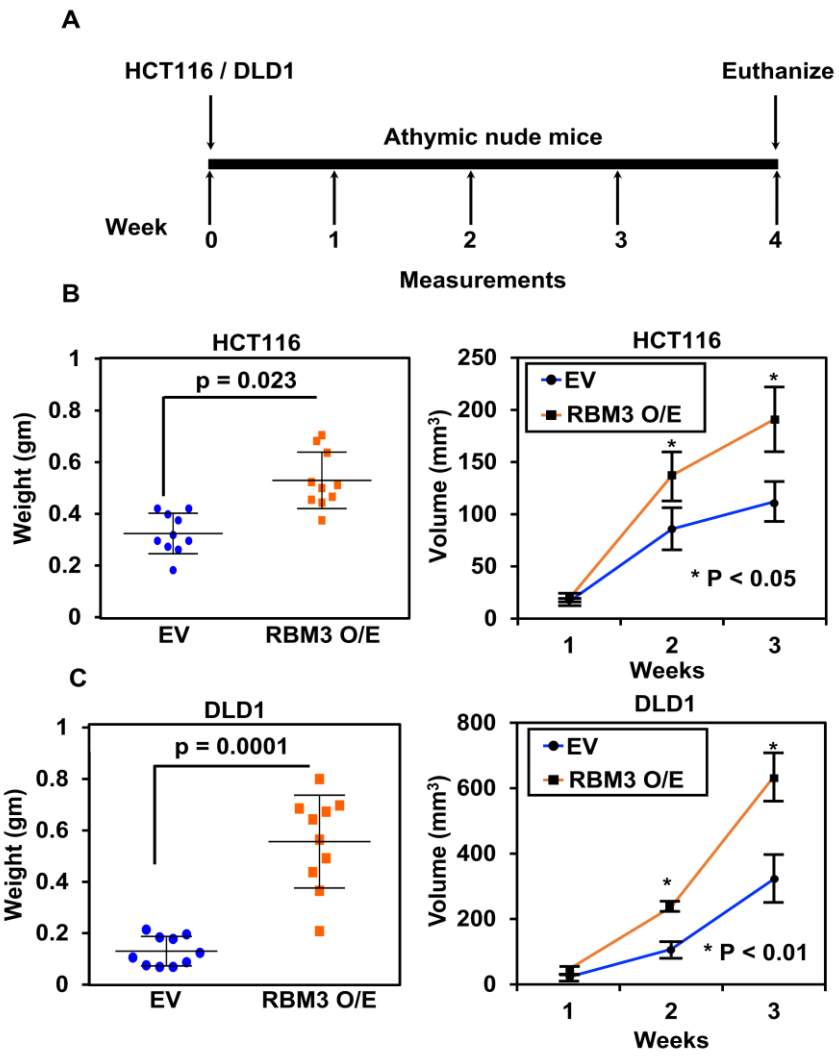

Figure 2-13 RBM3 increases tumor growth in the xenograft model

A. Schematic of xenograft model.

B. Plot for tumor weight and volume for HCT116 xenograft, represented as the means ± SEM (n = 10 for each group). Both tumor weight and volume were significantly increased in RBM3 overexpression (orange) compared to vector control (blue) ($p<0.05$)

C. Plot for tumor weight and volume for DLD1 xenograft, represented as the means ± SEM (n = 10 for each group). Both tumor weight and volume were significantly increased in RBM3 overexpression (orange) compared to vector control (blue) ($p<0.01$)

validated the expression of the mRNAs VEGFA, ZEB1 and TWIST in the tumor xenograft tissues by PCR. The RBM3 overexpressing HCT116 and DLD1 xenografts showed increased expression of mRNA transcripts of angiogenesis and EMT markers, VEGFA, ZEB1 and TWIST, compared to empty vector (Figure 2.14 A). RBM3 overexpressing

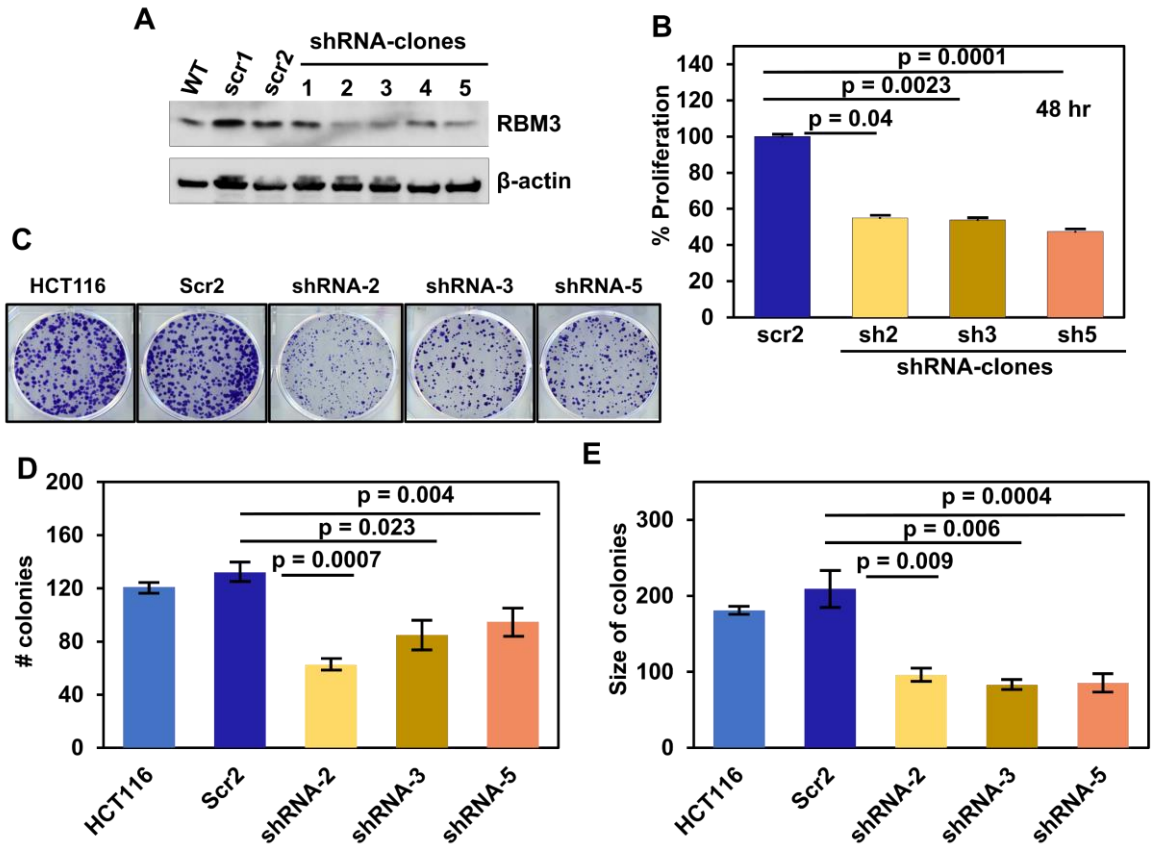

Figure 2-14 RBM3 knockdown decreases growth in colon cancer cell line

A. Western blot showing the knockdown of RBM3 in HCT116 cells.Clones 2,3 and 5 show more than 50% reduction in RBM3 levels.

B. Proliferation assay for HCT116 after RBM3 knockdown shows decrease in proliferation after 48 hours as compared to scramble control sh2 (proliferation= 55.06%) (p=0.04), sh3 (proliferation= 53.8%) (p=0.0023), sh5 (proliferation= 47.45%) (p=0.0001)

C. Representative images for colony formation in HCT116 after RBM3 knockdown

D. Plot for number of colonies shows reduction after RBM3 knockdown sh2 (p=0.0007), sh3 (p=0.023), sh5 (p=0.004) as compared to scramble control.

E. Plot for size of colonies shows reduction after RBM3 knockdown sh2 (p=0.009), sh3 (p=0.006), sh5 (p=0.0004) as compared to scramble control.

tumors also had higher levels of VEGF protein compared to empty vector in both HCT116 and DLD1 xenografts as seen by western blot analysis of the xenograft tumors (Figure 2-14 B). Immunohistochemistry was performed to assess the protein levels of RBM3 along with markers for proliferation (PCNA) and angiogenesis (CD31) on the tumor tissues. We found that the RBM3 overexpressing xenografts expressed higher protein levels of RBM3 and PCNA compared to the empty vector xenografts (Figure 2-

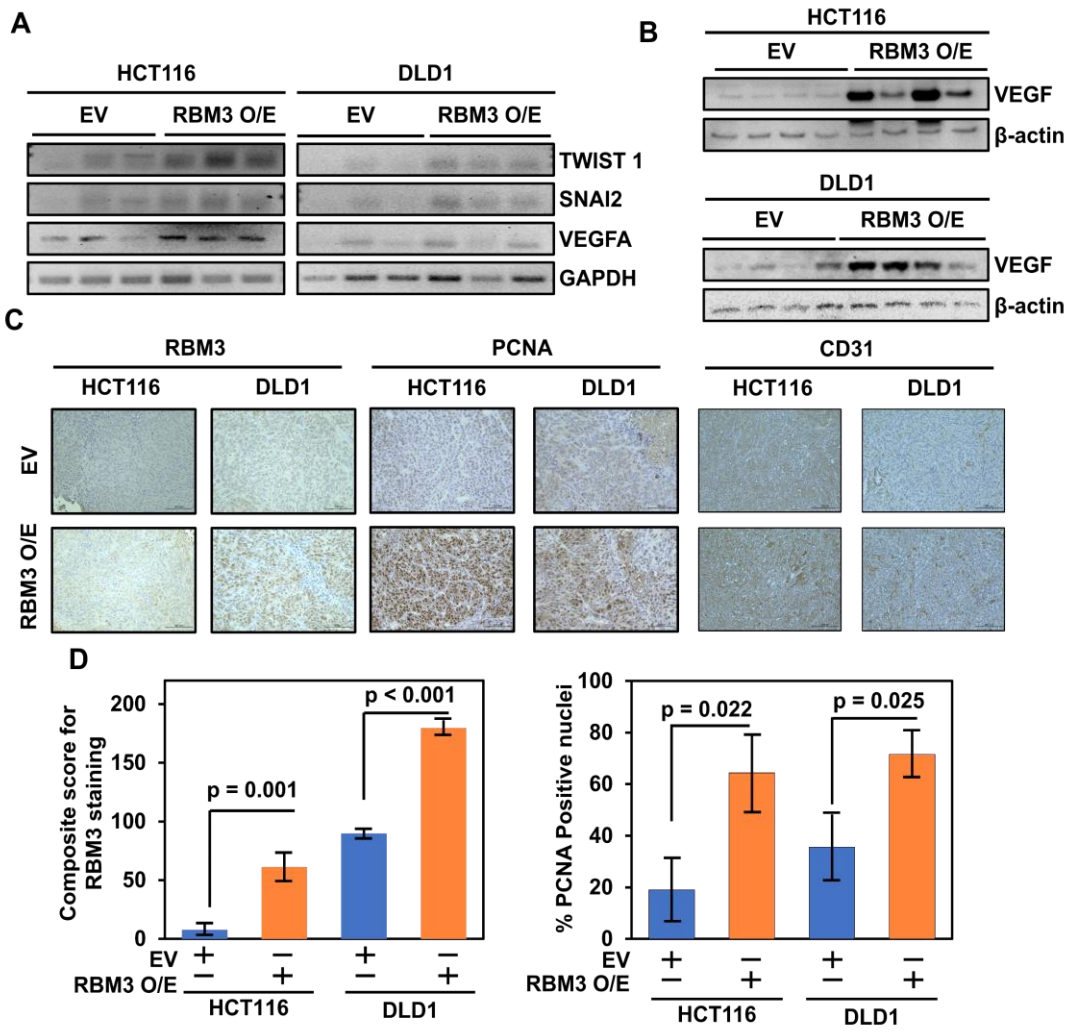

Figure 2-15 RBM3 facilitates tumor growth and increases EMT and angiogenesis

A. PCR and gel for EMT markers TWIST1, SNA2 and VEGFA shows increase in RBM3 overexpressing HCT116 and DLD1 xenograft compared to vector control xenograft.

B. Western blot analysis of tumors from HCT116 and DLD1 xenograft tissues for VEGF expression shows increase in VEGF protein levels in RBM3 overexpressing HCT116 and DLD1 xenograft compared to vector control xenograft.

C. Representative images of immunohistochemistry analysis of RBM3, CD31 and PCNA levels in HCT116 and DLD1 xenograft show increased level of staining in RBM3 overexpressing xenograft tissues as compared to vector control.

D. Composite score shows increased RBM3 levels in HCT116 and DLD1 xenograft overexpressing RBM3 compared to vector control. RBM3 overexpressing xenograft show increased in the percent of PCNA positive nuclei compared to vector control.

14 C and D), CD31 staining was also showed increased vessel density for RBM3

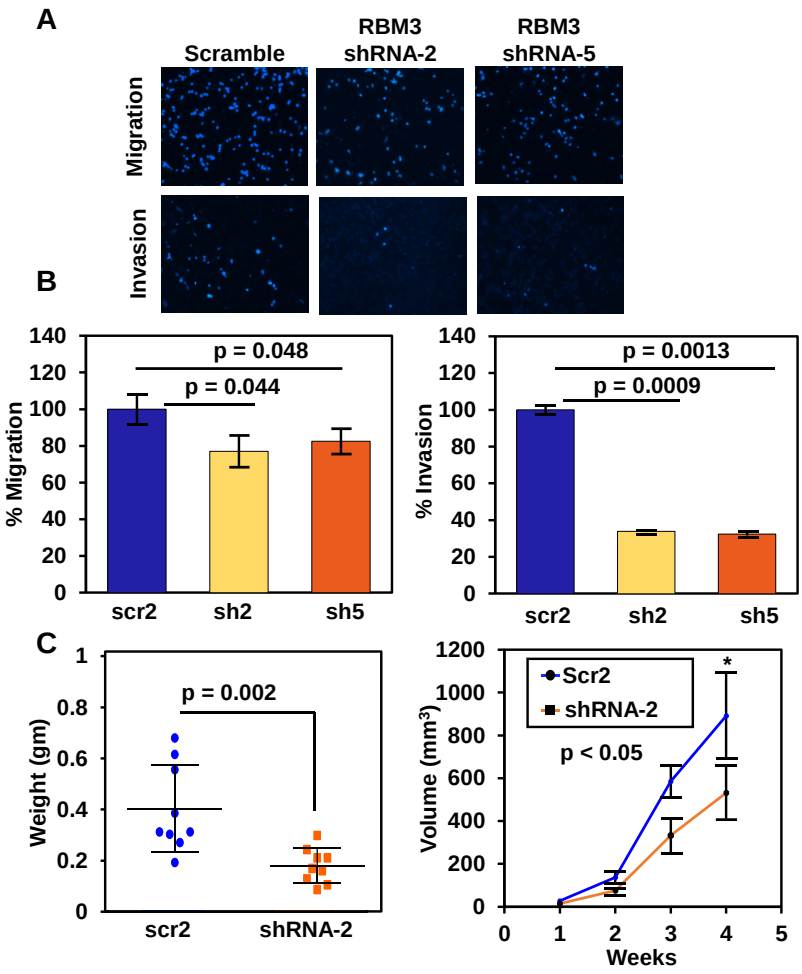

Figure 2-16 RBM3 knockdown decreases migration and xenograft growth in colon cancer cell line

A. Representative images of transwell migration and invasion assay shows decrease in the number of cells migrated and invaded after RBM3 knockdown HCT116 cells.

B. Plot for percent migration and invasion of HCT116 scramble and shRNA knocked shows reduction in invasion (sh2 p=<0.001 and sh5 p=0.001) and migration (sh2 p=.044 and sh5 p=0.048) after RBM3 knockdown.

C. The tumor weight (p=0.002) and volumes (p<0.05) were significantly reduced in RBM3 knockdown xenograft (orange) compared to scramble control xenograft (blue).

overexpressing cells compared to vector control. The data suggest that RBM3 facilitates tumor growth and increases EMT and angiogenesis.

2.3.5 RBM3 knockdown decreases tumor progression *in vitro* and *in vivo*

Having tested the tumor-promoting effects of overexpressing RBM3, we sought to validate these findings by knocking down RBM3 in colon cancer cells. Using shRNA for

RBM3 in the HCT116 cells, we achieved more than 50% reduction in RBM3 protein levels as seen by the western blot analysis (Figure 2.15 A). To validate our previous findings that RBM3 is important for tumor progression, we performed *in vitro* assays for RBM3 knockdown cells. We first assessed the proliferative capacity of the RBM3 shRNA knockdown clones over the scramble control cells. RBM3 shRNA knockdown significantly reduced the proliferation rate of shRNA clones -2, -3 and -5, by close to 50% ($p<0.05$) compared to the scramble controls (Figure 2.15 B). We also assessed the effect of RBM3 knockdown on the colony forming capacity. The shRNA knockdown clones of RBM3 showed a decrease in the number and size of colonies as compared to the scrambled controls (Figure 2.15 C-E). We next validated the role of RBM3 in cell migration and invasion by performing transwell assays. We found that knockdown of RBM3 significantly reduced the migration and invasion of cells (shRNA-2 migration $p=0.04$ and invasion $p<0.001$, and shRNA-5 migration $p=0.04$ and invasion $p=0.001$) (Figure 2.16 A and B). We also evaluated the capacity of RBM3 knockdown to impede tumor xenograft formation. For this we performed subcutaneous injection of scramble and RBM3 knockdown shRNA-2 of HCT116 cells in the flanks of athymic mice. We found that knockdown of RBM3 significantly impaired the increase in tumor weight ($p=0.007$) and volume ($p<0.05$) compared to that of scrambled control tumors (Figure 2.16 C). This corroborates with our data for RBM3 overexpressing cells. Our cumulative data thus demonstrate that RBM3 regulates tumor proliferation, migration and invasion.

2.4 Discussion

RNA binding proteins are important players in post-transcriptional control on mRNAs and have been shown to affect the various hallmarks of cancer leading to tumorigenesis

(Glisovic et al., 2008b). RBM3 is one such protein that is upregulated in several cancers including breast, colon, melanoma, prostrate, astrocytoma, ovarian and plays important role in tumorigenesis (Ehlén et al., 2010, Shaikhibrahim et al., 2013a, Zhang et al., 2013a, Siesing et al., 2017b, Zhou et al., 2017b).

We confirmed the expression of RBM3 in colon cancer by analyzing TCGA data for mRNA expression and patient tumor microarray for RBM3 protein expression. We found both RNA and protein expression of RBM3 is upregulated in a stage-dependent manner in colon cancer. Looking at the patient characteristics we found that RBM3 expression is high irrespective of age, sex and tumor histology. A gold standard RNA binding protein that is well studied is HuR, which has functions similar to RBM3 in that it can also bind and stabilize mRNAs and it is implicated in tumorigenesis for various cancers. However, HuR expression does not seem to significantly change, but rather it may be cytoplasmic localization that determines HuR activity (Denkert, 2006). However, in established cancer cell lines, HuR expression was found to be is varied. For example, HuR was higher in HT29 when compared to LoVo cells (Dixon et al., 2001). Similarly, in breast cancer cell lines, it was reported that MCF7 had five times more mRNA expression than MCF10A and MCF12A (Kotta-Loizou, 2016). RBM3 protein expression is also higher in established cell lines as compared to the fetal human colon normal cell line. However, similar results are seen in cancer tissues, suggesting that unlike HuR, RBM3 expression in cancer cells mirrors that seen cancer tissues. Overexpression of RBM3 did not increase expression of HuR.

An important aspect of RNA binding proteins is that localization dictates their functional role. In colon tissue immunohistochemistry, the expression of HuR is minimal in the

normal crypt but staining for the noeplastic epithelial cells ranges from weak to strong showing a heterogenous expression (Dixon et al., 2001). However, in cancers HuR is present in both the nucleus and the cytoplasm (Dixon et al., 2001). In breast cancer, higher cytoplasmic levels of HuR were observed in MB-231 cells compared to MCF7 cells (Kotta-Loizou et al., 2016). In our current studies, we have also observed that RBM3 is present in both the nuclear and the cytoplasm, suggesting a similar function to HuR in stability and translation.

A controversy does exist on the RBM3 expression and tumor prognosis. High RBM3 protein expression was predicted to have poor prognosis in prostate cancer (Grupp et al., 2018). Similarly, RBM3 enhanced proliferation and carcinogenesis of astrocytoma, resulting in poor prognosis (Zhang et al., 2013a). While these studies correlate well with our observations, others have suggested that RBM3 expression correlates with better prognosis. Indeed, RBM3 expression was found to correlate with good prognosis in several cancers including breast cancer, cisplatin sensitivity in epithelial ovarian cancer, prostate cancer, and colorectal cancers (Jonsson et al., 2011a, Siesing et al., 2017a, Zhou et al., 2017b). However, all these studies were based on immunohistochemistry and only focused on nuclear localization of RBM3. Moreover, several functional studies have demonstrated that overexpression of RBM3 results in increased proliferation and stemness and enhanced drug resistance (Sureban, 2008). It is quite possible that these functions are encoded by cytoplasmic RBM3, which can be missed in studies just looking at immunohistochemical analyses of tissues with antibody that may not have been validated. Nevertheless, studies are required to determine the role of cytoplasmic localization of RBM3 on tumor aggressiveness.

As such a few targets for RBM3 have been validated and RBM3 may bind and stabilize the mRNAs of many other unknown genes that may be important for tumorigenesis. Also, the role of RBM3 in proliferation, survival and stemness has been studied but it can also be involved in other pathways important for tumor progression (Sureban et al., 2008, Venugopal et al., 2016a). Here, we utilized an unbiased approach to find new RNA targets for RBM3 and to evaluate the effect of RBM3 overexpression on the differentially expressed genes (DEGs) involved in signaling pathways important for tumor progression. While genes involved in every aspect of the hallmarks of cancer were found to be upregulated, we chose to focus our studies on a select group of genes involved in tumor angiogenesis and epithelial mesenchymal transition and determine the mechanism by which RBM3 mediated their mRNA translation. There is much more that needs to be done related to the changes in gene expression in response to RBM3 including looking at genes regulating other hallmark pathways, and how all of these together can affect tumor progression and metastasis. Towards this, to get a comprehensive understanding we have begun constructing mouse models, one of which is described later.

Chapter 3 RBM3 induces tumor progression by modulating lncRNAs

3.1 Introduction

LncRNAs are noncoding RNA molecules involved at multiple levels for the regulation of gene expression (Fernandes et al., 2019). They are involved in various cellular processes from chromatin remodeling, transcriptional control, posttranscriptional and translational regulation, enzymatic regulation and signaling. LncRNAs function by binding to RNA, protein and DNA in combination acting as scaffolds, decoys or shuttling molecules (Fernandes et al., 2019). Due to their central role in gene expression, the dysregulation of lncRNAs is involved in various human diseases (DiStefano, 2018). Studies have shown that several lncRNAs are associated with colon cancer, including H19, DANCR, BLACAT1, HOTAIR, Xist, CCAT1, UCA, PCAT1, GAS5 (He et al., 2019a, Kalmár et al., 2019, Siddiqui et al., 2019). These lncRNAs are important for colon cancer cell migration, proliferation and act as biomarkers for prognosis (Bermúdez et al., 2019). Even with these studies, a vast majority of lncRNAs remain largely unknown for their role in colon cancer. RBPs also play an important role in post-transcriptional and translational regulation of the lncRNAs (Xu et al., 2019). Recent high throughput studies evaluating lncRNA-protein interactome have discovered that a large number of RBPs also bind lncRNA (Bierhoff, 2018, Chu and Chang, 2018). The RBP-lncRNA interaction and its role in cancer is still vastly understudied. Some examples of RBP and lncRNA interaction studied in cancer include hnRNPK interactions with lncRNAs lnc-p21, XIST, PTOV1-ASI; HuR interactions with lncRNAs NEAT1, HGBC, lincBRN1a; and hnRNP A2/B1 interactions with lncRNA HOTAIR (Kawasaki et al., 2016, Meredith et al., 2016, Sun et al., 2017b, Hu et al., 2019, Xu et al., 2019). As discussed in the earlier chapter, RNA binding protein RBM3 is a protooncogene that is upregulated in colon cancer and is important for stemness and cell

survival (Sureban et al., 2008). It is involved in the stability and translation of mRNAs, and can affect the biogenesis of miRNA at the DICER step (Pilotte et al., 2011). However, few studies exist on the effect of RBM3 on other noncoding RNAs. Dong et al evaluated the role of RBM3 on circular RNAs (circRNA) in HCC using ribosomal-depleted RNA-seq. They found that several circRNAs were upregulated in HCC compared to normal tissue. They focused on the circRNA SCD-circRNA 2 that is encoded within the stearoyl-CoA desaturase (SCD) gene and its expression predicts poor prognosis in HCC. Their results indicate that RBM3 may be involved in the production of SCD-circRNA 2 and RBM3 promotes the proliferation of HCC through SCD-circRNA 2 (Dong et al., 2019b). A recent study in TNBC evaluated the role of lncRNAs in tumor invasion and proliferation. They found lncRNA LINC00096 increased the proliferation and invasion of TNBC cells by regulation expression of miR-383-5p and in turn RBM3 (Tian et al., 2019). However, the role of RBM3 in lncRNA interaction and regulation has not been evaluated. Therefore, there is a dire need to evaluate the role of both RBM3 and lncRNAs in cancer progression. This study uses an unbiased approach to analyze the lncRNAs modulated by RBM3 and its role in colon cancer progression.

3.2 Materials and Methods

RNA-sequencing and IPA analyses:

RNA from HCT116 and DLD1 empty vector and RBM3 overexpressing cells was extracted and used for immunoprecipitations. To perform RNA-immunoprecipitation, we grew the cells to 90% confluency in 150-mm dishes and then removed the media. Any traces of media were removed using ice-cold phosphate-buffered saline. The lysates were prepared with polysomal lysis buffer which is made up of 100 mmol/L KCl, 25

mmol/L EDTA, 5 mmol/L $MgCl_2$, 10 mmol/L HEPES, pH 7.0, 0.5% Nonidet P-40, 10% glycerol, 2 mmol/L dithiothreitol, 0.4 mmol/L vanadyl ribonucleoside complex, one tablet of complete protease inhibitor (Roche Applied Sciences Penzberg, Germany), and RNaseOUT (Invitrogen Carlsbad, CA). We added 1.5 volumes of the buffer to the cells to lyse them and then centrifuged the mixture. We removed the supernatant and stored lysates at −80ºC. For immunoprecipitation, the supernatant was incubated with Protein A/G Plus Agarose beads (Thermo Fisher Waltham, MA) and incubated overnight at 4ºC with either anti-RBM3 monoclonal antibody (Abcam) or anti-rabbit-IgG-antibody (Cell signaling). The beads that are coated with antibody were resuspended in NT2 buffer supplemented with RNaseOUT, 0.2% vanadyl ribonucleoside complex, 2 mmol/L dithiothreitol, and 25 mmol/L EDTA. We incubated the beads with the cell lysates at 4ºC and ensure that this was constantly mixing for 4 hours. At the end of the incubation, the beads were spun down and washed three times with ice-cold NT2 buffer. Subsequently, we digested the material with proteinase K for 2 hours and extracted the RNA with TRIzol reagent. To assess the quality of the RNA, we used an Agilent 2100 Bioanalyzer (Agilent Technologies, Santa Clara, CA) according to the manufacturer protocol.

For RNA sequencing, we used the method developed by Quick Biology Inc, Pasadena, CA. After the samples passed QC for alignment and gene body coverage, they were used for library preparation, and subsequently subjected to developing sequencing **l**ibraries with the KAPA Stranded RNA-Seq Kit, where we first enrich the mRNA followed by generation of cDNA generation, end repair to generate blunt ends, A-tailing, adaptor ligation, and finally PCR amplification. We used different adaptors were for multiplexing samples in one lane. Finally, we performed sequencing on Illumina

Hiseq3000 for a pair-end 150 run. To check for data quality, we used Illumina SAV. Finally, we performed demultiplexing with Illumina Bcl2fastq 2 v 2.17 program.

Once the sequencing was completed and the data quality was assured, we first mapped the sequences to the latest UCSC transcript set using Bowtie2 version 2.1.0, and used RSEM v1.2.15 to estimate gene expression levels (Li and Dewey, 2011). To normalize gene expression, we use usedTMM (trimmed mean of M-values). To identify differentially expressed genes we used the edgeR program. Only genes showing altered expression with $p < 0.05$ and more than two-fold changes were considered differentially expressed. Subsequently, we performed analyses in the Ingenuity (IPA) pathway and network analysis software to determine the networks according to the fit of the set of supplied focus genes. These scores indicate the likelihood of focus genes to belong to a network versus those obtained by chance. A score > two indicates a ≤ 99% confidence that a focus gene network was not generated by chance alone. The canonical pathways generated by IPA are the most significant for the uploaded data set. Fischer's exact test with the FDR option was used to calculate the significance of the canonical pathway.

The lncRNA transcript sets were downloaded from Lncpedia (Volders et al., 2018) (https://www.lncipedia.org/). The reads were mapped to the Lncpedia transcript set using Bowtie2 version 2.1.0 (Langmead and Salzberg, 2012) and the gene expression level was estimated using RSEM v1.2.15. Trimmed mean of M-values (TMM) were used to normalize the gene expression. Differentially expressed genes were identified using the edgeR program (Robinson et al., 2010). Genes showing altered expression with $p < 0.05$ with a more than two-fold change, were considered differentially expressed.

GO analysis:

The Gene Ontology (GO) terms enriched in lncRNA-seq for HCT116 RBM3 overexpressing cells, compared to control having the lowest over-represented *p* values were analyzed by REVIGO (http://revigo.irb.hr) (Supek et al., 2011). The GO terms that are more closely related circles are in closer proximity. The size of the circle indicates the number of mutated genes. The statistical significance of the enriched GO terms is represented by the color of the circle which is based on the over-represented *p*-value. These GO enrichment terms were also plotted as bar graphs against the p-value.

Lnc-RNA structure and lncRNA-mRNA interaction prediction:

The secondary structure of lncRNA lnc-HOTAIR, lnc-TUG1, lnc-Flii-1, lnc-LSAMP-3 along with the secondary structure of the two IRES in VEGFA mRNA was predicted using RNAfold (Lorenz et al., 2011) (The ViennaRNA Web Services, http://rna.tbi.univie.ac.at/) and illustrated using VARNA GUI. The software calculates the minimum free energy (MEF) for a given RNA sequence. This is the most stable structure for the molecule found in a state of equilibrium. The structure of the lncRNA is colored by the base-pairing probabilities with the unpaired regions colored by the probability of being paired. (Lorenz et al., 2011). Putative interactions between lnc-Flii-1 or lnc-LSAMP-3 with the 5' and 3'UTRs of VEGFA, ZEB1, SNAI2, and TWIST mRNA were determined using IntaRNA (Mann et al., 2017) (http://rna.informatik.uni-freiburg.de/IntaRNA). Hybridization scores for lncRNA-mRNA interaction were calculated using the IntaRNA tool.

siRNA and LNA gapmer transfection

We designed siRNA for lnc-FLii-1 and lnc-LSAMP-3 using the siRNA Design Center (Dharmacon) (Table 3-1). These siRNA was purchased along with Lincode non-targeting

siRNA#1 control from Dharmacon. The LNA gapmers for lnc-FLii-1 and lnc-LSAMP-3 were designed and purchased along with negative control LNA from Qiagen. Transfection was performed using Lipofectamine-2000 (Invitrogen) and OptiMEM according to manufacturer recommendations (Life Technologies). Briefly, cells were plated at 2 $X10^5$ cells per well into 6-well plates and transfected using either a combination of si scramble + LNA scramble or siRNA + LNA for LSAMP-3 or Flii-1. The concentration of siRNA and LNA gapmer used was 200 nM each. Lipofectamine-2000 (Invitrogen) was used as the transfection reagent. Six hours following transfection, cells were washed with PBS and treated with 10% serum containing DMEM. Twenty-four hours following siRNA transfection, cells were then assayed for migration on the scratch plate assay and RT-PCR studies as indicated above. The supernatant was collected 24 hours after transfection for tube formation assay. Each experiment was performed in replicates and each experiment repeated three times. All data plotted was statistically analyzed.

Generating RBM3 overexpressing transgenic mice model

We generated RBM3 overexpressing transgenic mice model by knockin (KI) of the mice RBM3 CDS at ROSA26 locus of in C57BL/6 mice. Cyagen Biosciences INC used CRISPR/Cas-mediated genome engineering to insert the ORF of mice RBM3 under the CMV promoter into the ROSA26 locus. In the knockin mice the “CAG-mouse Rbm3 cDNA-Myc-IRES-mCherry-polyA” cassette was cloned into intron 1 of ROSA26 in reverse direction. To engineer the donor vector, homology arms were generated by PCR using a BAC clone from the C57BL/6J library as a template. Cas9 and gRNA were co-injected into fertilized eggs with donor vector for KI mice production. RBM3 was constitutively expressed by this method in the entire mice. The pups born were then genotyped by PCR

followed by sequencing of PCR product. For experiment littermates or age matched C57BL/6 mice were used. Mice were genotyped before experiments. Western blot analysis for different tissues was done to confirm overexpression of RBM3. The lncRNA expression in the mice tissue was determined by RT-PCR using mice specific primers.

Colon cancer xenograft model

Athymic Foxn1nu mice were injected with 1×10^6 cells subcutaneously in the flank. Either empty vector or RBM3 overexpressing DLD1 or HCT1 cells, or HCT116 cells stably expressing scramble or RBM3 shRNA were used. The tumors were allowed to grow for three weeks. Tumor volume were measured with calipers weekly and the volume calculated [(length × width^2) × 0.5]. At the end of three weeks, the animals were euthanized, and the tumors were weighed and photographed. For lncRNA knockdown siRNA+LNA gapmer were incorporated into DOPC (1,2-Dioleoyl-*sn*-Glycero-3-Phosphocholine) (Mangala et al., 2009). Xenograft tumors were generated by injecting HCT116 and DLD1 cells (1×10^6 cells) subcutaneously into the flanks of male athymic Foxn1nu mice and housed under specific pathogen-free conditions. Tumors were measured with calipers and the volume calculated [(length × width^2) × 0.5]. When tumors reached 150 mm^3, they were injected intratumorally with 25ul (10 µM) siRNA+LNA gapmer on every third day from day 15 for a total of 5 doses. Tumor volume were measured every third day. We included five mice per group and the experiment was repeated thrice. All tumors were excised after four weeks of treatment and photographed; for each tumor, about half of the tumor was frozen in liquid nitrogen and stored at −80°C, and the rest part was fixed with 10% formalin and embedded in paraffin. The tissue protein and RNA were extracted using RIPA buffer and TRIzol

method respectively. The paraffin-embedded tissues were used for immunohistochemical analysis. Tumor volume and weight was plotted and represented as mean±S.E.M.

Table 3-1 siRNA sequence for lncRNA

No	Name	Sequence
1	Lnc-Flii-1 : 1	Sense: 5' GAGGCUUGAGGAUCACACUCUUU 3'
		Antisense: 5' AGAGUGUGAUCCUCAAGCCUCUU 3'
2	Lnc-Flii-1 : 2	Sense: 5' GAUGCUCAGUGGAUCUAUACUUU 3'
		Antisense: 5' AGUAUAGAUCCACUGAGCAUCUU3'
3	Lnc-LSAMP-3 : 1	Sense: 5' GCAGGGACACCUCUGUGAUUAUU 3'
		Antisense: 5' UAAUCACAGAGGUGUCCCUGCUU 3’
4	Lnc-LSAMP-3 : 2	Sense: 5' AUACCUGAAUCCAAAUCUAUGAAAAUU 3'
		Antisense: 5' UUUUCAUAGAUUUGGAUUCAGGUAUUU 3'

Table 3-2 LNA Gapmer sequences

No	Name	Sequence
1	Lnc-Flii-1	5’ ATTTGCACACGCTGAT 3’
2	Lnc-LSAMP-3	5’ GATTGAAGTGTAGTGC 3’

Statistical analyses

Statistical determinations were performed using the GraphPad Prism Software (v. 8.1.2, GraphPad Software, San Diego, CA). Student *t* tests are used to calculate statistical significance between groups, and data are reported as mean ± standard error of the mean (SEM), unless otherwise noted. Correlation analysis was done using Pearson correlation.

Comparison of survival curves was done by Log-Rank (Mantel-cox) test. Non-parametric, Mann-Whitney test was used to assess the significance in tumor volumes and weights, and immunohistochemistry biomarker determinations. Statistical significance between test groups determined by p <0.05. All experiments were validated by two or more biological repeats.

Table 3-3 Primer sequences

No	Name	Forwad primer	Reverse primer
1.	lnc-Flii-1 (H)	GATCACTTGAGGCAAGGAGT	ACTACAACCTCTGCTTCCCC
2.	lnc-LSAMP-3 (H)	CCCTGTCCTCCTGTTCTTTG	GAGGCCGCTTACTGGATTT
3.	lnc-HOTAIR (H)	GGTAGAAAAAGCAACCACGAAGC	ACATAAACCTCTGTCTGTGAGTGCC
4.	lnc-TUG1	AGGTAGAACCTCTATGCATTTTGTG	ACTCTTGCTTCACTACTTCATCCAG
5.	GAPDH (H)	GGAAGGTGAAGGTCGGAGTCA	GTCATTGATGGCACCAATATCCACT
6.	lnc-Flii-1 (M)	ATCCTGACTGAAGAGCCGGA	GGGACCACCAAGCGGAAATA
7.	lnc-LSAMP-3 (M)	CTCCTTCCTCCTGAGCACAA	TATCAGATGCAGGCTGAAAGT
8.	GAPDH (M)	GACTTCAACAGCGACACCCAC	CTCTTCCTCTTGTGCTCTTGC

H: *Homo sapiens*; M: *Mus musculus*

3.3 Results

3.3.1 RBM3 regulates long non-coding RNA expression

RBM3 interacts with mRNAs, and upon binding to the 3'UTR of client mRNA, it can affect the stability and translation of the mRNA (Cok et al., 2004, Smart et al., 2007b). Previous studies have also shown that RBM3 regulates the posttranscriptional biogenesis of miRNA by regulating their association with dicer complexes (Pilotte et al., 2011). Previous studies have also shown that RBM3 can promote HCC cell proliferation by regulating circular RNA SCD-circRNA 2 (Dong, 2019). However, the effect of RBM3 on long non-coding RNA (lncRNA) has not yet been explored. Accordingly, we performed two studies. First, we analyzed the RNA-sequencing (RNA-seq) data generated from RBM3 overexpressing or empty vector control HCT116 and DLD1 cell lines to identify lncRNA differentially regulated by RBM3. We also analyzed the data from the RNA-immunoprecipitation coupled sequencing (RNA-IP seq) studies to identify lncRNAs that interact with RBM3 protein. We then analyzed the lncRNA in both our sequencing datasets. We found differentially expressed lncRNAs between RBM3 overexpressing and empty vector cells, which were then visualized by volcano plots. HCT116 RBM3 overexpressing cells have 718 upregulated and 715 downregulated lncRNA as compared to empty vector. The DLD1 RBM3 overexpressing cells showed 551 upregulated and 556 down regulated lncRNAs as compared to empty vector (Figure 3-1 A). The breakdown of the differentially expressed lncRNAs is depicted in the Venn diagram. The numbers in the Venn diagram represent lncRNAs that are significantly expressed based on an absolute fold-change greater than 1.5 and a p-value less than 0.05. The intersection represents the number of lncRNAs that are similarly expressed

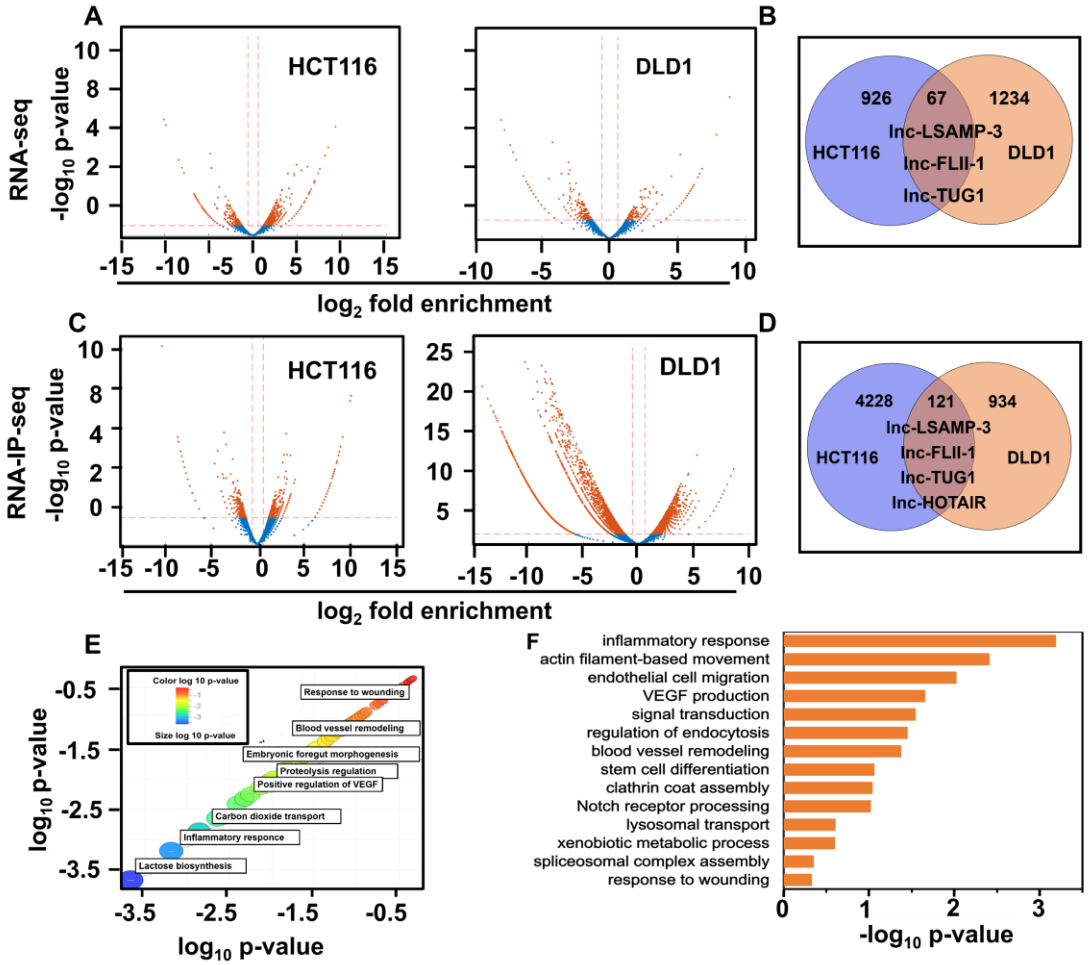

Figure 3-1 RBM3 causes differential expression of lncRNAs

A. Volcano plots (A) for differentially expressed lncRNAs found in RNA-sequencing (RNA seq) for HCT116 and DLD1 RBM3 overexpressing and vector control cell lines.

B. Venn diagram showing the commonly expressed lncRNAs found in RNA-sequencing (RNA seq) found in HCT116 (blue) and DLD1 (orange) from RNA seq. Highlighted are the lncRNAs further examined in the studies.

C. Volcano plots for differentially expressed lncRNAs found in RNA-immunoprecipitation coupled sequencing (RNA-IP seq) for HCT116 and DLD1 RBM3 overexpressing and vector control cell lines.

D. Venn diagram showing the commonly expressed lncRNAs found in RNA-IP seq found in HCT116 (blue) and DLD1 (orange) from RNA seq. Highlighted are the lncRNAs further examined in the studies

E. The sequencing data was evaluated using Gene Ontology (GO) and the different pathways visualized by REVIGO software. The graph shows that RBM3 upregulates lncRNAs involved in important cellular pathways like positive regulation of VEGF and blood vessel remodeling.

F. The sequencing data was evaluated using Gene Ontology (GO) and the different pathways that the lncRNA were involved was plotted against the -log10 p-value. The plot shows lncRNA which were associated with response to wound healing, VEGF production and blood vessel remodeling.

subject to these cutoffs. In the RNA-seq experiment, we found that HCT116 RBM3 overexpressing cells had 926 and DLD1 RBM3 overexpressing had 1234 unique

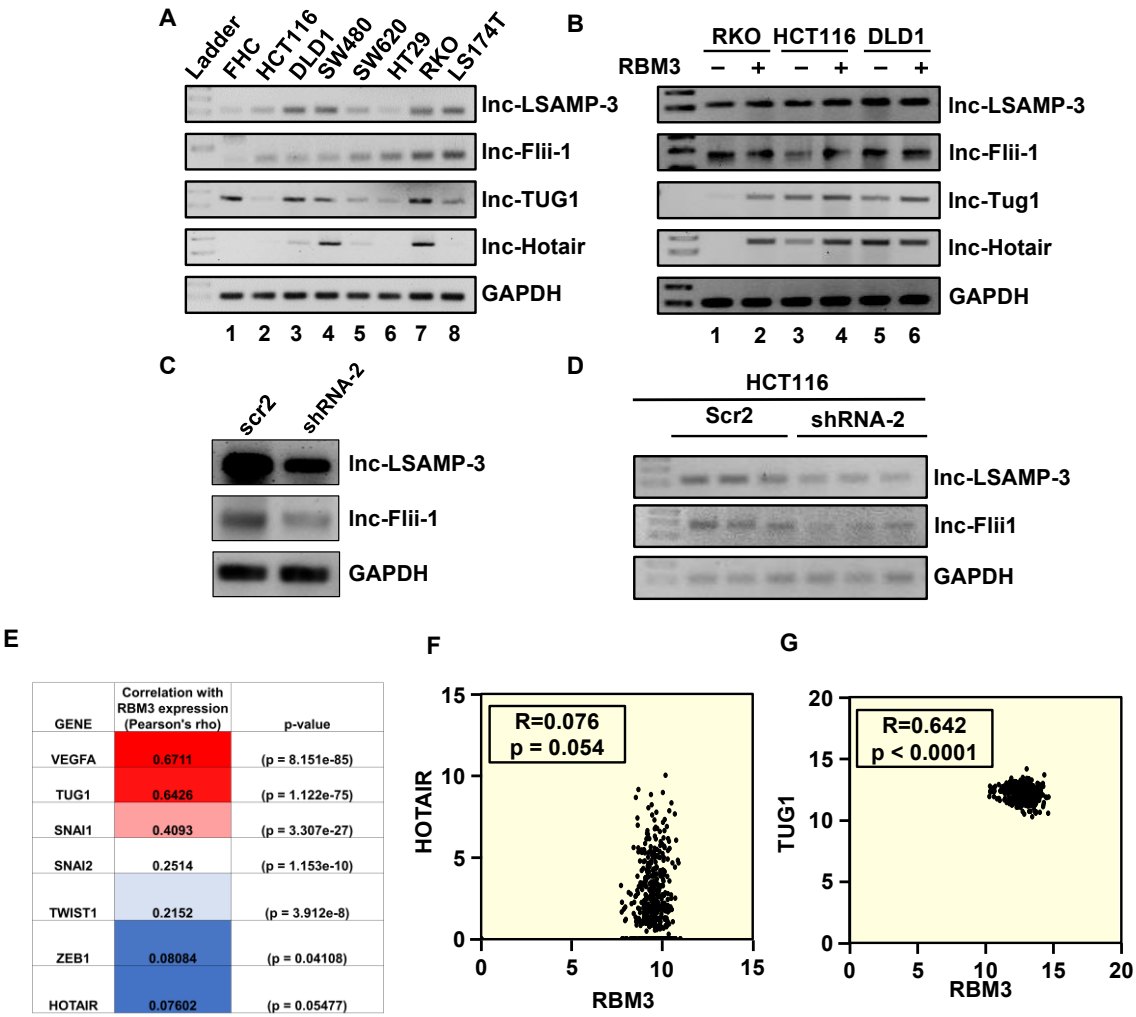

GENE	Correlation with RBM3 expression (Pearson's rho)	p-value
VEGFA	0.6711	(p = 8.151e-85)
TUG1	0.6426	(p = 1.122e-75)
SNAI1	0.4093	(p = 3.307e-27)
SNAI2	0.2514	(p = 1.153e-10)
TWIST1	0.2152	(p = 3.912e-8)
ZEB1	0.08084	(p = 0.04108)
HOTAIR	0.07602	(p = 0.05477)

Figure 3-2 Expression of lncRNA correlates with RBM3
A. PCR for all four lncRNAs (lnc-HOTAIR, lnc-TUG1, lnc-Flii-1, lnc-LSAMP-3) show differential expression in colon cancer cell lines.
B. PCR of the four lncRNA from RNA-seq in the cell lines overexpressing RBM3 (RKO, HCT116 and DLD1) shows increased lncRNA expression with RBM3 overexpression.
C and D. RBM3 knockdown decreases the expression of the lncRNA in HCT116 cells (C) and xenogaft (D).
E. Correlation analysis of RBM3 expression with VEGFA, TUG1, SNAI1, SNAI2, TWIST1, ZEB1, HOTAIR using TCGA database.
F. No significant correlation was found between the expression of RBM3 and HOTAIR using TCGA database
G. Positive correlation between TUG1 and RBM3 expression from TCGA database ($p<0.0001$)

expressed lncRNAs. There were 67 lncRNAs that were co-expressed in both cell lines (Figure 3-1 B).

The RNA-IP seq showed 368 upregulated and 746 downregulated lncRNA in HCT116 RBM3 overexpressing cells. In the DLD1 RBM3 overexpressing cells, there were 2882 upregulated and 1467 downregulated lncRNA compared to control (Figure 3-1 C). The Venn diagram for the RNA-IP seq, showed 4228 unique lncRNA in HCT116 and 934 in the DLD1 cell line, while 121 lncRNAs were co-expressed in both cell lines (Figure 3-1 D). We identified two known (HOTAIR and TUG1) and two novel (lnc-Flii-1 and lnc LSAMP-3) lncRNA, which are highlighted in the Venn diagram. These four lncRNAs were common in RNA-Seq and RNA-IP-Seq to both cell lines (Figure 3-1 B and D). The lncRNAs are both cis and trans acting. Lnc-HOTAIR is antisense, lnc-TUG1 is intergenic, lnc-LSAMP-3 is intergenic and lnc-Flii-1 is antisense. To identify the putative targets of lnc-HOTAIR, lnc-TUG1, lnc-Flii-1 and lnc-LSAMP-3, we used the IntaRNA software to perform *in silico* analysis of mRNA regulating cell movement and angiogenesis found in the RNA-seq. Based on IntaRNA analysis, we found that the lncRNAs lnc-Flii-1 and lnc-LSAMP-3 showed predicted interactions with the 5'UTR and 3'UTR of VEGFA, ZEB1, SNAI2, and TWIST mRNA (Mann et al., 2017) (Table 3.1-3.4). This result gave us promising evidence that RBM3 may regulate the mRNAs through these lncRNAs. We also characterized the secondary structure of the lncRNAs using the RNAfold software (The Vienna RNA Web Services, http://rna.tbi.univie.ac.at/). The software gave us the predicted secondary structure of the lncRNA showing the base pairing probabilities and then highlighted the paired and unpaired regions in the lncRNA. These regions are important for interaction with protein and other RNAs (Appendix Figure 3A) (Lorenz et al., 2011). To annotate the role of lncRNAs in biological functions and diseases, we used Gene Ontology (GO) and LncDisease databases. The LncDisease database is used to

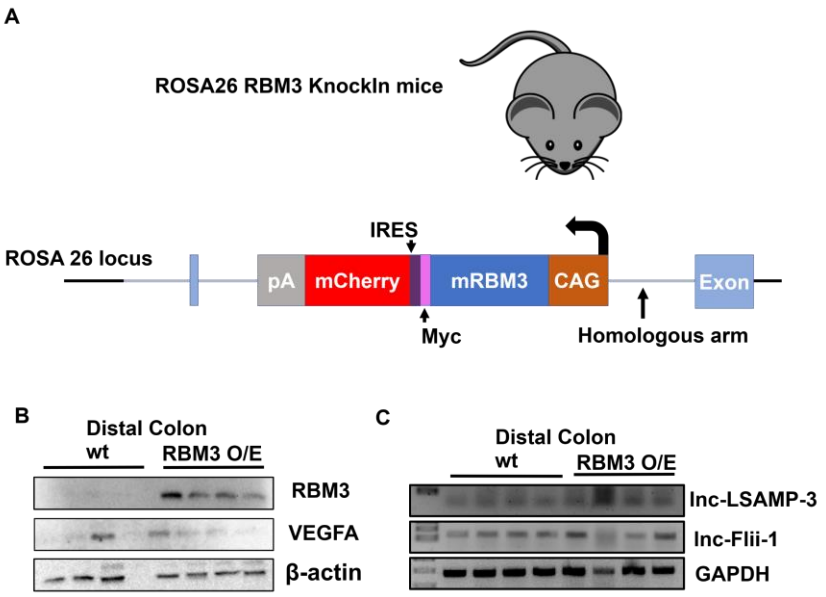

Figure 3-3 LncRNAs are upregulated in RBM3 transgenic mice
A. Schematic for the RBM3 KnockIn mice generation. The "CAG-mouse Rbm3 cDNA-Myc-IRES-mCherry-polyA" cassette was inserted in the ROSA26 locus for a constitutive expression of RBM3. B. Western blot analysis for the expression of RBM3 and VEGFA in the distal colon of the RBM3 transgenic and wild type mice, show increased expression compared to wild type controls.
C. RT-PCR analysis for the lncRNAs lnc-LSAMP-3 and lnc-Flii-1 in the distal colon tissues of the transgenic mice show increased expression compared to wild type mice.

assign the association of lncRNA to the ascribed functions and diseases. The significance of the association of the differentially expressed lncRNA with the functions and diseases was calculated by the database. These GO terms enriched in lncRNA seq for HCT116 RBM3 overexpressing cells compared to control were visualized by REVIGO software (Supek et al., 2011). The REVIGO software provides a graph of GO term and functions for the lncRNA in the sequencing data. The circle size represents the frequency of GO terms and the color scale represents $\log_{10}$ P-value of RNA seq. In analyzing the data for significantly enriched GO terms, we found that RBM3 overexpression caused differential expression of lncRNAs involved in response to wound healing, VEGF production and blood vessel remodeling (Figure 3.1 E and F). This result corroborated

with our previous results showing RBM3 involvement in cell movement and angiogenesis.

We next validated the expression of the lnc-Flii-1, lnc-LSAMP-3, lnc-HOTAIR and lnc-TUG1 in colon cancer and normal colonic epithelial cells. The expression of all four lncRNAs were increased in colon cancer cell lines compared to normal FHC cells (Figure 3-2 A). We also evaluated the expression of the four lncRNAs in RKO, HCT116, and DLD1 RBM3 overexpressing cells and found that their expression increased with RBM3 levels in colon cancer cell lines. (Figure 3.2 B). While knockdown of RBM3 decreased the expression of the lncRNAs. We then sought to determine whether RBM3 levels correlate with the expression of these lncRNA and with the EMT markers evaluated in our studies. We performed correlation analysis of RBM3 expression with VEGFA, SNAI1, SNAI2, TWIST1, ZEB1, TUG1 and HOTAIR using TCGA database. We found that RBM3 expression shows positive correlation with VEGFA, SNAI1, SNAI2, TWIST1 (Figure 3.2 E). We then determined if RBM3 expression correlates with lncRNAs HOTAIR and TUG1 in the patient samples. There was no significant correlation between lnc-HOTAIR and RBM3 levels in interrogating data from TCGA ($R=0.076$, $p=0.054$) (Figure 3-2 F). However, a positive correlation was observed between the expression of RBM3 and lnc-TUG1 ($r=0.64$, $p<0.01$) (Figure 3-2 G). Gene expression data for lnc-Flii-1 and lnc-LSAMP-3 were not available on TCGA for correlation analysis. We also validated the expression of the lncRNAs in the RBM3 knockdown HCT116 cell line and found that the expression of both lnc-Flii-1 and lnc-LSAMP-3 was decreased with RBM3 knockdown in both cell line and the xenograft (Figure 3-2 C-D).

3.3.2 LncRNAs are upregulated in RBM3 transgenic mice

We generated a constitutive RBM3 overexpressing mouse model. In this mouse the RBM3 ORF was inserted into the first exon of the ROSA26 locus for constitutive expression, using the CRISPR/Cas-mediated genome engineering. The “CAG-mouse Rbm3 cDNA-Myc-IRES-mCherry-polyA” cassette was used for robust expression of the protein. The mice were genotyped and RBM3 overexpressing mice were then utilized to detect the expression of RBM3 in the tissues. The distal colon tissue was analyzed for expression of RBM3 and VEGFA by western blot. We found that the RBM3 transgenic mice had elevated level of RBM3 compare to wild type mice in the distal colon. Along with RBM3, the expression of VEGFA was also increased in the colon of the transgenic mice. We then evaluated the expression of the lncRNAs in these tissues by RT-PCR analysis. We found that the distal colon showed an increased expression of both lnc-LSAMP-3 and lnc-Flii-1 in RBM3 transgenic mice compared to wild type (Figure 3-3).

3.3.3 RBM3 regulated lncRNA interact with mRNA involved in angiogenesis and migration

It is well established that lncRNA regulates mRNA at various levels including chromatin remodeling, and transcriptional and post-transcriptional regulation (Wang and Chang, 2011, Mercer and Mattick, 2013). To identify the putative targets of lnc-HOTAIR, lnc-TUG1, lnc-Flii-1 and lnc-LSAMP-3, we used the IntaRNA software to carry out *in silico* analysis of mRNAs regulating cell movement and angiogenesis. We identified predicted interaction of lnc-Flii-1 and lnc-LSAMP-3 with the 5'UTR and 3'UTR of VEGFA, ZEB1, SNAI2, and TWIST mRNA (Mann et al., 2017) (Table 3-1 to 3-4). The table indicates the position of lncRNA and mRNA interaction along with the minimal energy associated with the interaction. The interaction between the lncRNA sequence and the target mRNA

predicted by IntaRNA was also visualized (Appendix Figure 3-2 to 3-5).

Since lncRNAs were predicted to interact with mRNA at the 5'UTR, we determined if there were binding sites for lncRNA on 5'UTR regulatory elements. VEGFA mRNA has several regulatory elements, notable of these are the two Internal Ribosome Entry Sites (IRES) present on the 5'UTR. The two IRES on VEGFA mRNA are the IRES-A which drives the expression of the AUG-initiated forms, and IRES-B which drives expression of the CUG-initiated isoforms and helps in cap-independent translation (Arcondéguy et al., 2013). We determined the predicted structure of IRES-A and IRES-B at the 5'UTR of VEGFA mRNA by RNAfold software. The interactions of the lncRNAs on these structures were then highlighted. We found that the lnc-HOTAIR and lnc-TUG1 showed *in silico* interaction with the IRES-B (Appendix Figure 3A) while lnc-Flii-1, lnc-LSAMP-3 interacted with IRES-A (Appendix Figure 3B).

We also determined whether the lncRNAs interact with 5'UTR of mRNAs that undergo cap-dependent translation. We choose ZEB1 mRNA that does not have any IRES and determined the secondary structure of ZEB1 5'UTR by RNAfold software. We found that both lnc-Flii-1, lnc-LSAMP-3 interact with ZEB1 5'UTR (Appendix Figure 3A) showing that the lncRNAs can bind mRNAs that undergo either cap-dependent or independent translation.

3.3.4 lncRNA knockdown decreases *in vitro* cell migration, angiogenesis and tumor growth

To address the role of lnc-Flii-1 and lnc-LSAMP-3 in RBM3 driven cell migration and angiogenesis, we used a combination of siRNA and locked nucleic acid (LNA) oligomers to knockdown the lncRNAs. The lncRNAs were knocked down in the HCT116 and DLD1

Table 3-4 Predicted interaction of lnc-LSAMP-3 and lnc-Flii-1 with the 5'UTR and 3'UTR of VEGFA.

VEGFA	**IRES/ 5'UTR**			**3'UTR**		
lncRNA	**mRNA 5'UTR**	**lncRNA position**	**DG (Kcal/ mol)**	**mRNA 3'UTR**	**lncRNA position**	**DG (Kcal /mol)**
lnc-LSAMP-3	774 – 815	1723 –1772	-45.2	2452 – 2486	1104 – 1136	-20.4
lnc-Flii-1	767 – 791	290 – 266	-18.8	3022 – 3170	1505 – 1647	-31.5

The table indicates the position of lncRNA and mRNA interaction along with the minimal energy associated with the interaction (DG Kcal/mol).

Table 3-5 Predicted interaction of lnc-LSAMP-3 and lnc-Flii-1 with the 5'UTR and 3'UTR of ZEB1.

ZEB1	**IRES/ 5'UTR**			**3'UTR**		
lncRNA	**mRNA 5'UTR**	**lncRNA position**	**DG (Kcal/ mol)**	**mRNA 3'UTR**	**lncRNA position**	**DG (Kcal/ mol)**
lnc-LSAMP-3	243 – 308	795 – 869	-15.4	3937 – 4074	1643 – 1789	-18.7
lnc-Flii-1	99 – 132	783 – 811	-12.6	5601 – 5631	1066 – 1105	-17.3

The table indicates the position of lncRNA and mRNA interaction along with the minimal energy associated with the interaction (DG Kcal/mol).

Table 3-6 Predicted interaction of lnc-LSAMP-3 and lnc-Flii-1 with the 5'UTR and 3'UTR of SNAI2.

SNAI2	**IRES/ 5'UTR**			**3'UTR**		
lncRNA	**mRNA 5'UTR**	**lncRNA position**	**DG (Kcal/ mol)**	**mRNA 3'UTR**	**lncRNA position**	**DG (Kcal/ mol)**
lnc-LSAMP-3	4 – 34	495 – 525	-14.9	1670 – 1696	1642 – 1697	-21.8
lnc-Flii-1	30 – 70	1611 – 1648	-12.8	1628 – 1622	266 – 292	-21.4

The table indicates the position of lncRNA and mRNA interaction along with the minimal energy associated with the interaction (DG Kcal/mol).

Table 3-7 Predicted interaction of lnc-LSAMP-3 and lnc-Flii-1 with the 5'UTR and 3'UTR of TWIST1.

TWIST1	**IRES/ 5'UTR**			**3'UTR**		
lncRNA	**mRNA 5'UTR**	**lncRNA position**	**DG (Kcal/ mol)**	**mRNA 3'UTR**	**lncRNA position**	**DG (Kcal/ mol)**
lnc-LSAMP-3	279 - 294	515 – 530	-18.8	1023 – 1157	1239 – 1335	-22.9
lnc-Flii-1	132 – 176	1060 – 1102	-21.2	984 – 1220	1604 – 1671	-18.9

The table indicates the position of lncRNA and mRNA interaction along with the minimal energy associated with the interaction (DG Kcal/mol).

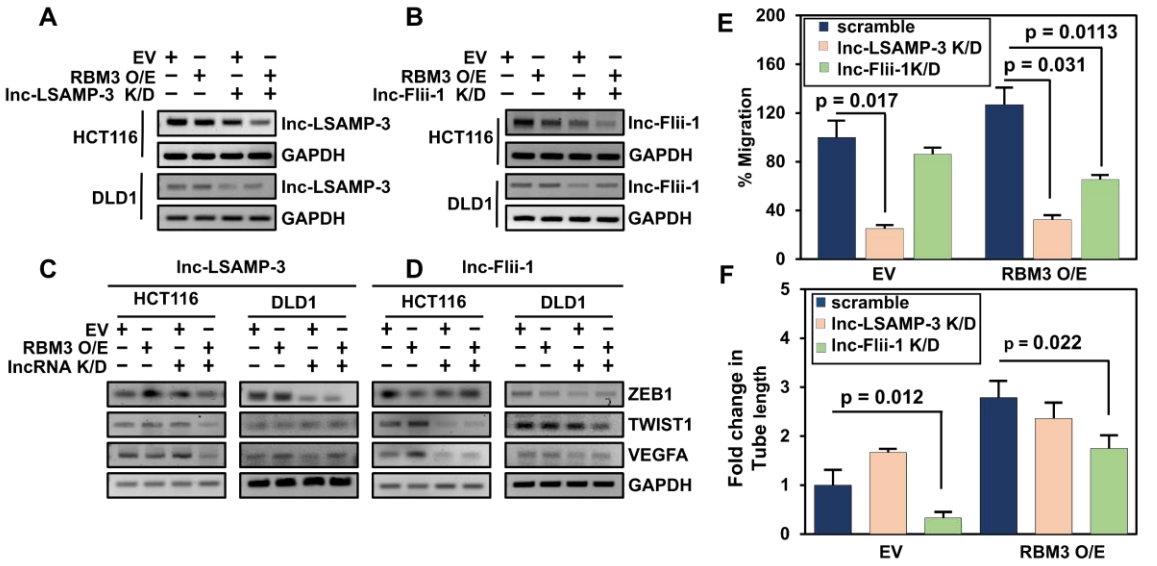

Figure 3-4 RBM3 modulates EMT and angiogenesis through lncRNAs

A and B. Knockdown of lncRNAs (lnc-Flii-1, lnc-LSAMP-3) was performed by combination of siRNA and LNA gapmers and the expression in HCT116 and DLD1 RBM3 overexpressing and vector control cells is shown by PCR analysis.

C. PCR of EMT markers ZEB1, TWIST1 AND VEGFA after the knockdown of lncRNA lnc-LSAMP-3 (C) lnc-Flii-1 (D) shows reduction in their expression.

E. Plot for percent migration of HCT116 vector control and RBM3 overexpressing cells having knock down of lncRNA lnc-LSAMP-3 (orange) and lnc-Flii-1(green). There is reduction in cell movement of cells after lncRNA knockdown.

F. Plot for tube length of the endothelial tubular network formed by HUVEC cell treated by condition media from lncRNA (LSAMP-3 or Flii-1) knockdown in HCT116 vector control and RBM3 overexpressing cells. Knockdown of lnc-Flii-1 shows reduction in tube length.

RBM3 overexpressing and empty vector cells. The extent of lncRNA knockdown was confirmed by RT-PCR (Figure 3-1 A-B). We then evaluated the effect of lncRNA knockdown on the expression of VEGFA, ZEB1 and TWIST. The knockdown for either lncRNA lnc-Flii-1 or lnc-LSAMP-3 attenuated mRNA expression of VEGFA, ZEB1 and TWIST1 in both HCT116 and DLD1 cells despite RBM3 overexpression (Figure 3-2 C-D). We next assessed the role of lncRNA in RBM3-mediated cell movement and angiogenesis. We performed wound closure assays after lncRNA knockdown with siRNA+LNA gapmer for lnc-Flii-1 and lnc-LSAMP-3 respectively in HCT116 RBM3 overexpressing and vector control cells. Knockdown of lnc-LSAMP-3, significantly

reduced migration in empty vector and RBM3 overexpressing cells, while lnc-Flii-1 knockdown had a significant reduction in migration only in the RBM3 overexpressing cells (p=0.0113) (Figure 3-2 E). This may be because the basal level of expression of lnc-Flii-1 is low in vector control cells compared to RBM3 overexpressing cells. We also sought to evaluate the effect of lncRNA knockdown on angiogenesis by treating the endothelial cells (HUVEC) with condition media from lnc-Flii-1 and lnc-LSAMP-3 knockdown cells. Interestingly, RBM3 induced angiogenesis was effectively mitigated by lnc-Flii-1 knockdown (p=0.012) but not lnc-LSAMP-3 knockdown (Figure 3-2 F). RBM3 exerts its tumor-promoting effects through differential use of lncRNA. We next evaluated the role of lnc-LSAMP-3 and lnc-Flii-1 in tumor growth using xenograft model. We first injected HCT116 and DLD1 cells in the flank of athymic nude mice. After the tumor reached 150 mm^3 mice were treated intratumorally with a combination of siRNA and LNA gapmer targeting lnc-LSAMP-3 or lnc-Flii-1. Knockdown of both lnc-LSAMP-3 and lnc-Flii-1 reduced the tumor volume and weight as compared to tumors treated with scramble controls in HCT116 and DLD1 xenografts (Figure 3-5 A-D). We validated the knockdown of lnc-Flii-1 and lnc-LSAMP-3 by PCR and found that the tumors treated with siRNA+LNA gapmer showed decreased expression of lnc-Flii-1 and lnc-LSAMP-3 (Figure 3-5 E-F). We also performed western blot analysis on the tumor tissue to analyze the effect of the knockdown on EMT marker protein Slug and VEGFA. We found that the tumors treated with siRNA+LNA gapmer for lnc-Flii-1 and lnc-LSAMP-3 also showed a corresponding decrease in the protein expression of VEGF and Slug (SNAI2) (Figure 3-5 G-H). This shows that lnc-LSAMP-3 and lnc-Flii-1 regulate colon cancer growth in part through the modulation of angiogenic factor VEGF, and EMT marker SNAI2 (Slug).

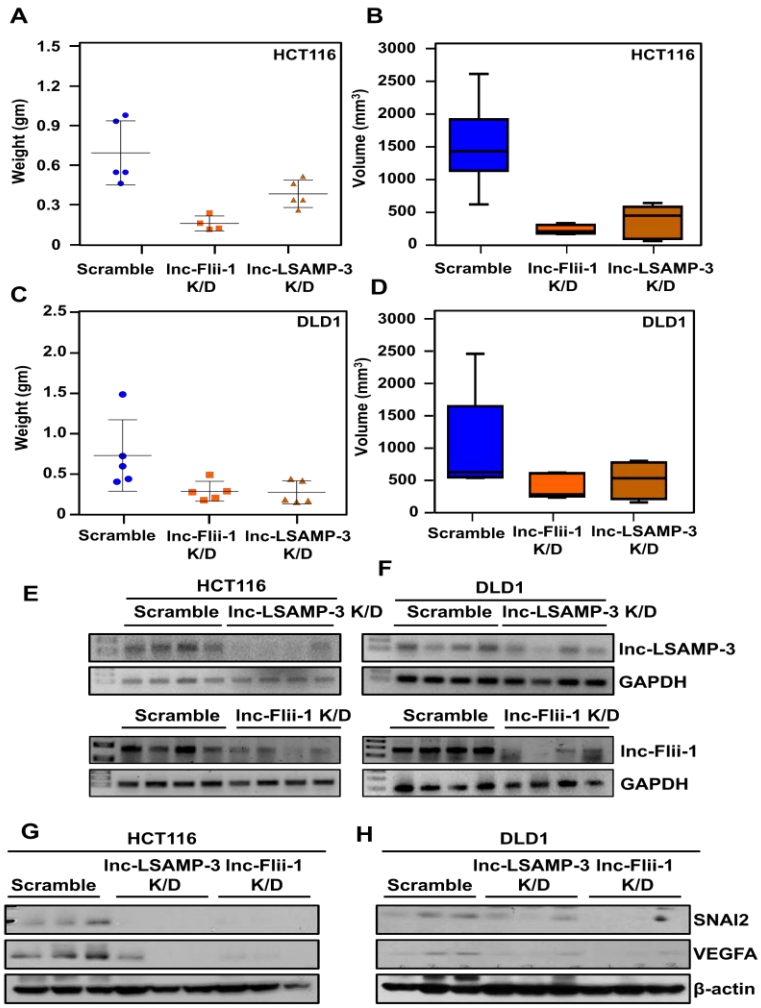

Figure 3-5 LncRNAs knockdown decreases cell growth in xenograft model

A Plot for tumor weight of HCT116 xenograft after intratumoral knockdown of lnc-Flii-1(red), lnc-LSAMP-3 (brown) and scramble control (blue). The result shows reduction in xenograft weight after knockdown of both lncRNAs compared to control.

B. Plot for tumor volume of HCT116 xenograft after intratumoral knockdown of lnc-Flii-1(red), lnc-LSAMP-3 (brown) and scramble control (blue). The result shows reduction in xenograft volume after knockdown of both lncRNAs compared to control.

C. Plot for tumor weight of DLD1 xenograft after intratumoral knockdown of lnc-Flii-1(red), lnc-LSAMP-3 (brown) and scramble control (blue). The result shows reduction in xenograft weight after knockdown of both lncRNAs compared to control.

D. Plot for tumor volume of DLD1 xenograft after intratumoral knockdown of lnc-Flii-1(red), lnc-LSAMP-3 (brown) and scramble control (blue). The result shows reduction in xenograft volume after knockdown of both lncRNAs compared to control.

E and F. PCR confirming the knockdown of lnc-LSAMP-3 and lnc-Flii-1 after treatment with siRNA + LNA Gapmer for each lncRNA, as compared to scramble in HCT116 (E) and DLD1 (F) xenograft.

G and H. Western blot analysis for SNAI2 and VEGFA protein in xenograft after knockdown of lnc-LSAMP-3 and lnc-Flii-1 respectively in HCT116 (G) and DLD1 (H) xenograft. There is reduction in protein expression after lncRNA knockdown as compared to scramble control.

3.4 Discussion

LncRNAs are an important components of the transcriptome and play a central role in controlling various cellular processes (Mongelli et al., 2019). The interaction between RBP and lncRNA is crucial for many post transcriptional functions of lncRNA and is implicated in several cancers (Hu et al., 2019, Liu et al., 2019). This makes it important to study the role of RBP and lncRNA together in cancer. The RNA binding protein HuR has been previously shown to interact with various lncRNAs including NEAT1, HGBC, lincBRN1a, RMST, OIP5-ASI, OCC1. HuR expression was found to positively correlate with that of lnc-HGBC, and that HuR binds lnc-HGBC (Hu et al., 2019). Similarly, HuR was found to bind lncRNA-p2, but this led to the degradation of the lncRNA (Yoon et al., 2012). More importantly, these studies demonstrate that lncRNA and RNA binding protein are collaborative, although the significance of this interaction on tumorigenesis process is not well understood. HuR has been shown to bind and stabilize lncRNA NEAT1 in ovarian cancer cells, and that knockdown of HuR also reduced NEAT1 levels (Chai et al., 2016). This is similar to RBM3 enhancing expression of lnc-Flii-1 and LSAMP3. HuR has also been shown to be a target for lncRNA OCC-1 mediated degradation by the ubiquitination-proteosome system (Lan et al., 2018). However, a lncRNA that targets and degrades RBM3 has not been identified. Identifying one such lncRNA could be of utility in treating cancers where RBM3 is overexpressed. Our studies identified multiple lncRNAs of which, four were of interest because it was observed both in RNA seq and RIP seq. While we focused much of our studies on the two novel lncRNAs lnc-Flii-1, lnc-LSAMP-3, the other two lncRNAs HOTAIR and TUG1 are also interesting. Both HOTAIR and TUG1 have been previously been shown to be involved in stemness and EMT (Zhang

et al., 2014, Tan et al., 2015, Yu and Li, 2015, Xu et al., 2016). Many other studies have also shown these lncRNAs to affect angiogenesis, EMT and stemness in other cancer types (Xu et al., 2013, Xu et al., 2016, Cai et al., 2017, Chen et al., 2017, Lei et al., 2017, Li et al., 2017). Our laboratory has also shown that RBM3 regulates stemness and EMT, and we now show that this is in part due to FLii-1 and LSAMP-3 (Venugopal et al., 2016b). Nevertheless, it would be important to also check the role of HOTAIR and TUG1 in this process.

Collectively, we believe that RBM3 and lncRNAs together facilitate the circularization of mRNA thereby enhancing mRNA translation of transcripts involved in stemness and EMT related mRNAs, thereby leading to tumor progression.

Chapter 4 RBM3 Knockout mice show reduced tumor formation after AOM/DSS treatment

4.1 Introduction

Animal models enable us to study and understand carcinogenesis, biology of tumor and its impact on molecular events (Cheon and Orsulic, 2011a, Yee et al., 2015). Given the promising results observed *in vitro*, we sought to assess the role of RBM3 on tumor initiation and progression in murine models. Two studies are published on RBM3 modulation in murine model mice, both studies have been with RBM3 knockdown mice. Matsuda et al, generated a RBM3 knockout mice (*RBM3*$^{-/-}$) to study the role of RBM3 in immune response and cell growth. They found that RBM3 deficient mice showed no major phenotypic changes and it did not affect the immune cell differentiation. However, they found that the embryonic fibroblasts in these *RBM3*$^{-/-}$mice showed decreased proliferation compared to control MEFs. They inferred the decreased cell proliferation was due to an increase in number of cells in G-2 phase of cell cycle, highlighting the role of RBM3 in cell cycle progression (Matsuda et al., 2011). Xinzhou et al, also generated RBM3 deficient mice to study the role of RBM3 in neurodegenerative disease. They investigated role of RBM3 in cell cycle regulation of the mouse neural stem cells (NSCs) under hypoxic conditions. They found that though RBM3 is expressed in brain under physiological conditions, yet its deficiency did not show any obvious effect on brain development. However, under pathological conditions such as hypoxic ischemia (HI), RBM3 is indisputably important for protection and regeneration of neuron. They showed that RBM3 protected the NSCs from HI-induced apoptosis, while stimulating its proliferation and differentiation. The mechanism by which RBM3 promotes NSPC proliferation after HI is by regulating the IMP2-IGF2 pathway (Zhu et al., 2019).
Our laboratory has previously shown that RBM3 is a novel proto-oncogene that induces

transformation when overexpressed and is essential for cells to progress through mitosis. They showed that NIH3T3 cells stably expressing RBM3 had a significantly higher level of proliferation compared to the wild-type, vector-transfected controls. These cells could also grow in an anchorage-independent manner, a characteristic seen in transformed cells. Moreover, RBM3 overexpression increased the proliferation of already transformed cells such as SW480 colon cancer cells. But overexpressing HuR did not have similar effect showing their roles may be different (Sureban et al., 2008). Even though a lot of studies have been done that show differential RBM3 expression in various cancers, very little is known on the role of RBM3 in cancer initiation or progression. Accordingly, we hypothesized that RBM3 is important for mucosal priming for neoplasia. To test the hypothesis, we established a RBM3 knockout model to study effects on tumor formation. Many mice models including transgenic, knockout, conditional-knockout, or knock-in mice are available to study the involvement of specific genes in development, disease and disorders (Lampreht Tratar et al., 2018). One of the most widely used system for the conditional gene targeting to a specific tissue is the Cre-loxP system (Kim et al., 2018). The system consists of the Cre protein, a site-specific DNA recombinase that recognizes a 34-bp loxP sequence and, in the presence of two directly repeating loxP sites, excises the intervening DNA sequence (Abremski and Hoess, 1984). The loxP site is made up of an 8-bp nonpalindromic core region flanked by two 13-bp inverted repeats (Sauer and Henderson, 1988). Cre-loxP system has been used for studying the function of tumor suppressor genes and oncogenes that can be mutated or activated in a spatial and temporal manner (Kim et al., 2018). We performed knockout of RBM3 gene expression by introducing the lox sites in the mice RBM3 gene. The mice RBM3 gene has seven

exons and is located at the X chromosome the start codon is on exon 2 and stop codon on exon 6. The lox sites were introduced in the mice C57BL/6 ES cells, spanning exon 2-6 for completely deleting the coding sequence of the gene. To achieve conditional knockout, we then crossed these mice with C57BL/6 mice having CDX2-Cre/ERT2. The Cre recombinase in the CDX2-Cre/ERT2 mice will be under the promoter for CDX2 gene and will be expressed only after tamoxifen treatment. The Caudal type homeo box 2 (CDX2) promoter/enhancer sequence is used for directing expression of Cre recombinase predominantly to colonic epithelium during late gestation and in adult tissues (Xue et al., 2010). Using CDX2 as promoter we can get the Cre recombinase expression in epithelium from the distal ileum and cecum, and throughout the colon from the crypt base to the luminal surface. Cre recombinase is also observed throughout the caudal region of the embryo during early development (Xue et al., 2010). The fusion gene CreERT2 combines Cre recombinase fused to ligand binding domain of a human estrogen receptor. This restricts the Cre recombinase to the cytoplasm and the Cre-ERT2 can transfer to the nucleus after tamoxifen treatment (Maitra et al., 2019). Breeding these mice to the loxP-flanked RBM3 mice will result in a tamoxifen induced deletion of RBM3 floxed exon and finally RBM3 knockdown in colon. We will also generate RBM3 overexpressing transgenic mice model having RBM3 overexpression by knockin (KI) of RBM3 CDS at ROSA26 locus of in C57BL/6 mice.

To study the effect of RBM3 on colon cancer initiation and progression we then subjected the RBM3 knockout mice to chemically induced carcinogen. Several chemicals have been used to mimic the sporadic colon cancer model in mice. These chemically induced colon cancer models have several advantages in that they are rapid, reproducible and

mimic the events of human colon carcinogenesis (Rosenberg et al., 2009). Several carcinogens are available for colon cancer model example methylazoxymethanol (MAM), azoxymethane (AOM) and 1,2-dimethylhydrazine; aromatic amines like, 3,2′-dimethyl-4-aminobiphenyl; heterocyclic amines, like 2-amino-33-methylimidazo[4,5-f] quinoline and 2-amino-1-methyl-6-phenylimidazo[4,5-b]pyridine (Rosenberg et al., 2009, Nandan and Yang, 2010). One of the most frequently used models for colon carcinogenesis is the colitis associated AOM/DSS model. It utilizes a single dose of azoxymethane (AOM) causing DNA damage followed by several rounds of dextran sodium sulfate (DSS) causing colitis (De Robertis et al., 2011, Parang et al., 2016).

DSS is a heparin-like polysaccharide that can induce colitis in mice mimicking features of inflammatory bowel disease (IBD) (De Robertis et al., 2011). DSS is given to mice in three rounds dissolved in the drinking water and it acts by damaging the colonic epithelial (Parang et al., 2016). AOM is given as a single dose of nearly 10 mg/kg body weight. AOM is an alkylating agent that is metabolized by cytochrome p450 (CYP2E1) and concerted to highly reactive methylazocymethanol (MAM). MAM is excreted through bile and taken up by colonic epithelial where it can induce mutagenesis by O6 methylguanine adducts in DNA resulting in G→A transitions (Thaker et al., 2012). The tumors formed by the AOM/DSS model can recapitulate human colon cancer pathogenesis. These tumors are formed mostly in the distal colon, start from polyp and are histopathologically similar to human CRC. One major drawback of this model is the lack of mucosal invasion seen by the tumors hence, it cannot be used for metastasis model (Boivin et al., 2003). Tumors induced in mice exposed to AOM/DSS treatment accurately recapitulate the pathogenesis observed in human CRC. For example, tumors are very frequent in the

distal part of the colon, which is also the predominant location of spontaneous CRC in man. They often start with a polypoid growth and frequently exhibit histopathological features like human CRC. However, AOM-induced tumors often lack mucosal invasiveness (Boivin et al., 2003, De Robertis et al., 2011). AOM/DSS-induced tumors frequently mimic the mutation found in CRC, they have high frequency mutations in β-catenin and K-Ras but low frequency of mutation in APC and rarely any mutations in p53 gene. The tumors also have high levels of enzymes like nitric oxide synthase and COX-2 that are involved in nitric oxide synthesis and prostaglandin. They also exhibit microsatellite instability resulting from defective mismatch repair (MMR) (De Robertis et al., 2011). This makes it a good model to study the role of RBM3 in colon carcinogenesis.

4.2 Materials and methods

Generating RBM3 knockout mice

The RBM3 cre-inducible knockout mice were created from Cyagen Biosciences INC. The mouse RBM3 gene (NCBI Reference Sequence: NM_016809.6; Ensembl: ENSMUSG00000031167) is located on the X chromosome and has seven exons. The ATG start codon is present in exon 2 and the TGA stop codon in exon 6 (Transcript: RBM3-005 ENSMUST00000040010). Exons 2~6 were selected as the conditional knockout region (cKO) where the loxP sites was introduced. To engineer the targeting vector, homology arms and cKO region was generated by PCR using BAC clone RP23-224M4 and RP23-77B24 from the C57BL/6J library as a template. The floxed cassette was then inserted into ES cells generated from C57BL/6 mice. Genomic integration of the cassette was assessed by PCR using specific primers. The mice obtained from having the flox site at RBM3 gene were then used for further studies. To obtain colon specific

knockout of RBM3 (intRBM3KO), the RBM3 floxed mice were crossed with CDX2-Cre/ERT2. The progeny was again genotyped for both presence of flox site and CDX2-Cre recombinase by tail-tip biopsies. The mice containing both the floxed RBM3 gene and CDX2-Cre/ERT2 were the used for the experiments. Tamoxifen at a dose of 40mg/kg body weight was given by IP injections daily for 5 days to induce RBM3 knockout.This was confirmed by PCR. For AOM/DSS experiments, littermates or age matched C57BL/6 mice were used.

AOM/DSS model in RBM3 knockout mice

Six to 8-week-old intRBM3KO mice and age-matched wild type C57BL/6 controls were used for experimental and control groups, respectively. The weight of the mice was recorded on Day 0 and each mouse was injected intraperitoneally (IP) with 10 mg/kg of AOM working solution (1 mg/ml in isotonic saline, diluted from 10 mg/ml stock solution in dH2O kept at -20ºC). On day 7, DSS (2.5%) solution was supplied to mice as their drinking water for 5 days (Approximately 250 ml/cage). DSS solution was replaced in clean bottles three times (every 2-3 days) during this period. On day 14, the cages were switched back to standard drinking water for two weeks. This cycle was repeated on days 28 and 49. A DSS "cycle" consists of one week of DSS in the drinking water followed by 2 weeks of regular (autoclaved) water. The mice were euthanized after 24 weeks from the start of the study. AOM/DSS can cause other disease symptoms like blood in feces, diarrhea, rectal prolapse and dehydration (Seamons et al., 2013). Animals were monitored for these symptoms and euthanized when disease symptoms were severe. DSS-induces colitis damages the distal colon; therefore, the entire colon was assessed for tumor burden. The gross tumor burden was recorded, and tumors were photographed

and excised, about half of the tumor was frozen in liquid nitrogen and stored at −80℃, and the rest was fixed with 10% formalin and embedded in paraffin. The tissue protein and RNA were extracted using RIPA buffer and TRIzol method, respectively. The paraffin-embedded tissues were used for immunohistochemistry analysis. As the lncRNAs in human and mice are not same. We looked for orthologs and made primes for those.

We also assayed the gut permeability after the AOM/DSS treatment at the end of the study. Briefly, 200μl of 4kD FITC-dextran at a concentration of 600mg/kg body weight was given by gavage to mice and after 4 hours blood was collected. The serum concentration of the FITC-dextran was then determined using a fluorimeter with an excitation wavelength at 490 nm and an emission wavelength of 530 nm. The concentration of FITC-dextran was calculated from the standard curve of serially diluted FITC-dextran. The intestinal permeability is represented as the concentration of serum FITC-dextran (Wang et al., 2015a, Woting and Blaut, 2018).

Table 4-1 Genotyping primers

No	Name	Primer sequence
1.	RBM3 Knockout mice	F: AGGCACTCAGGATTATTGTTTCTGGC R:CTTCCTGACTTGCCTCTCGCTCTA

4.3 Results

4.3.1 Generating RBM3 knock out mice

We previously reported the malignant transformation of NIH-3T3 cells caused by RBM3 overexpression (Sureban et al., 2008). Our *in vitro* results show that RBM3 increases

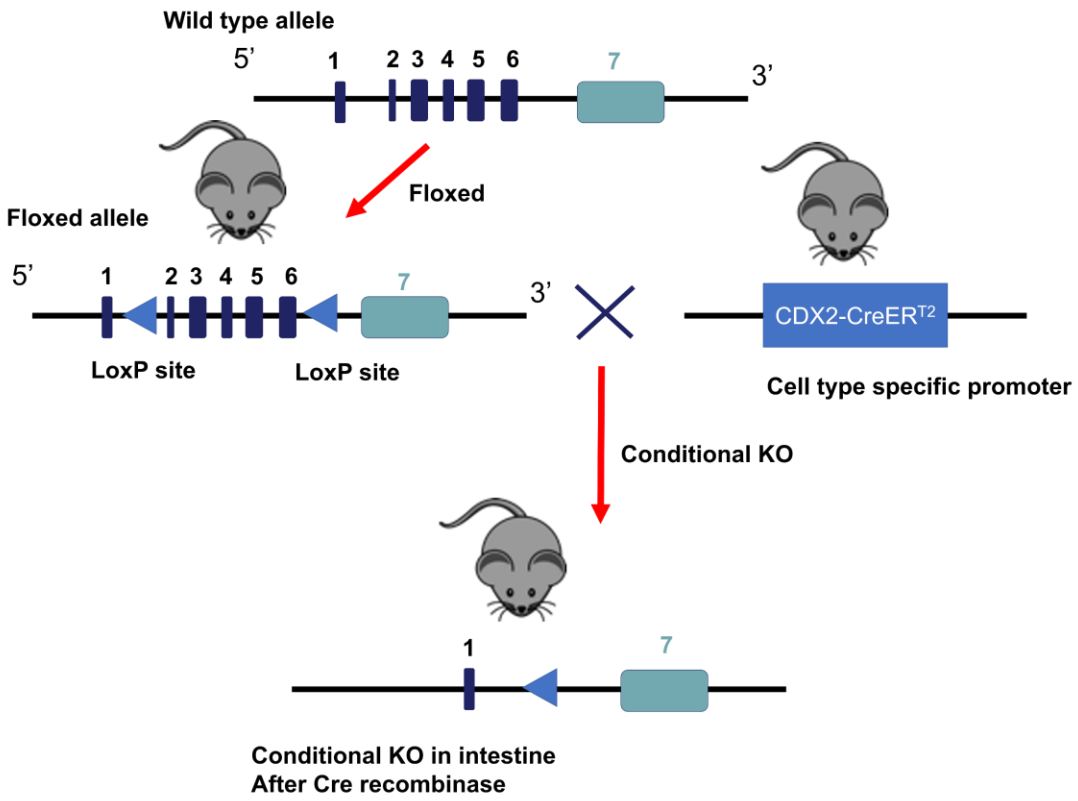

Figure 4-1 Establishing RBM3 knockout mice model
A Schematic for the RBM3 knockout mice generation. The exons 2-6 were chosen for knockout and were floxed. The floxed RBM3 mice, these mice were crossed with mice carrying a colon-specific promoter driven Cre (CDX2-driven-Cre/ER^{T2}) construct from Jackson Labs for colon specific knockout. The conditional knockout for RBM3 in the colon was done by tamoxifen treatment to mice containing the RBM3 floxed gene and the CDX2-Cre.

cell survival, stemness, invasion and angiogenesis in colon cancer cell lines. Hence,

to evaluate the role of RBM3 in colon carcinogenesis, we employed a carcinogen induced colon tumor model with the intRBM3KO mice (presented below). First, we generated RBM3 floxed mice from Cyagen biosciences, having the exons 2-6 were floxed (Figure 4-1). For conditional knockout of RBM3 in the colon, these mice were bred with mice carrying a colon-specific CDX2 promoter driven Cre (CDX2-driven-Cre/ER^{T2}) construct from Jackson Labs. The mice were genotyped for both the floxed gene and presence of CDX2-Cre/ER^{T2} and mice positive for both were included in the

further studies. To generate the knockout, the mice were administered tamoxifen ip at a dose of 5 mg/kg body weight for five days (Figure 4-1).

4.3.2 RBM3 knockout protects mice against colitis induced carcinogenesis

The carcinogen AOM/DSS is frequently used to induce colon cancer in mice. These mice develop colitis which then rapidly progresses to colon adenocarcinoma (Pan et al., 2017). We employed the AOM/DSS to induce colon adenocarcinoma to determine whether RBM3 mediates the alteration of intestinal epithelia for induction of cancer. For this, we first administered a single AOM dose by intraperitoneal injection, followed by three rounds of oral DSS (Figure 4-2 A). For the experiment, we utilized age matched wild-type and RBM3 knockout (intRBM3KO) mice (n=10, per group). We monitored these mice for symptoms of colitis especially rectal prolapse which is an indicator of colitis. We found that the mice developed symptoms of colitis as early as 14 weeks after carcinogen induction. Rectal prolapse was found in 86.6% of the wild-type mice while only 36.3% of RBM3 knockout mice showed the similar condition. We monitored the mice for up to 20-week post treatment with AOM/DSS, and found that at the experimental end point, only 40% of wild-type mice survived while in RBM3 knockout group 80% of the mice survived (Figure 4-2 D). AOM/DSS causes colitis-induced adenocarcinoma and has features like IBD. One key feature observed in IBD and in AOM/DSS induced carcinoma is the disturbance in the intestinal mucosal barrier. This breach in the intestinal barrier can aggravate inflammation and promote tumor progression (Liu et al., 2017a). Therefore, we investigated effects of RBM3 expression on intestinal barrier function by assessing wall permeability. We used fluorescent-labeled dextran (FITC-dextran) to access gut permeability of wild-type and intRBM3KO mice. We found that the wild-type mice treated

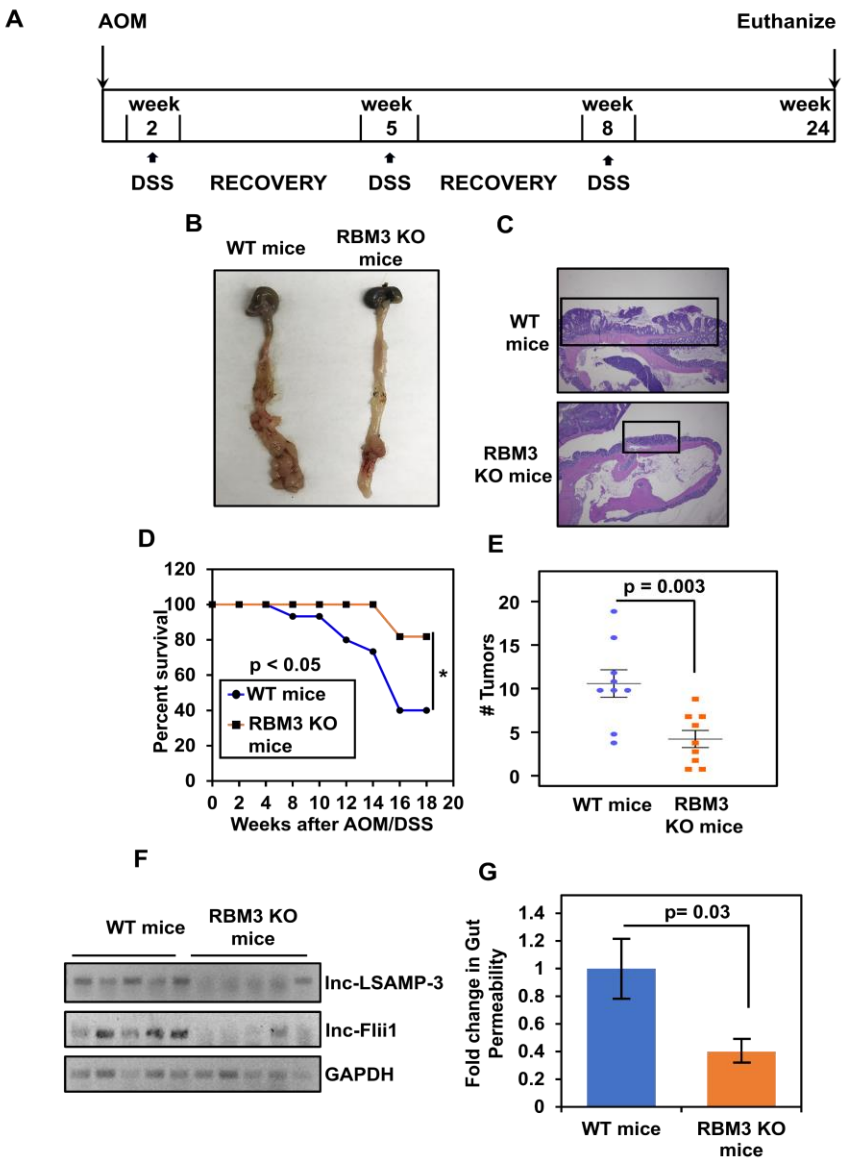

Figure 4-2 RBM3 knockout protects mice against colitis induced carcinogenesis

A Schematic for AOM/DSS induced colon adenocarcinoma. AOM 10 mg/kg was injected intraperitoneally (IP) to the mice followed by three cycles of DSS (2.5%) in drinking water. The mice were monitored.

B. Representative images of distal colon from wild type and RBM3 knockout mice after AOM/DSS treatment.

C. Representative images of H&E staining of the distal colon from wild type and RBM3 knockout mice after AOM/DSS treatment. Highlighted the area of tumor in both mice.

D. The survival curve for wild type and RBM3 knockout mice after AOM/DSS treatment shows RBM3 knockout increases survival after AOM/DSS treatment.

E. The plot for number of tumors formed after AOM/DSS treatment in mice. There is reduction in the number of tumors formed after AOM/DSS treatment in RBM3 knockout mice compared to wild type mice.

F. PCR analysis shows reduction in the expression of lnc-LSAMP-3 and lnc-Flii-1 after AOM/DSS in the RBM3 knockout mice.

G. Plot for fold change in the gut permeability shows reduction in RBM3 knockdown mice compared to wild type mice after AOM/DSS treatment.

with AOM/DSS showed over two-fold increase in intestinal permeability as compared to the intRBM3KO mice treated with AOM/DSS (Figure 4-2 G). This shows that RBM3 plays an important role in the progression of colitis to cancer, severely impacting survival of the mice. The mice colons were then examined for tumors at the end of the study. The gross examination of the distal colon from mice itself demonstrated a significant reduction in the number of tumors in the colon of intRBM3KO mice compared to that from wild-type animals after AOM/DSS treatment. We found that 100% of the wild type mice treated with AOM/DSS developed tumors in the colon but in contrast, only 80% of intRBM3KO mice treated with AOM/DSS developed tumors. We calculated the average number of tumors per mouse and found that the AOM/DSS treatment induced 10.77±1.26 tumors per wild-type mouse, which was about three times higher than the 3.2±0.85 tumors per mouse in intRBM3KO mice. (Figure 4-2 E). We performed hematoxylin and eosin (H&E) staining to analyze the histology of the distal colon from both WT and intRBM3KO mice treated with AOM/DSS. The colon tissues of mice treated with AOM/DSS typically show adenomatous growth and are infiltrated with immune cells including T lymphocytes (Tanaka et al., 2003). The H&E staining for the colon from our experimental AOM/DSS treated mice showed pathological features indicative of injury and inflammatory infiltration. Of the 10 intRBM3KO mice treated with AOM/DSS, two did not have any tumors and showed histology similar to normal mucosa, while one mouse had low-grade adenocarcinoma. The remaining intRBM3KO mice had tumors that were histopathologically like the wild-type mice. These tumors showed intra-tumoral crypt abscess and glands that are consistent with a well-differentiated adenocarcinoma (Figure 4-2 C). Just like the number of tumors, we found a decrease in the number of tumor foci

and the average size of foci in intRBM3KO mice compared to wild-type mice (Figure 4-2 C). The expression of RBM3 does not change in the stroma in colon. We also accessed the expression of the lncRNAs evaluated in our previous experiments. We found that the expression of both lnc-LSAMP-3 and lnc-Flii-1 was decreased in the tumors of intRBM3KO mice compared to wild-type mice (Figure 4-2 F). These cumulative findings demonstrate that RBM3 facilitates colon cancer progression and lnc-LSAMP-3 and lnc-Flii-1 are involved in the process.

4.4 Discussion

We established the role of RBM3 in increasing cell movement and angiogenesis through lncRNA modulation through our previous experiments. But most of these experiments were with established cell lines. To fully evaluate the role of RBM3 in tumor formation and progression, we need to study it in animal models. Genetically engineered models help understand the biology of cancer and allow testing of new chemo-preventive agents (Walrath et al., 2010). The Cre-Lox system allows a conditional and time specific modulation of genes. This has opened wide avenues to study the role of genes in specific cancers (Cheon and Orsulic, 2011b). Genetically engineered RBM3 mice have been previously used in the study for neurodegenerative disease and its role in immunity. Both studies involved RBM3 knockout in all the tissues, and not a tissue specific knockout of the gene (Matsuda et al., 2011, Zhu et al., 2019). Moreover, the role of RBM3 in tumorigenesis in these models have not been evaluated. Hence, we generated a Cre-inducible RBM3 knockout mouse to study the role of RBM3 in colon cancer. We achieved colon-specific conditional RBM3 knockdown (inRBM3KO) by crossing RBM3 floxed mice with CDX2-Cre/ERT2 mice and treating them with tamoxifen. These mice did not show

any phenotypic abnormalities. We do not know the effect of RBM3 knockout on embryo as we did not induce knockout in embryonic stage. Matsuda et.al, studied the role of RBM3 in immunity by generating mice deficient in RBM3 (Matsuda et al., 2011). They found that the RBM3 deficient mice had no abnormalities; however, there was decreased proliferation in the mouse embryonic fibroblasts (MEFs) compared to control MEFs (Matsuda et al., 2011). Xinzhou et al. utilized RBM3 knockout mice to study the role of RBM3 in neurodegenerative disease. They also did not find any abnormalities in the mice but under hypoxic conditions RBM3 protected the mouse neuronal stem cells from apoptosis and promoted its proliferation (Zhu et al., 2019).

Previously, several RBP have been studied for their role in colon cancer using AOM/DSS model including HuR, Lin28, Lin28b and IMP1. Intestine specific HuR knockout mice treated with AOM/DSS demonstrated lower tumor burden than wild type mice (Giammanco et al., 2014). On the other hand, knockout of HuR in the myeloid cells increased tumor size, proliferation, and grading after AOM/DSS. Knockout of both *Lin28a* and *Lin28b*, genes also did not show any phenotypic changes in the intestine or difference in tumor formation compared to wild type mice following treatment with AOM/DSS. Finally, IMP1 is an RBP that is upregulated in colon cancer and is associated with metastasis and poor prognosis. Again, knockdown of IMP1 in stromal cells of mice lead to increased tumor burden after AOM/DSS treatment (Hamilton, 2015). Therefore, varying and contradictory results have been seen with various RNA binding proteins and their role in colon cancer. More importantly, in all four cases manipulating the expression of these genes in established cell lines suggested that they are all pro-tumorigenic. Therefore, to fully understand the role of RBM3 in tumorigenesis, we performed

AOM/DSS-induced colitis-associated carcinogenesis in the RBM3 knockout mice. We found that loss of RBM3 knockout in the colon reduced the number and size of tumors compared to wild-type mice, similar to that see with HuR (Giammanco et al., 2014).

AOM/DSS can cause inflammation in the intestinal barrier and cause it to dysfunction leading increased gut permeability (Song et al., 2018). We found that gut permeability was decreased in RBM3 knockout mice as compared to wild-type mice after AOM/DSS treatment. This shows that RBM3 has a protective role on the intestinal barrier in the transition stage from inflammation to cancer in the colon. This finding corroborates previous studies demonstrating that HuR helps in intestinal epithelial regeneration following injury by increasing CDC42 translation (Liu, 2017). However, the studies did not look at gut permeability in these mice and therefore it is not clear whether this regeneration protected from gut permeability or by another mechanism. We have also observed that RBM3 affects the expression of lncRNAs lnc-LSAMP-3 and lnc-Flii-1 in the colon tissues following AOM/DSS treatment. This suggests that RBM3 may play an important role in colon carcinogenesis by modulating these lncRNAs. This is similar to lncRNAs SPRY4-IT1, which regulates intestinal barrier function by modulating expression of tight junction proteins (PMID 26680741). Whether FLii-1 and LSAMP-3 also modulate tight junction proteins still need to be determined.

Chapter 5 : Conclusions and Significance

5.1 Conclusions and Significance

RNA binding proteins are important for mRNA post-transcriptional control and deregulation of RBPs is seen in various cancers. (Glisovic et al., 2008b). We have previously shown that RBM3 is a protooncogene and important for cell survival and stemness in cancer REF. RBM3 is upregulated in several cancers like breast, colon, melanoma, prostrate, astrocytoma, ovarian and plays important role in tumorigenesis (Ehlén et al., 2010, Shaikhibrahim et al., 2013a, Zhang et al., 2013a, Siesing et al., 2017b, Zhou et al., 2017b). We have now confirmed that RBM3 is upregulated in a stage-dependent manner in colon cancers. Moreover, we have discovered two novel lncRNAs in addition to two known ones. Recent studies have also identified the important role of RBP interaction with lncRNAs (Ferrè et al., 2015). However, this is the first study to demonstrate that lncRNAs cooperate with an RNA binding protein to enhance circularization of the mRNA, the consequence of which is increased translation of the mRNA.

We first investigated the stemness/EMT phenotype associated with RBM3 overexpression. We found that RBM3 increased stemness, cell movement, and angiogenesis. We focused on VEGFA because recent studies have also shown the role of VEGFA in tumor proliferation, migration and invasion (Geng et al., 2013, Zeng et al., 2016). Similarly, transcription factors ZEB1, Snail, Slug, and TWIST are important regulators of EMT. They act by repressing the expression of adhesion protein E-cadherin contributing to a mesenchymal phenotype (Lamouille et al., 2014). Studies have also shown that EMT can play a role in switching dormant cells to the proliferative phenotype (Weidenfeld and Barkan, 2018). The transcription factors ZEB1 and TWIST1 have also

been shown to promote CSC traits in cancer (Wellner et al., 2009, Pang et al., 2016). While we only focused on a few of the markers, there are multiple factors that regulate stemness and EMT. These may also need to be further examined, especially in the context of RBM3 overexpression. The role of lncRNA in translational control is vastly understudied. Recent studies applying techniques such as translating ribosome affinity purification (TRAP) and ribosome profiling have shown that lncRNA are present and associated with the ribosomes and poly-ribosomal fractions (Guttman et al., 2013, Pircher et al., 2015). This ribosome association of lncRNA opens the possibility of translational control by lncRNA which needs further investigation (Long et al., 2017). RBM3 and lncRNA interaction appears to influence translational control of the mRNAs involved in EMT and stemness suggesting a role in cancer progression. RBM3 is a well-known regulator of mRNA translation. In fact, RBM3 overexpression enhances phosphorylation of translation initiation factors eIF4E and 4EBP1. 4EBP1 is a translation inhibitor that interacts with eIF4E. However, phosphorylated 4EBP1 cannot interact with eIF4E, thereby releasing eIF4E to enhance mRNA translation (Dresios et al., 2005). RBM3 can also enhance global protein translation by interacting with the 60S ribosomal subunit and increases the formation of active polysomes (Smart et al., 2007b). lncRNA can also interact with ribosomes and polysomes (Pircher et al., 2015). The cis-acting structures in the 5'UTR of mRNA like the IRES are important in the translation of transcripts especially under stress conditions like hypoxia (Komar and Hatzoglou, 2011). As the tumor environment has increases hypoxia the translation by a cap-independent mechanism becomes increasingly important where IRES can recruit ribosomes for translation initiation (Morfoisse et al., 2014). Our molecular modeling studies suggest that all four

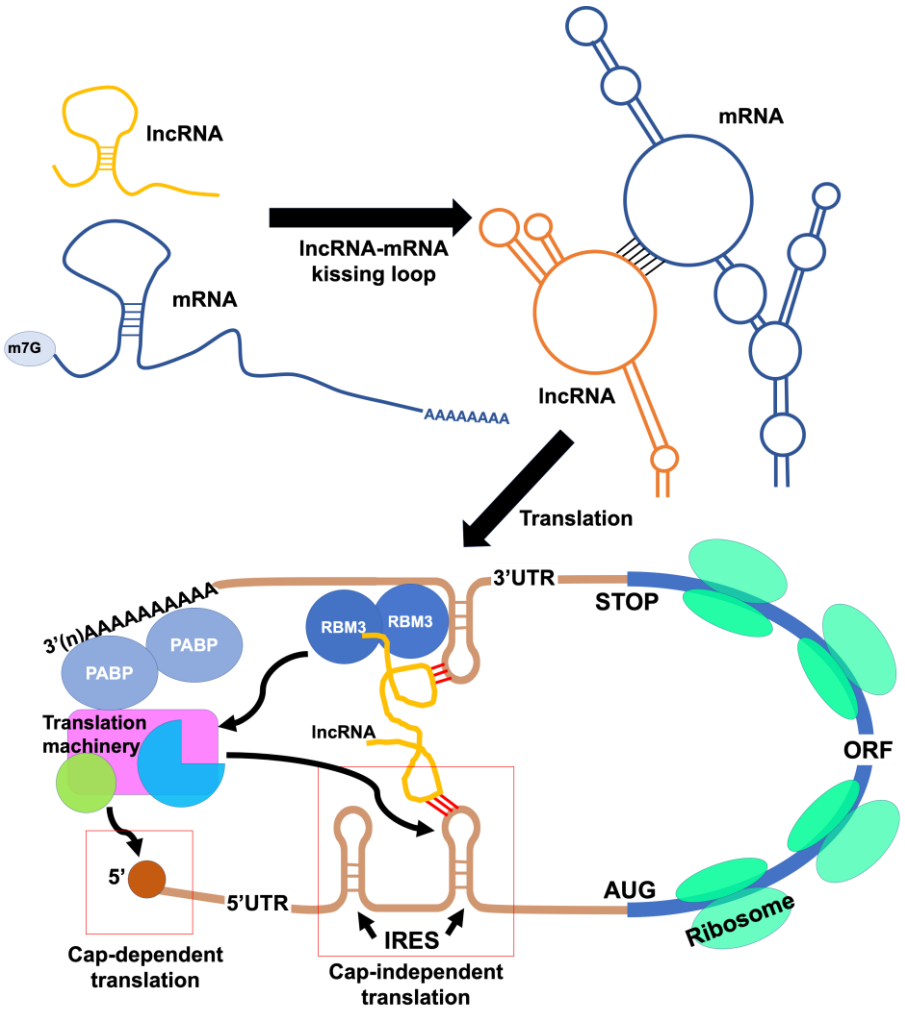

Figure 5-1 Proposed model
The schematic for the proposed model. The working model for our hypothesis is that both lnc-Flii-1, lnc-LSAMP-3 the lncRNAs can interact with the mRNA 5'UTR and 3'UTR of the mRNA. The interaction between lncRNA and mRNA is in the loop region coined as kissing loop interaction. The lncRNAs can bind at 5' of the cis acting element IRES containing or no IRES containing transcripts. RBM3 thus facilitates the binding of the lncRNAs at 5' and 3' and circularization of the mRNA. This circular structure facilitates the recruitment of translation machinery and elongation factors and enables multiple rounds of mRNA translation through polysome formation. Therefore, RBM3 can increase translation by either cap-dependent or independent mechanisms highlighted by boxes in the figure.
lncRNA: long non-coding RNA; UTR: untranslated region; IRES: Internal ribosome entry site; AUG: start codon; ORF: open reading frame; Stop: stop codon; PABP: poly A binding protein

lncRNAs lnc-Flii-1, lnc-LSAMP-3, HOTAIR, and TUG1 can interact with the EMT related mRNAs. The interactions detected were with cis-acting structural elements located in the 5'UTR of both IRES containing and IRES lacking transcripts. This suggests that these lncRNAs can possibly work on both cap-dependent and independent translation.

Interacting with both the 5'UTR and the 3'UTR results in the formation of a bridge to keep the mRNA in a circular structure. This circularization of mRNA is important for the recruitment of ribosomes to facilitate multiple rounds of mRNA translation (Wells et al., 1998). Collectively, we envision that binding of RBM3 and lncRNA to facilitate the circularization of mRNA can contribute to the increased translation of stemness and EMT related mRNAs leading to tumor progression. Thus, the working model for our hypothesis is that RBM3 and select lncRNAs can interact with both the 5'UTR and 3'UTR ends of specific mRNAs and thereby stabilize the complex in a circular structure, which then facilitates multiple rounds of mRNA translation through polysome formation (Figure 5.1). Further studies are needed to evaluate the mechanism and working of this model.

Chapter 6 Future directions

Characterizing sites of RBM3-lncRNA binding

To gain insight into the underlying mechanism of RBM3-lncRNA interaction, we performed structure-function studies. As RBM3 has two functional domains, we performed truncations of RBM3 to either have only the RRM domain or the glycine-arginine-serine (GAS) rich domain (Figure 6-1 A). Primers for the truncation were made to amplify the full length (FL), GAS truncation (ΔGAS), and RRM domain truncation (ΔRRM) (Figure 6-1 B). The truncated RBM3 proteins were generated by *in vitro* transcription and translation adding a N-terminal Flag-tag, to enable immunoprecipitation (IP). The truncated domains were then used for RNA-IP using beads coated with anti-flag antibodies. The cell lysate was used for RNA-IP and the lncRNA levels after the immunoprecipitation were determined by RT-PCR for lnc-Flii-1 and lnc-LSAMP-3. To further characterize where RBM3 binds to the lncRNA we performed truncations for the lncRNA. RBM3 is known to bind to AU rich elements on the RNA. Analyzing the sequence of the lncRNAs, we found that the AU-rich element was present at the 5' end of lnc-Flii-1 and at the 3' end of lnc-LSAMP-3. Therefore, we made truncations of the lncRNA removing either 5' end or the 3' end of both the lncRNAs. The lnc-Flii-1 truncation was done by the invitro transcription of region on 5' end Flii-1(1-305) and 3' end Flii-1(1818 to 2158) containing the AU-rich elements (Figure 6-1 D). The lnc- LSAMP-3 truncation was done by the invitro transcription of region on 5' end LSAMP-3 (1-231) and 3' end LSAMP-3 (1584 to 1794) containing the AU-rich elements (Figure 6-1 F).

Materials and Methods:

RBM3 and lncRNA truncations:

The RBM3 protein was truncated to encompass just the RRM domain and GAS domain. PCR primers were designed encompassing the RRM and GAS domain. The primers included the flag tag and sequence for S6 transcriptase. The lncRNAs were truncated by designing primers encompassing 200-300 bp at the 5' and 3' end of each lncRNA. The primer for lncRNA contained the S6 transcriptase. The cDNA from HCT116 cells was used for PCR using the designed primers. The PCR products were run on agarose gel to validate the correct size. The PCR products of appropriate size were purified and further used for in vitro transcription and translation.

In vitro transcription and translation:

The RBM3 and lncRNA truncation PCR products were further utilized for transcription using the MAX1script SP6 transcription kit (#AM1334; Thermo-Fisher) following the manufacturer's protocol with PCR products containing the SP6 promoter. RNA was extracted by phenol/chloroform/isoamyl alcohol (25:24:1) and precipitated with 3 M sodium acetate (pH, 5.2) and 100% ethanol. To label RNA for downstream RNA pull-down assay, RNAs were 3′ end-labeled with a biotinylation kit (#20160; Thermo-Fisher) following the manufacturer's instructions.

Immunoprecipitations:

To identify which domain of RBM3 interacted with the lncRNA the flag tagged truncations of RRM and GAS were used for immunoprecipitation assays. Briefly, HCT116 cells were grown to 90% confluency in 150-mm dishes and then washed twice with ice-cold phosphate-buffered saline. Lysates were prepared with 1.5 volumes of polysomal lysis buffer [100 mmol/L KCl, 25 mmol/L EDTA, 5 mmol/L $MgCl_2$, 10 mmol/L HEPES, pH 7.0, 0.5% Nonidet P-40, 10% glycerol, 2 mmol/L dithiothreitol, 0.4 mmol/L

vanadyl ribonucleoside complex, one tablet of complete protease inhibitor (Roche Applied Sciences Penzberg, Germany), and RNaseOUT (Invitrogen Carlsbad, CA) and centrifuged, and the supernatant was removed and stored at −80ºC. The supernatant was then incubated overnight at 4ºC with the truncated protein and anti-flag beads in NT2 buffer supplemented with RNaseOUT, 0.2% vanadyl ribonucleoside complex, 2 mmol/L dithiothreitol, and 25 mmol/L EDTA. After incubation, the beads were spun down and washed four times with ice-cold NT2 buffer. Subsequently, the material was digested with proteinase K for 2 hours and RNA extracted with TRIzol reagent. The lncRNA interacting with RBM3 truncated protein were identified by PCR using specific primers for lncRNA.

To identify the region on the lncRNA where RBM3 binds we performed immunoprecipitation using the in vitro transcribed truncated lncRNAs. The truncated lncRNAs were incubated individually with either full length, RRM or GAS domain of RBM3 and were precipitated using anti-flag beads. The lncRNA region interacting with RBM3 truncation was determined by PCR using specific primers for that region.

Results

The truncated RBM3 proteins were generated by *in vitro* transcription and translation adding a N-terminal Flag-tag, to enable immunoprecipitation (IP). The truncated domains were then used for RNA-IP using beads coated with anti-flag antibodies. The cell lysate was used for RNA-IP and the lncRNA levels after the immunoprecipitation was determined by RT-PCR for lnc-Flii-1 and lnc-LSAMP-3. The PCR results show that the RRB domain pulled down both lnc-Flii-1 ad lnc-LSAMP-3. There was no pulldown of lncRNA in bead control group. While lnc-Flii-1 only interacted with the RRM domain, lnc-LSAMP-3 was pulled down by both RRM and GAS domains (Figure 6-1 C).

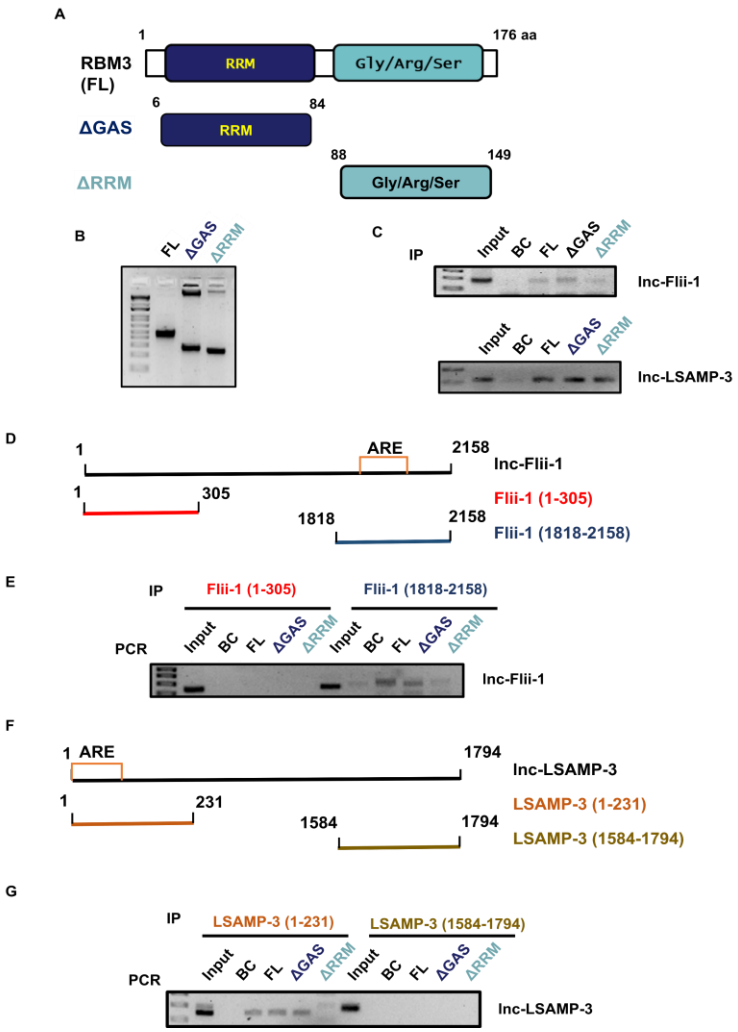

Figure 6-1 RRM domain of RBM3 associates with lncRNAs

A. Schematic of the RBM3 truncations. Invitro protein translation was done for RBM3 full length (FL), GAS domain truncation (ΔGAS), RRM domain truncation (ΔRRM).

B. The PCR products depicting the full length (FL), GAS truncation (ΔGAS), RRM domain truncation (ΔRRM) run on gel.

C. Immunoprecipitation was done using full length (FL), GAS truncation (ΔGAS), RRM truncation (ΔRRM) protein. PCR for lnc-Flii-1 and lnc-LSAMP-3 was done after pulldown. Whole cell cDNA was used as input and flag beads for bead control (BC). We found that lnc-Flii-1 was pulled down by FL and ΔGAS, while lnc-LSAMP-3 was pulled down by FL, ΔGAS and ΔRRM using full length, RRM and GAS domain for RBM3.

D. Schematic for lnc-Flii-1 truncation showing the invitro transcribed region on 5' end Flii-1(1-305) and 3' end Flii-1(1818 to 2158) containing the AU-rich elements.

E. Immunoprecipitation followed by PCR of the lnc-Flii-1 5' and 3' region incubated with either FL, ΔGAS and ΔRRM truncation of RBM3 using flag beads. The PCR was performed using primers specific for 5' end and 3' end region. The 5' end of end Flii-1(1-305) was not pulled down by any truncations, while the 3' end Flii-1(1818 to 2158) was pulled down by FL and ΔGAS.

F. Schematic for lnc-LSAMP-3 truncation showing the invitro transcribed region on 5' end LSAMP-3 (1-231) and 3' end LSAMP-3 (1584 to 1794) containing the AU-rich elements.

G. Immunoprecipitation followed by PCR of the lnc-LSAMP-3 5' and 3' region incubated with either FL, ΔGAS and ΔRRM truncation of RBM3 using flag beads. The PCR was performed using primers specific for 5' end and 3' end region. The 3' end of end LSAMP-3 (1584 to 1794) was not pulled down by any truncations, while the 5' end LSAMP-3 (1-231) was pulled down by FL, ΔRRM and ΔGAS.

The truncated lncRNA transcripts were also generated by *in vitro* transcription. We then subjected the truncations of lncRNA to either RBM3 full length protein or the RRM and GAS truncated proteins and performed pulled down assay using the anti-Flag beads. Subsequently, lncRNA truncations interacting with the RBM3 truncations were determined by RT-PCR using primer specific to the 5' end or 3' end of each lncRNA. We found that the 5' end of lnc-Flii-1 interacted with the full length and RRM domain of RBM3, while no interaction was seen in the 3' end to any RBM3 domain suggesting that the RRM domain in RBM3 interacts with the AU rich element at the 5' end of the lnc-Flii-1 (Figure 6-1 E). For the lnc-LSAMP-3, we found interactions at the 3' end of lncRNA and the RBM3, but not at 5' end, suggesting that RBM3 most likely interacts with the 3' end of lnc-LSAMP-3 where the AU- rich element is present (Figure 6-1 G).

Discussion

To identify precisely where RBM3 and lncRNAs Fliii-1 and LSAMP-3 interact, we performed deletion studies. The deletions were chosen based on our predicted molecular models. Not surprisingly, the RRM domain in RBM3 bound the AU-rich sequences located near the 5' and 3' ends of LASMP-3 and Flii-1, respectively. Surprisingly, the GAS domain also interacts with LSAMP-3 RNA, suggesting that this domain can have RNA binding properties. Further studies are required to delineate the differences in RNA binding between the RRM and GAS domains in RBM3, and the role of this binding on tumorigenesis. Interestingly, RBM3 encodes only one RRM domain. Previous studies with ELAV family proteins have suggested that a combination of two RRMS has a higher affinity of binding to AU rich elements (Abe et al., 1996, Park et al., 2000). The possibility therefore exists that the GAS domain in RBM3 enhances RRM binding function, and this

can be further determined by performing additional structure-function studies. Another study of importance in evaluating the role of lncRNA and RBM3 in the translation of mRNAs would be to perform a polysome assay. Polysome assays could help identify the presence of RBM3 and lncRNAs with the translation machinery to help increase translation of transcripts involved in tumor progression.

References

ABBASI, N., PARK, Y.-I. & CHOI, S.-B. 2011. Pumilio Puf domain RNA-binding proteins in Arabidopsis. *Plant signaling & behavior,* 6**,** 364-368.

ABE, R., SAKASHITA, E., YAMAMOTO, K. & SAKAMOTO, H. 1996. Two different RNA binding activities for the AU-rich element and the poly(A) sequence of the mouse neuronal protein mHuC. *Nucleic acids research,* 24**,** 4895-4901.

ALLAIN, F. H., BOUVET, P., DIECKMANN, T. & FEIGON, J. 2000. Molecular basis of sequence-specific recognition of pre-ribosomal RNA by nucleolin. *The EMBO journal,* 19**,** 6870-6881.

ALLEN, S. E., DARNELL, R. B. & LIPSCOMBE, D. 2010. The neuronal splicing factor Nova controls alternative splicing in N-type and P-type CaV2 calcium channels. *Channels (Austin, Tex.),* 4**,** 483-489.

ARCONDÉGUY, T., LACAZETTE, E., MILLEVOI, S., PRATS, H. & TOURIOL, C. 2013. VEGF-A mRNA processing, stability and translation: a paradigm for intricate regulation of gene expression at the post-transcriptional level. *Nucleic Acids Research,* 41**,** 7997-8010.

BALAS, M. M. & JOHNSON, A. M. 2018. Exploring the mechanisms behind long noncoding RNAs and cancer. *Non-coding RNA research,* 3**,** 108-117.

BAO, X., WU, H., ZHU, X., GUO, X., HUTCHINS, A. P., LUO, Z., SONG, H., CHEN, Y., LAI, K., YIN, M., XU, L., ZHOU, L., CHEN, J., WANG, D., QIN, B., FRAMPTON, J., TSE, H.-F., PEI, D., WANG, H., ZHANG, B. & ESTEBAN, M. A. 2015. The p53-induced lincRNA-p21 derails somatic cell reprogramming by sustaining H3K9me3 and CpG methylation at pluripotency gene promoters. *Cell Research,* 25**,** 80-92.

BARBOSA-MORAIS, N. L., CARMO-FONSECA, M. & APARÍCIO, S. 2006. Systematic genome-wide annotation of spliceosomal proteins reveals differential gene family expansion. *Genome research,* 16**,** 66-77.

BARREAU, C., PAILLARD, L. & OSBORNE, H. B. 2005. AU-rich elements and associated factors: are there unifying principles? *Nucleic Acids Res,* 33**,** 7138-50.

BARTONICEK, N., MAAG, J. L. V. & DINGER, M. E. 2016. Long noncoding RNAs in cancer: mechanisms of action and technological advancements. *Molecular Cancer,* 15**,** 43.

BASS, B. L. 2002. RNA editing by adenosine deaminases that act on RNA. *Annual review of biochemistry,* 71**,** 817-846.

BATTISTELLI, C., CICCHINI, C., SANTANGELO, L., TRAMONTANO, A., GRASSI, L., GONZALEZ, F. J., DE NONNO, V., GRASSI, G., AMICONE, L. & TRIPODI, M. 2017. The Snail repressor recruits EZH2 to specific genomic sites through the enrollment of the lncRNA HOTAIR in epithelial-to-mesenchymal transition. *Oncogene,* 36**,** 942-955.

BERMÚDEZ, M., AGUILAR-MEDINA, M., LIZÁRRAGA-VERDUGO, E., AVENDAÑO-FÉLIX, M., SILVA-BENÍTEZ, E., LÓPEZ-CAMARILLO, C. & RAMOS-PAYÁN, R. 2019. LncRNAs as Regulators of Autophagy and Drug Resistance in Colorectal Cancer. *Frontiers in oncology,* 9**,** 1008-1008.

BHAN, A., SOLEIMANI, M. & MANDAL, S. S. 2017. Long Noncoding RNA and Cancer: A New Paradigm. *Cancer Research,* 77**,** 3965.

BIERHOFF, H. 2018. Analysis of lncRNA-Protein Interactions by RNA-Protein Pull-Down Assays and RNA Immunoprecipitation (RIP). *Methods Mol Biol,* 1686**,** 241-250.

BLANCO, F. F., PREET, R., AGUADO, A., VISHWAKARMA, V., STEVENS, L. E., VYAS, A., PADHYE, S., XU, L., WEIR, S. J., ANANT, S., MEISNER-KOBER, N., BRODY, J. R. & DIXON, D. A. 2016. Impact of HuR inhibition by the small molecule MS-444 on colorectal cancer cell tumorigenesis. *Oncotarget,* 7**,** 74043-74058.

BOIVIN, G. P., WASHINGTON, K., YANG, K., WARD, J. M., PRETLOW, T. P., RUSSELL, R., BESSELSEN, D. G., GODFREY, V. L., DOETSCHMAN, T., DOVE, W. F., PITOT, H. C., HALBERG, R. B., ITZKOWITZ, S. H., GRODEN, J. & COFFEY, R. J. 2003. Pathology of mouse models of intestinal cancer: Consensus report and recommendations. *Gastroenterology,* 124**,** 762-777.

BOLAND, C. R., THIBODEAU, S. N., HAMILTON, S. R., SIDRANSKY, D., ESHLEMAN, J. R., BURT, R. W., MELTZER, S. J., RODRIGUEZ-BIGAS, M. A., FODDE, R., RANZANI, G. N. & SRIVASTAVA, S. 1998. A National Cancer Institute Workshop on Microsatellite Instability for Cancer Detection and Familial Predisposition: Development of International Criteria for the Determination of Microsatellite Instability in Colorectal Cancer. *Cancer Research,* 58**,** 5248.

BOLHA, L., RAVNIK-GLAVAČ, M. & GLAVAČ, D. 2017. Long Noncoding RNAs as Biomarkers in Cancer. *Disease markers,* 2017**,** 7243968-7243968.

BRAY, F., FERLAY, J., SOERJOMATARAM, I., SIEGEL, R. L., TORRE, L. A. & JEMAL, A. 2018. Global cancer statistics 2018: GLOBOCAN estimates of incidence and mortality worldwide for 36 cancers in 185 countries. *CA: A Cancer Journal for Clinicians,* 68**,** 394-424.

BRODY, J. R. & DIXON, D. A. 2018. Complex HuR function in pancreatic cancer cells. *WIREs RNA,* 9**,** e1469.

CAI, H., LIU, X., ZHENG, J., XUE, Y., MA, J., LI, Z., XI, Z., LI, Z., BAO, M. & LIU, Y. 2017. Long non-coding RNA taurine upregulated 1 enhances tumor-induced angiogenesis through inhibiting microRNA-299 in human glioblastoma. *Oncogene,* 36**,** 318-331.

CASTELLO, A., FISCHER, B., FRESE, C. K., HOROS, R., ALLEAUME, A.-M., FOEHR, S., CURK, T., KRIJGSVELD, J. & HENTZE, M. W. 2016. Comprehensive Identification of RNA-Binding Domains in Human Cells. *Molecular cell,* 63**,** 696-710.

CHAI, Y., LIU, J., ZHANG, Z. & LIU, L. 2016. HuR-regulated lncRNA NEAT1 stability in tumorigenesis and progression of ovarian cancer. *Cancer medicine,* 5**,** 1588-1598.

CHANDRASHEKAR, D. S., BASHEL, B., BALASUBRAMANYA, S. A. H., CREIGHTON, C. J., PONCE-RODRIGUEZ, I., CHAKRAVARTHI, B. V. S. K. & VARAMBALLY, S. 2017. UALCAN: A Portal for Facilitating Tumor Subgroup Gene Expression and Survival Analyses. *Neoplasia (New York, N.Y.),* 19**,** 649-658.

CHANG, K.-Y. & RAMOS, A. 2005. The double-stranded RNA-binding motif, a versatile macromolecular docking platform. *The FEBS Journal,* 272**,** 2109-2117.

CHEN, C.-Y. A. & SHYU, A.-B. 1995a. AU-rich elements: characterization and importance in mRNA degradation. *Trends in Biochemical Sciences,* 20**,** 465-470.

CHEN, C. Y. & SHYU, A. B. 1995b. AU-rich elements: characterization and importance in mRNA degradation. *Trends Biochem Sci,* 20**,** 465-70.

CHEN, P., YUE, X., XIONG, H., LU, X. & JI, Z. 2019. RBM3 upregulates ARPC2 by binding the 3'UTR and contributes to breast cancer progression. *Int J Oncol,* 54**,** 1387-1397.

CHEN, S., ZHU, J., WANG, F., GUAN, Z., GE, Y., YANG, X. & CAI, J. 2017. LncRNAs and their role in cancer stem cells. *Oncotarget,* 8**,** 110685-110692.

CHEN, Z.-Z., HUANG, L., WU, Y.-H., ZHAI, W.-J., ZHU, P.-P. & GAO, Y.-F. 2016. LncSox4 promotes the self-renewal of liver tumour-initiating cells through Stat3-mediated Sox4 expression. *Nature communications,* 7**,** 12598-12598.

CHEON, D.-J. & ORSULIC, S. 2011a. Mouse Models of Cancer. *Annual Review of Pathology: Mechanisms of Disease,* 6**,** 95-119.

CHEON, D. J. & ORSULIC, S. 2011b. Mouse models of cancer. *Annu Rev Pathol,* 6**,** 95-119.

CHIP, S., ZELMER, A., OGUNSHOLA, O. O., FELDERHOFF-MUESER, U., NITSCH, C., BÜHRER, C. & WELLMANN, S. 2011. The RNA-binding protein RBM3 is involved in hypothermia induced neuroprotection. *Neurobiology of Disease,* 43**,** 388-396.

CHOTHIA, C., LEVITT, M. & RICHARDSON, D. 1981. Helix to helix packing in proteins. *Journal of Molecular Biology,* 145**,** 215-250.

CHU, C. & CHANG, H. Y. 2018. ChIRP-MS: RNA-Directed Proteomic Discovery. *Methods Mol Biol,* 1861**,** 37-45.

CIUZAN, O., HANCOCK, J., PAMFIL, D., WILSON, I. & LADOMERY, M. 2015. The evolutionarily conserved multifunctional glycine-rich RNA-binding proteins play key roles in development and stress adaptation. *Physiologia Plantarum,* 153**,** 1-11.

CLÉRY, A., BLATTER, M. & ALLAIN, F. H. T. 2008. RNA recognition motifs: boring? Not quite. *Current Opinion in Structural Biology,* 18**,** 290-298.

COK, S. J., ACTON, S. J., SEXTON, A. E. & MORRISON, A. R. 2004. Identification of RNA-binding proteins in RAW 264.7 cells that recognize a lipopolysaccharide-responsive element in the 3-untranslated region of the murine cyclooxygenase-2 mRNA. *J Biol Chem,* 279**,** 8196-205.

CONN, SIMON J., PILLMAN, KATHERINE A., TOUBIA, J., CONN, VANESSA M., SALMANIDIS, M., PHILLIPS, CAROLINE A., ROSLAN, S., SCHREIBER, ANDREAS W., GREGORY, PHILIP A. & GOODALL, GREGORY J. 2015. The RNA Binding Protein Quaking Regulates Formation of circRNAs. *Cell,* 160**,** 1125-1134.

CORLEY, S. M. & GREADY, J. E. 2008. Identification of the RGG box motif in Shadoo: RNA-binding and signaling roles? *Bioinformatics and biology insights,* 2**,** 383-400.

DANNO, S., ITOH, K., MATSUDA, T. & FUJITA, J. 2000. Decreased expression of mouse Rbm3, a cold-shock protein, in Sertoli cells of cryptorchid testis. *The American journal of pathology,* 156**,** 1685-1692.

DANNO, S., NISHIYAMA, H., HIGASHITSUJI, H., YOKOI, H., XUE, J. H., ITOH, K., MATSUDA, T. & FUJITA, J. 1997. Increased transcript level of RBM3, a member of the glycine-rich RNA-binding protein family, in human cells in response to cold stress. *Biochem Biophys Res Commun,* 236**,** 804-7.

DE HOOG, C. L., FOSTER, L. J. & MANN, M. 2004. RNA and RNA Binding Proteins Participate in Early Stages of Cell Spreading through Spreading Initiation Centers. *Cell,* 117**,** 649-662.

DE ROBERTIS, M., MASSI, E., POETA, M. L., CAROTTI, S., MORINI, S., CECCHETELLI, L., SIGNORI, E. & FAZIO, V. M. 2011. The AOM/DSS murine model for the study of colon carcinogenesis: From pathways to diagnosis and therapy studies. *Journal of carcinogenesis,* 10**,** 9-9.

DE RUBEIS, S. & BAGNI, C. 2010. Fragile X mental retardation protein control of neuronal mRNA metabolism: Insights into mRNA stability. *Mol Cell Neurosci,* 43**,** 43-50.

DE SILANES, I. L., FAN, J., YANG, X., ZONDERMAN, A. B., POTAPOVA, O., PIZER, E. S. & GOROSPE, M. 2003. Role of the RNA-binding protein HuR in colon carcinogenesis. *Oncogene,* 22**,** 7146-7154.

DEO, R. C., BONANNO, J. B., SONENBERG, N. & BURLEY, S. K. 1999. Recognition of Polyadenylate RNA by the Poly(A)-Binding Protein. *Cell,* 98**,** 835-845.

DERRIEN, T., JOHNSON, R., BUSSOTTI, G., TANZER, A., DJEBALI, S., TILGNER, H., GUERNEC, G., MARTIN, D., MERKEL, A., KNOWLES, D. G., LAGARDE, J., VEERAVALLI, L., RUAN, X., RUAN, Y., LASSMANN, T., CARNINCI, P., BROWN, J. B., LIPOVICH, L., GONZALEZ, J. M., THOMAS, M., DAVIS, C. A., SHIEKHATTAR, R., GINGERAS, T. R., HUBBARD, T. J., NOTREDAME, C., HARROW, J. & GUIGÓ, R. 2012. The GENCODE v7 catalog of human long noncoding RNAs: analysis of their gene structure, evolution, and expression. *Genome research,* 22**,** 1775-1789.

DERRY, J. M., KERNS, J. A. & FRANCKE, U. 1995a. RBM3, a novel human gene in Xp11.23 with a putative RNA-binding domain. *Hum Mol Genet,* 4**,** 2307-11.

DERRY, J. M. J., KERNS, J. A. & FRANCKE, U. 1995b. RBM3, a novel human gene in Xp11.23 with a putative RNA-binding domain. *Human Molecular Genetics,* 4**,** 2307-2311.

DICTENBERG, J. B., SWANGER, S. A., ANTAR, L. N., SINGER, R. H. & BASSELL, G. J. 2008. A Direct Role for FMRP in Activity-Dependent Dendritic mRNA Transport Links Filopodial-Spine Morphogenesis to Fragile X Syndrome. *Developmental Cell,* 14**,** 926-939.

DING, C., CHENG, S., YANG, Z., LV, Z., XIAO, H., DU, C., PENG, C., XIE, H., ZHOU, L., WU, J. & ZHENG, S. 2014. Long non-coding RNA HOTAIR promotes cell migration and invasion via down-regulation of RNA binding motif protein 38 in hepatocellular carcinoma cells. *International journal of molecular sciences,* 15**,** 4060-4076.

DISTEFANO, J. K. 2018. The Emerging Role of Long Noncoding RNAs in Human Disease. *In:* DISTEFANO, J. K. (ed.) *Disease Gene Identification: Methods and Protocols.* New York, NY: Springer New York.

DIXON, D. A., TOLLEY, N. D., KING, P. H., NABORS, L. B., MCINTYRE, T. M., ZIMMERMAN, G. A. & PRESCOTT, S. M. 2001. Altered expression of the mRNA stability factor HuR promotes cyclooxygenase-2 expression in colon cancer cells. *The Journal of clinical investigation,* 108**,** 1657-1665.

DJEBALI, S., DAVIS, C. A., MERKEL, A., DOBIN, A., LASSMANN, T., MORTAZAVI, A., TANZER, A., LAGARDE, J., LIN, W., SCHLESINGER, F., XUE, C., MARINOV, G. K., KHATUN, J., WILLIAMS, B. A., ZALESKI, C., ROZOWSKY, J., RÖDER, M., KOKOCINSKI, F., ABDELHAMID, R. F., ALIOTO, T., ANTOSHECHKIN, I., BAER, M. T., BAR, N. S., BATUT, P., BELL, K., BELL, I., CHAKRABORTTY, S., CHEN,

X., CHRAST, J., CURADO, J., DERRIEN, T., DRENKOW, J., DUMAIS, E., DUMAIS, J., DUTTAGUPTA, R., FALCONNET, E., FASTUCA, M., FEJES-TOTH, K., FERREIRA, P., FOISSAC, S., FULLWOOD, M. J., GAO, H., GONZALEZ, D., GORDON, A., GUNAWARDENA, H., HOWALD, C., JHA, S., JOHNSON, R., KAPRANOV, P., KING, B., KINGSWOOD, C., LUO, O. J., PARK, E., PERSAUD, K., PREALL, J. B., RIBECA, P., RISK, B., ROBYR, D., SAMMETH, M., SCHAFFER, L., SEE, L.-H., SHAHAB, A., SKANCKE, J., SUZUKI, A. M., TAKAHASHI, H., TILGNER, H., TROUT, D., WALTERS, N., WANG, H., WROBEL, J., YU, Y., RUAN, X., HAYASHIZAKI, Y., HARROW, J., GERSTEIN, M., HUBBARD, T., REYMOND, A., ANTONARAKIS, S. E., HANNON, G., GIDDINGS, M. C., RUAN, Y., WOLD, B., CARNINCI, P., GUIGÓ, R. & GINGERAS, T. R. 2012. Landscape of transcription in human cells. *Nature,* 489**,** 101-108.

DONG, W., DAI, Z.-H., LIU, F.-C., GUO, X.-G., GE, C.-M., DING, J., LIU, H. & YANG, F. 2019a. The RNA-binding protein RBM3 promotes cell proliferation in hepatocellular carcinoma by regulating circular RNA SCD-circRNA 2 production. *EBioMedicine,* 45**,** 155-167.

DONG, W., DAI, Z. H., LIU, F. C., GUO, X. G., GE, C. M., DING, J., LIU, H. & YANG, F. 2019b. The RNA-binding protein RBM3 promotes cell proliferation in hepatocellular carcinoma by regulating circular RNA SCD-circRNA 2 production. *EBioMedicine,* 45**,** 155-167.

DRESIOS, J., ASCHRAFI, A., OWENS, G. C., VANDERKLISH, P. W., EDELMAN, G. M. & MAURO, V. P. 2005. Cold stress-induced protein Rbm3 binds 60S ribosomal subunits, alters microRNA levels, and enhances global protein synthesis. *Proceedings of the National Academy of Sciences of the United States of America,* 102**,** 1865-1870.

DUNICAN, D. S., MCWILLIAM, P., TIGHE, O., PARLE-MCDERMOTT, A. & CROKE, D. T. 2002. Gene expression differences between the microsatellite instability (MIN) and chromosomal instability (CIN) phenotypes in colorectal cancer revealed by high-density cDNA array hybridization. *Oncogene,* 21**,** 3253-3257.

DYKES, I. M. & EMANUELI, C. 2017. Transcriptional and Post-transcriptional Gene Regulation by Long Non-coding RNA. *Genomics, proteomics & bioinformatics,* 15**,** 177-186.

EDWARDS, THOMAS A. 2015. Bespoke RNA recognition by Pumilios. *Biochemical Society Transactions,* 43**,** 801-806.

EHLÉN, Å., BRENNAN, D. J., NODIN, B., O'CONNOR, D. P., EBERHARD, J., ALVARADO-KRISTENSSON, M., JEFFREY, I. B., MANJER, J., BRÄNDSTEDT, J., UHLÉN, M., PONTÉN, F. & JIRSTRÖM, K. 2010. Expression of the RNA-binding protein RBM3 is associated with a favourable prognosis and cisplatin sensitivity in epithelial ovarian cancer. *Journal of Translational Medicine,* 8**,** 78.

EHLÉN, Å., NODIN, B., REXHEPAJ, E., BRÄNDSTEDT, J., UHLÉN, M., ALVARADO-KRISTENSSON, M., PONTÉN, F., BRENNAN, D. J. & JIRSTRÖM, K. 2011. RBM3-regulated genes promote DNA integrity and affect clinical outcome in epithelial ovarian cancer. *Translational oncology,* 4**,** 212-221.

FEARON, E. R. 2011. Molecular Genetics of Colorectal Cancer. *Annual Review of Pathology: Mechanisms of Disease,* 6**,** 479-507.

FEDOROV, V. B., GOROPASHNAYA, A. V., TØIEN, Ø., STEWART, N. C., CHANG, C., WANG, H., YAN, J., SHOWE, L. C., SHOWE, M. K. & BARNES, B. M. 2011. Modulation of gene expression in heart and liver of hibernating black bears (Ursus americanus). *BMC genomics,* 12**,** 171-171.

FERNANDES, J. C. R., ACUÑA, S. M., AOKI, J. I., FLOETER-WINTER, L. M. & MUXEL, S. M. 2019. Long Non-Coding RNAs in the Regulation of Gene Expression: Physiology and Disease. *Non-coding RNA,* 5**,** 17.

FERRÈ, F., COLANTONI, A. & HELMER-CITTERICH, M. 2015. Revealing protein–lncRNA interaction. *Briefings in Bioinformatics,* 17**,** 106-116.

FISHEL, R., LESCOE, M. K., RAO, M. R. S., COPELAND, N. G., JENKINS, N. A., GARBER, J., KANE, M. & KOLODNER, R. 1993. The human mutator gene homolog MSH2 and its association with hereditary nonpolyposis colon cancer. *Cell,* 75**,** 1027-1038.

FU, W.-M., LU, Y.-F., HU, B.-G., LIANG, W.-C., ZHU, X., YANG, H.-D., LI, G. & ZHANG, J.-F. 2016. Long noncoding RNA Hotair mediated angiogenesis in nasopharyngeal carcinoma by direct and indirect signaling pathways. *Oncotarget,* 7**,** 4712-4723.

GEBAUER, F., PREISS, T. & HENTZE, M. W. 2012. From cis-regulatory elements to complex RNPs and back. *Cold Spring Harb Perspect Biol,* 4**,** a012245.

GENG, L., CHAUDHURI, A., TALMON, G., WISECARVER, J. L. & WANG, J. 2013. TGF-Beta suppresses VEGFA-mediated angiogenesis in colon cancer metastasis. *PloS one,* 8**,** e59918-e59918.

GIAMMANCO, A., BLANC, V., MONTENEGRO, G., KLOS, C., XIE, Y., KENNEDY, S., LUO, J., CHANG, S.-H., HLA, T., NALBANTOGLU, I., DHARMARAJAN, S. & DAVIDSON, N. O. 2014. Intestinal Epithelial HuR Modulates Distinct Pathways of Proliferation and Apoptosis and Attenuates Small Intestinal and Colonic Tumor Development. *Cancer Research,* 74**,** 5322.

GLASGOW, S. C., YU, J., CARVALHO, L. P., SHANNON, W. D., FLESHMAN, J. W. & MCLEOD, H. L. 2005. Unfavourable expression of pharmacologic markers in mucinous colorectal cancer. *British journal of cancer,* 92**,** 259-264.

GLISOVIC, T., BACHORIK, J. L., YONG, J. & DREYFUSS, G. 2008a. RNA-binding proteins and post-transcriptional gene regulation. *FEBS letters,* 582**,** 1977-1986.

GLISOVIC, T., BACHORIK, J. L., YONG, J. & DREYFUSS, G. 2008b. RNA-binding proteins and post-transcriptional gene regulation. *FEBS Lett,* 582**,** 1977-86.

GRISHIN, N. V. 2001. KH domain: one motif, two folds. *Nucleic acids research,* 29**,** 638-643.

GRUPP, K., HOFMANN, B., KUTUP, A., BACHMANN, K., BOGOEVSKI, D., MELLING, N., UZUNOGLU, F. G., EL GAMMAL, A. T., KOOP, C., SIMON, R., STEURER, S., KRECH, T., BURDAK-ROTHKAMM, S., JACOBSEN, F., SAUTER, G., IZBICKI, J. & WILCZAK, W. 2018. Reduced RBM3 expression is associated with aggressive tumor features in esophageal cancer but not significantly linked to patient outcome. *BMC cancer,* 18**,** 1106-1106.

GUTTMAN, M. & RINN, J. L. 2012. Modular regulatory principles of large non-coding RNAs. *Nature,* 482**,** 339-346.

GUTTMAN, M., RUSSELL, P., INGOLIA, N. T., WEISSMAN, J. S. & LANDER, E. S. 2013. Ribosome profiling provides evidence that large noncoding RNAs do not encode proteins. *Cell,* 154**,** 240-251.

HANAHAN, D. & WEINBERG, R. A. 2011. Hallmarks of cancer: the next generation. *Cell,* 144**,** 646-74.
HANDA, N., NUREKI, O., KURIMOTO, K., KIM, I., SAKAMOTO, H., SHIMURA, Y., MUTO, Y. & YOKOYAMA, S. 1999. Structural basis for recognition of the tra mRNA precursor by the Sex-lethal protein. *Nature,* 398**,** 579-585.
HAYNES, C. & IAKOUCHEVA, L. M. 2006. Serine/arginine-rich splicing factors belong to a class of intrinsically disordered proteins. *Nucleic acids research,* 34**,** 305-312.
HE, M., LIN, Y. & XU, Y. 2019a. Identification of prognostic biomarkers in colorectal cancer using a long non-coding RNA-mediated competitive endogenous RNA network. *Oncology letters,* 17**,** 2687-2694.
HE, R.-Z., LUO, D.-X. & MO, Y.-Y. 2019b. Emerging roles of lncRNAs in the post-transcriptional regulation in cancer. *Genes & diseases,* 6**,** 6-15.
HENTZE, M. W., CASTELLO, A., SCHWARZL, T. & PREISS, T. 2018. A brave new world of RNA-binding proteins. *Nature Reviews Molecular Cell Biology,* 19**,** 327-341.
HOGAN, D. J., RIORDAN, D. P., GERBER, A. P., HERSCHLAG, D. & BROWN, P. O. 2008. Diverse RNA-binding proteins interact with functionally related sets of RNAs, suggesting an extensive regulatory system. *PLoS Biol,* 6**,** e255.
HONG, S. 2017. RNA Binding Protein as an Emerging Therapeutic Target for Cancer Prevention and Treatment. *Journal of Cancer Prevention,* 22**,** 203-210.
HONG, S. N. 2018. Genetic and epigenetic alterations of colorectal cancer. *Intestinal research,* 16**,** 327-337.
HU, Y.-P., JIN, Y.-P., WU, X.-S., YANG, Y., LI, Y.-S., LI, H.-F., XIANG, S.-S., SONG, X.-L., JIANG, L., ZHANG, Y.-J., HUANG, W., CHEN, S.-L., LIU, F.-T., CHEN, C., ZHU, Q., CHEN, H.-Z., SHAO, R. & LIU, Y.-B. 2019. LncRNA-HGBC stabilized by HuR promotes gallbladder cancer progression by regulating miR-502-3p/SET/AKT axis. *Molecular Cancer,* 18**,** 167.
HUANG, R., HAN, M., MENG, L. & CHEN, X. 2018. Transcriptome-wide discovery of coding and noncoding RNA-binding proteins. *Proceedings of the National Academy of Sciences,* 115**,** E3879.
HUARTE, M. 2015. The emerging role of lncRNAs in cancer. *Nature Medicine,* 21**,** 1253-1261.
HUARTE, M., GUTTMAN, M., FELDSER, D., GARBER, M., KOZIOL, M. J., KENZELMANN-BROZ, D., KHALIL, A. M., ZUK, O., AMIT, I., RABANI, M., ATTARDI, L. D., REGEV, A., LANDER, E. S., JACKS, T. & RINN, J. L. 2010. A large intergenic noncoding RNA induced by p53 mediates global gene repression in the p53 response. *Cell,* 142**,** 409-419.
HUGEN, N., VAN BEEK, J. J. P., DE WILT, J. H. W. & NAGTEGAAL, I. D. 2014. Insight into Mucinous Colorectal Carcinoma: Clues from Etiology. *Annals of Surgical Oncology,* 21**,** 2963-2970.
IINO, H., SIMMS, L., YOUNG, J., ARNOLD, J., WINSHIP, I. M., WEBB, S. I., FURLONG, K. L., LEGGETT, B. & JASS, J. R. 2000. DNA microsatellite instability and mismatch repair protein loss in adenomas presenting in hereditary non-polyposis colorectal cancer. *Gut,* 47**,** 37-42.
IYER, M. K., NIKNAFS, Y. S., MALIK, R., SINGHAL, U., SAHU, A., HOSONO, Y., BARRETTE, T. R., PRENSNER, J. R., EVANS, J. R., ZHAO, S., POLIAKOV, A., CAO, X., DHANASEKARAN, S. M., WU, Y.-M., ROBINSON, D. R., BEER, D. G.,

FENG, F. Y., IYER, H. K. & CHINNAIYAN, A. M. 2015. The landscape of long noncoding RNAs in the human transcriptome. *Nature genetics,* 47**,** 199-208.
JASS, J. R., WHITEHALL, V. L. J., YOUNG, J. & LEGGETT, B. A. 2002. Emerging concepts in colorectal neoplasia. *Gastroenterology,* 123**,** 862-876.
JIA, M., GAO, X., ZHANG, Y., HOFFMEISTER, M. & BRENNER, H. 2016. Different definitions of CpG island methylator phenotype and outcomes of colorectal cancer: a systematic review. *Clinical epigenetics,* 8**,** 25-25.
JOGI, A., BRENNAN, D. J., RYDEN, L., MAGNUSSON, K., FERNO, M., STAL, O., BORGQUIST, S., UHLEN, M., LANDBERG, G., PAHLMAN, S., PONTEN, F. & JIRSTROM, K. 2009. Nuclear expression of the RNA-binding protein RBM3 is associated with an improved clinical outcome in breast cancer. *Mod Pathol,* 22**,** 1564-74.
JOHNSON, J. M., CASTLE, J., GARRETT-ENGELE, P., KAN, Z., LOERCH, P. M., ARMOUR, C. D., SANTOS, R., SCHADT, E. E., STOUGHTON, R. & SHOEMAKER, D. D. 2003. Genome-Wide Survey of Human Alternative Pre-mRNA Splicing with Exon Junction Microarrays. *Science,* 302**,** 2141.
JONSSON, L., BERGMAN, J., NODIN, B., MANJER, J., PONTÉN, F., UHLÉN, M. & JIRSTRÖM, K. 2011a. Low RBM3 protein expression correlates with tumour progression and poor prognosis in malignant melanoma: an analysis of 215 cases from the Malmö Diet and Cancer Study. *Journal of translational medicine,* 9**,** 114-114.
JONSSON, L., GABER, A., ULMERT, D., UHLÉN, M., BJARTELL, A. & JIRSTRÖM, K. 2011b. High RBM3 expression in prostate cancer independently predicts a reduced risk of biochemical recurrence and disease progression. *Diagnostic pathology,* 6**,** 91-91.
JOVER, R., NGUYEN, T.-P., PÉREZ-CARBONELL, L., ZAPATER, P., PAYÁ, A., ALENDA, C., ROJAS, E., CUBIELLA, J., BALAGUER, F., MORILLAS, J. D., CLOFENT, J., BUJANDA, L., REÑÉ, J. M., BESSA, X., XICOLA, R. M., NICOLÁS-PÉREZ, D., CASTELLS, A., ANDREU, M., LLOR, X., BOLAND, C. R. & GOEL, A. 2011. 5-Fluorouracil adjuvant chemotherapy does not increase survival in patients with CpG island methylator phenotype colorectal cancer. *Gastroenterology,* 140**,** 1174-1181.
KALMÁR, A., NAGY, Z. B., GALAMB, O., CSABAI, I., BODOR, A., WICHMANN, B., VALCZ, G., BARTÁK, B. K., TULASSAY, Z., IGAZ, P. & MOLNÁR, B. 2019. Genome-wide expression profiling in colorectal cancer focusing on lncRNAs in the adenoma-carcinoma transition. *BMC Cancer,* 19**,** 1059.
KAWASAKI, Y., KOMIYA, M., MATSUMURA, K., NEGISHI, L., SUDA, S., OKUNO, M., YOKOTA, N., OSADA, T., NAGASHIMA, T., HIYOSHI, M., OKADA-HATAKEYAMA, M., KITAYAMA, J., SHIRAHIGE, K. & AKIYAMA, T. 2016. MYU, a Target lncRNA for Wnt/c-Myc Signaling, Mediates Induction of CDK6 to Promote Cell Cycle Progression. *Cell Reports,* 16**,** 2554-2564.
KECHAVARZI, B. & JANGA, S. C. 2014. Dissecting the expression landscape of RNA-binding proteins in human cancers. *Genome biology,* 15**,** R14-R14.
KHAN MOHSIN, A. F., RECKMAN YOLAN, J., AUFIERO, S., VAN DEN HOOGENHOF MAARTEN, M. G., VAN DER MADE, I., BEQQALI, A., KOOLBERGEN DAVE, R., RASMUSSEN TORSTEN, B., VAN DER VELDEN, J., CREEMERS ESTHER, E.

& PINTO YIGAL, M. 2016. RBM20 Regulates Circular RNA Production From the Titin Gene. *Circulation Research,* 119**,** 996-1003.
KIM, H., KIM, M., IM, S.-K. & FANG, S. 2018. Mouse Cre-LoxP system: general principles to determine tissue-specific roles of target genes. *Laboratory animal research,* 34**,** 147-159.
KOMAR, A. & HATZOGLOU, M. 2011. *Cellular IRES-mediated translation*.
KOTAKE, Y., NAKAGAWA, T., KITAGAWA, K., SUZUKI, S., LIU, N., KITAGAWA, M. & XIONG, Y. 2011. Long non-coding RNA ANRIL is required for the PRC2 recruitment to and silencing of p15(INK4B) tumor suppressor gene. *Oncogene,* 30**,** 1956-1962.
KOTTA-LOIZOU, I., VASILOPOULOS, S. N., COUTTS, R. H. A. & THEOCHARIS, S. 2016. Current Evidence and Future Perspectives on HuR and Breast Cancer Development, Prognosis, and Treatment. *Neoplasia (New York, N.Y.),* 18**,** 674-688.
KRAUSOVA, M. & KORINEK, V. 2014. Wnt signaling in adult intestinal stem cells and cancer. *Cellular Signalling,* 26**,** 570-579.
KRISHNA, S. S., MAJUMDAR, I. & GRISHIN, N. V. 2003. Structural classification of zinc fingers: SURVEY AND SUMMARY. *Nucleic Acids Research,* 31**,** 532-550.
KUNG, J. T. Y., COLOGNORI, D. & LEE, J. T. 2013. Long noncoding RNAs: past, present, and future. *Genetics,* 193**,** 651-669.
LAMOUILLE, S., XU, J. & DERYNCK, R. 2014. Molecular mechanisms of epithelial-mesenchymal transition. *Nature reviews. Molecular cell biology,* 15**,** 178-196.
LAMPREHT TRATAR, U., HORVAT, S. & CEMAZAR, M. 2018. Transgenic Mouse Models in Cancer Research. *Frontiers in oncology,* 8**,** 268-268.
LAN, Y., XIAO, X., HE, Z., LUO, Y., WU, C., LI, L. & SONG, X. 2018. Long noncoding RNA OCC-1 suppresses cell growth through destabilizing HuR protein in colorectal cancer. *Nucleic acids research,* 46**,** 5809-5821.
LANGMEAD, B. & SALZBERG, S. L. 2012. Fast gapped-read alignment with Bowtie 2. *Nature methods,* 9**,** 357-359.
LEE, G. H., MALIETZIS, G., ASKARI, A., BERNARDO, D., AL-HASSI, H. O. & CLARK, S. K. 2015. Is right-sided colon cancer different to left-sided colorectal cancer? – A systematic review. *European Journal of Surgical Oncology (EJSO),* 41**,** 300-308.
LEI, H., GAO, Y. & XU, X. 2017. LncRNA TUG1 influences papillary thyroid cancer cell proliferation, migration and EMT formation through targeting miR-145. *Acta Biochimica et Biophysica Sinica,* 49**,** 588-597.
LENGAUER, C., KINZLER, K. W. & VOGELSTEIN, B. 1997. Genetic instability in colorectal cancers. *Nature,* 386**,** 623-627.
LI, B. & DEWEY, C. N. 2011. RSEM: accurate transcript quantification from RNA-Seq data with or without a reference genome. *BMC Bioinformatics,* 12**,** 323.
LI, E., ZHAO, Z., MA, B. & ZHANG, J. 2017. Long noncoding RNA HOTAIR promotes the proliferation and metastasis of osteosarcoma cells through the AKT/mTOR signaling pathway. *Exp Ther Med,* 14**,** 5321-5328.
LI, R., ZHU, H. & LUO, Y. 2016. Understanding the Functions of Long Non-Coding RNAs through Their Higher-Order Structures. *International journal of molecular sciences,* 17**,** 702.

LIU, C., LIU, E.-D., MENG, Y.-X., DONG, X.-M., BI, Y.-L., WU, H.-W., JIN, Y.-C., ZHAO, K., LI, J.-J., YU, M., ZHAN, Y.-Q., CHEN, H., GE, C.-H., YANG, X.-M. & LI, C.-Y. 2017a. Keratin 8 reduces colonic permeability and maintains gut microbiota homeostasis, protecting against colitis and colitis-associated tumorigenesis. *Oncotarget,* 8**,** 96774-96790.

LIU, L., CHEN, X., ZHANG, Y., HU, Y., SHEN, X. & ZHU, W. 2017b. Long non-coding RNA TUG1 promotes endometrial cancer development via inhibiting miR-299 and miR-34a-5p. *Oncotarget,* 8**,** 31386-31394.

LIU, L., LI, T., SONG, G., HE, Q., YIN, Y., LU, J Y., BI, X., WANG, K., LUO, S., CHEN, Y.-S., YANG, Y., SUN, B.-F., YANG, Y.-G., WU, J., ZHU, H. & SHEN, X. 2019. Insight into novel RNA-binding activities via large-scale analysis of lncRNA-bound proteome and IDH1-bound transcriptome. *Nucleic Acids Research,* 47**,** 2244-2262.

LONG, Y., WANG, X., YOUMANS, D. T. & CECH, T. R. 2017. How do lncRNAs regulate transcription? *Science advances,* 3**,** eaao2110-eaao2110.

LORENZ, R., BERNHART, S. H., HÖNER ZU SIEDERDISSEN, C., TAFER, H., FLAMM, C., STADLER, P. F. & HOFACKER, I. L. 2011. ViennaRNA Package 2.0. *Algorithms for molecular biology : AMB,* 6**,** 26-26.

LOUGHLIN, F. E., MANSFIELD, R. E., VAZ, P. M., MCGRATH, A. P., SETIYAPUTRA, S., GAMSJAEGER, R., CHEN, E. S., MORRIS, B. J., GUSS, J. M. & MACKAY, J. P. 2009. The zinc fingers of the SR-like protein ZRANB2 are single-stranded RNA-binding domains that recognize 5′ splice site-like sequences. *Proceedings of the National Academy of Sciences,* 106**,** 5581.

LUKONG, K. E., CHANG, K.-W., KHANDJIAN, E. W. & RICHARD, S. 2008. RNA-binding proteins in human genetic disease. *Trends in Genetics,* 24**,** 416-425.

LUO, C., CEN, S., DING, G. & WU, W. 2019. Mucinous colorectal adenocarcinoma: clinical pathology and treatment options. *Cancer communications (London, England),* 39**,** 13-13.

MAITRA, R., THAVORNWATANAYONG, T., VENKATESH, M. K., CHANDY, C., VACHSS, D., AUGUSTINE, T., GUZIK, H., KOBA, W., LIU, Q. & GOEL, S. 2019. Development and Characterization of a Genetic Mouse Model of KRAS Mutated Colorectal Cancer. *International journal of molecular sciences,* 20**,** 5677.

MANGALA, L. S., HAN, H. D., LOPEZ-BERESTEIN, G. & SOOD, A. K. 2009. Liposomal siRNA for Ovarian Cancer. *In:* RONDINONE, C. M. & REIDHAAR-OLSON, J. F. (eds.) *Therapeutic Applications of RNAi: Methods and Protocols.* Totowa, NJ: Humana Press.

MANN, M., WRIGHT, P. R. & BACKOFEN, R. 2017. IntaRNA 2.0: enhanced and customizable prediction of RNA–RNA interactions. *Nucleic Acids Research,* 45**,** W435-W439.

MARIS, C., DOMINGUEZ, C. & ALLAIN, F. H. T. 2005. The RNA recognition motif, a plastic RNA-binding platform to regulate post-transcriptional gene expression. *The FEBS Journal,* 272**,** 2118-2131.

MARKOWITZ, S. D. & BERTAGNOLLI, M. M. 2009. Molecular origins of cancer: Molecular basis of colorectal cancer. *The New England journal of medicine,* 361**,** 2449-2460.

MASUDA, K. & KUWANO, Y. 2019. Diverse roles of RNA-binding proteins in cancer traits and their implications in gastrointestinal cancers. *WIREs RNA,* 10**,** e1520.

MATSUDA, A., OGAWA, M., YANAI, H., NAKA, D., GOTO, A., AO, T., TANNO, Y., TAKEDA, K., WATANABE, Y., HONDA, K. & TANIGUCHI, T. 2011. Generation of mice deficient in RNA-binding motif protein 3 (RBM3) and characterization of its role in innate immune responses and cell growth. *Biochemical and Biophysical Research Communications,* 411**,** 7-13.

MATSUI, K., NISHIZAWA, M., OZAKI, T., KIMURA, T., HASHIMOTO, I., YAMADA, M., KAIBORI, M., KAMIYAMA, Y., ITO, S. & OKUMURA, T. 2008. Natural antisense transcript stabilizes inducible nitric oxide synthase messenger RNA in rat hepatocytes. *Hepatology,* 47**,** 686-697.

MERCER, T. R. & MATTICK, J. S. 2013. Structure and function of long noncoding RNAs in epigenetic regulation. *Nature Structural &Amp; Molecular Biology,* 20**,** 300.

MEREDITH, E. K., BALAS, M. M., SINDY, K., HAISLOP, K. & JOHNSON, A. M. 2016. An RNA matchmaker protein regulates the activity of the long noncoding RNA HOTAIR. *RNA (New York, N.Y.),* 22**,** 995-1010.

MOHIBI, S., CHEN, X. & ZHANG, J. 2019. Cancer the'RBP'eutics–RNA-binding proteins as therapeutic targets for cancer. *Pharmacology & Therapeutics,* 203**,** 107390.

MONGELLI, A., MARTELLI, F., FARSETTI, A. & GAETANO, C. 2019. The Dark That Matters: Long Non-coding RNAs as Master Regulators of Cellular Metabolism in Non-communicable Diseases. *Frontiers in Physiology,* 10.

MORFOISSE, F., KUCHNIO, A., FRAINAY, C., GOMEZ-BROUCHET, A., DELISLE, M.-B., MARZI, S., HELFER, A.-C., HANTELYS, F., PUJOL, F., GUILLERMET-GUIBERT, J., BOUSQUET, C., DEWERCHIN, M., PYRONNET, S., PRATS, A.-C., CARMELIET, P. & GARMY-SUSINI, B. 2014. Hypoxia Induces VEGF-C Expression in Metastatic Tumor Cells via a HIF-1α-Independent Translation-Mediated Mechanism. *Cell Reports,* 6**,** 155-167.

NANDAN, M. O. & YANG, V. W. 2010. Genetic and Chemical Models of Colorectal Cancer in Mice. *Current colorectal cancer reports,* 6**,** 51-59.

NEW, J., SUBRAMANIAM, D., RAMALINGAM, S., ENDERS, J., SAYED, A. A. A., PONNURANGAM, S., STANDING, D., RAMAMOORTHY, P., O'NEIL, M., DIXON, D. A., SAHA, S., UMAR, S., GUNEWARDENA, S., JENSEN, R. A., THOMAS, S. M. & ANANT, S. 2019. Pleotropic role of RNA binding protein CELF2 in autophagy induction. *Molecular Carcinogenesis,* 58**,** 1400-1409.

NILAND, C., MERRY, C. & KHALIL, A. 2012. Emerging Roles for Long Non-Coding RNAs in Cancer and Neurological Disorders. *Frontiers in Genetics,* 3.

OLIVEIRA, C., FAORO, H., ALVES, L. R. & GOLDENBERG, S. 2017. RNA-binding proteins and their role in the regulation of gene expression in Trypanosoma cruzi and Saccharomyces cerevisiae. *Genetics and molecular biology,* 40**,** 22-30.

OSTARECK, D. H., OSTARECK-LEDERER, A., SHATSKY, I. N. & HENTZE, M. W. 2001. Lipoxygenase mRNA Silencing in Erythroid Differentiation: The 3′UTR Regulatory Complex Controls 60S Ribosomal Subunit Joining. *Cell,* 104**,** 281-290.

PAN, Q., LOU, X., ZHANG, J., ZHU, Y., LI, F., SHAN, Q., CHEN, X., XIE, Y., SU, S., WEI, H., LIN, L., WU, L. & LIU, S. 2017. Genomic variants in mouse model induced by azoxymethane and dextran sodium sulfate improperly mimic human colorectal cancer. *Scientific Reports,* 7**,** 25.

PANG, M.-F., SIEDLIK, M. J., HAN, S., STALLINGS-MANN, M., RADISKY, D. C. & NELSON, C. M. 2016. Tissue Stiffness and Hypoxia Modulate the Integrin-Linked Kinase ILK to Control Breast Cancer Stem-like Cells. *Cancer Research,* 76**,** 5277.

PARANG, B., BARRETT, C. W. & WILLIAMS, C. S. 2016. AOM/DSS Model of Colitis-Associated Cancer. *Methods in molecular biology (Clifton, N.J.),* 1422**,** 297-307.

PARK, S., MYSZKA, D. G., YU, M., LITTLER, S. J. & LAIRD-OFFRINGA, I. A. 2000. HuD RNA recognition motifs play distinct roles in the formation of a stable complex with AU-rich RNA. *Molecular and cellular biology,* 20**,** 4765-4772.

PENG, C., HU, W., WENG, X., TONG, R., CHENG, S., DING, C., XIAO, H., LV, Z., XIE, H., ZHOU, L., WU, J. & ZHENG, S. 2017. Over Expression of Long Non-Coding RNA PANDA Promotes Hepatocellular Carcinoma by Inhibiting Senescence Associated Inflammatory Factor IL8. *Scientific reports,* 7**,** 4186-4186.

PENG, S. S., CHEN, C. Y., XU, N. & SHYU, A. B. 1998. RNA stabilization by the AU-rich element binding protein, HuR, an ELAV protein. *The EMBO journal,* 17**,** 3461-3470.

PÉREZ-CAÑADILLAS, J.-M. & VARANI, G. 2001. Recent advances in RNA–protein recognition. *Current Opinion in Structural Biology,* 11**,** 53-58.

PILOTTE, J., CUNNINGHAM, B. A., EDELMAN, G. M. & VANDERKLISH, P. W. 2009. Developmentally regulated expression of the cold-inducible RNA-binding motif protein 3 in euthermic rat brain. *Brain Research,* 1258**,** 12-24.

PILOTTE, J., DUPONT-VERSTEEGDEN, E. E. & VANDERKLISH, P. W. 2011. Widespread regulation of miRNA biogenesis at the Dicer step by the cold-inducible RNA-binding protein, RBM3. *PLoS One,* 6**,** e28446.

PILOTTE, J., KIOSSES, W., CHAN, S. W., MAKARENKOVA, H. P., DUPONT-VERSTEEGDEN, E. & VANDERKLISH, P. W. 2018. Morphoregulatory functions of the RNA-binding motif protein 3 in cell spreading, polarity and migration. *Scientific Reports,* 8**,** 7367.

PINO, M. S. & CHUNG, D. C. 2010. The chromosomal instability pathway in colon cancer. *Gastroenterology,* 138**,** 2059-2072.

PIQUÉ, L., MARTINEZ DE PAZ, A., PIÑEYRO, D., MARTÍNEZ-CARDÚS, A., CASTRO DE MOURA, M., LLINÀS-ARIAS, P., SETIEN, F., GOMEZ-MIRAGAYA, J., GONZALEZ-SUAREZ, E., SIGURDSSON, S., JONASSON, J. G., VILLANUEVA, A., VIDAL, A., DAVALOS, V. & ESTELLER, M. 2019. Epigenetic inactivation of the splicing RNA-binding protein CELF2 in human breast cancer. *Oncogene,* 38**,** 7106-7112.

PIRCHER, A., GEBETSBERGER, J. & POLACEK, N. 2015. Ribosome-associated ncRNAs: an emerging class of translation regulators. *RNA biology,* 11**,** 1335-1339.

PULLMANN, R., JR., KIM, H. H., ABDELMOHSEN, K., LAL, A., MARTINDALE, J. L., YANG, X. & GOROSPE, M. 2007. Analysis of turnover and translation regulatory RNA-binding protein expression through binding to cognate mRNAs. *Mol Cell Biol,* 27**,** 6265-78.

RAO, C. V. & YAMADA, H. Y. 2013. Genomic instability and colon carcinogenesis: from the perspective of genes. *Frontiers in oncology,* 3**,** 130-130.

RINN, J. L., KERTESZ, M., WANG, J. K., SQUAZZO, S. L., XU, X., BRUGMANN, S. A., GOODNOUGH, L. H., HELMS, J. A., FARNHAM, P. J., SEGAL, E. & CHANG, H.

Y. 2007. Functional demarcation of active and silent chromatin domains in human HOX loci by noncoding RNAs. *Cell,* 129**,** 1311-1323.
ROBINSON, M. D., MCCARTHY, D. J. & SMYTH, G. K. 2010. edgeR: a Bioconductor package for differential expression analysis of digital gene expression data. *Bioinformatics (Oxford, England),* 26**,** 139-140.
ROSENBERG, D. W., GIARDINA, C. & TANAKA, T. 2009. Mouse models for the study of colon carcinogenesis. *Carcinogenesis,* 30**,** 183-196.
ROSENTHAL, L.-M., TONG, G., WALKER, C., WOWRO, S. J., KRECH, J., PFITZER, C., JUSTUS, G., BERGER, F. & SCHMITT, K. R. L. 2017. Neuroprotection via RNA-binding protein RBM3 expression is regulated by hypothermia but not by hypoxia in human SK-N-SH neurons. *Hypoxia (Auckland, N.Z.),* 5**,** 33-43.
RUSTGI, A. K. 1994. Hereditary Gastrointestinal Polyposis and Nonpolyposis Syndromes. *New England Journal of Medicine,* 331**,** 1694-1702.
RYAN, K., CALVO, O. & MANLEY, J. L. 2004. Evidence that polyadenylation factor CPSF-73 is the mRNA 3' processing endonuclease. *RNA (New York, N.Y.),* 10**,** 565-573.
SÁNCHEZ, Y., SEGURA, V., MARÍN-BÉJAR, O., ATHIE, A., MARCHESE, F. P., GONZÁLEZ, J., BUJANDA, L., GUO, S., MATHEU, A. & HUARTE, M. 2014. Genome-wide analysis of the human p53 transcriptional network unveils a lncRNA tumour suppressor signature. *Nature communications,* 5**,** 5812-5812.
SAUER, B. & HENDERSON, N. 1988. Site-specific DNA recombination in mammalian cells by the Cre recombinase of bacteriophage P1. *Proceedings of the National Academy of Sciences of the United States of America,* 85**,** 5166-5170.
SCHMITT, A. M. & CHANG, H. Y. 2016. Long Noncoding RNAs in Cancer Pathways. *Cancer cell,* 29**,** 452-463.
SCHORDERET, P. & DUBOULE, D. 2011. Structural and functional differences in the long non-coding RNA hotair in mouse and human. *PLoS genetics,* 7**,** e1002071-e1002071.
SEAMONS, A., TREUTING, P. M., BRABB, T. & MAGGIO-PRICE, L. 2013. Characterization of Dextran Sodium Sulfate-Induced Inflammation and Colonic Tumorigenesis in Smad3−/− Mice with Dysregulated TGFβ. *PLOS ONE,* 8**,** e79182.
SHAIKHIBRAHIM, Z., LINDSTROT, A., OCHSENFAHRT, J., FUCHS, K. & WERNERT, N. 2013a. Epigenetics-related genes in prostate cancer: expression profile in prostate cancer tissues, androgen-sensitive and -insensitive cell lines. *International journal of molecular medicine,* 31**,** 21-25.
SHAIKHIBRAHIM, Z., LINDSTROT, A., OCHSENFAHRT, J., FUCHS, K. & WERNERT, N. 2013b. Epigenetics-related genes in prostate cancer: expression profile in prostate cancer tissues, androgen-sensitive and -insensitive cell lines. *Int J Mol Med,* 31**,** 21-5.
SHIH, J.-W., CHIANG, W.-F., WU, A. T. H., WU, M.-H., WANG, L.-Y., YU, Y.-L., HUNG, Y.-W., WANG, W.-C., CHU, C.-Y., HUNG, C.-L., CHANGOU, C. A., YEN, Y. & KUNG, H.-J. 2017. Long noncoding RNA LncHIFCAR/MIR31HG is a HIF-1α co-activator driving oral cancer progression. *Nature communications,* 8**,** 15874-15874.

SIDDIQUI, H., AL-GHAFARI, A., CHOUDHRY, H. & AL DOGHAITHER, H. 2019. Roles of long non-coding RNAs in colorectal cancer tumorigenesis: A Review. *Molecular and clinical oncology,* 11**,** 167-172.

SIEGEL, R. L., TORRE, L. A., SOERJOMATARAM, I., HAYES, R. B., BRAY, F., WEBER, T. K. & JEMAL, A. 2019. Global patterns and trends in colorectal cancer incidence in young adults. *Gut,* 68**,** 2179.

SIESING, C., SORBYE, H., DRAGOMIR, A., PFEIFFER, P., QVORTRUP, C., PONTÉN, F., JIRSTRÖM, K., GLIMELIUS, B. & EBERHARD, J. 2017a. High RBM3 expression is associated with an improved survival and oxaliplatin response in patients with metastatic colorectal cancer. *PLOS ONE,* 12**,** e0182512.

SIESING, C., SORBYE, H., DRAGOMIR, A., PFEIFFER, P., QVORTRUP, C., PONTÉN, F., JIRSTRÖM, K., GLIMELIUS, B. & EBERHARD, J. 2017b. High RBM3 expression is associated with an improved survival and oxaliplatin response in patients with metastatic colorectal cancer. *PloS one,* 12**,** e0182512-e0182512.

SIMONE, L. E. & KEENE, J. D. 2013. Mechanisms coordinating ELAV/Hu mRNA regulons. *Current opinion in genetics & development,* 23**,** 35-43.

SIOMI, H., MATUNIS, M. J., MICHAEL, W. M. & DREYFUSS, G. 1993a. The pre-mRNA binding K protein contains a novel evolutionarily conserved motif. *Nucleic acids research,* 21**,** 1193-1198.

SIOMI, H., SIOMI, M. C., NUSSBAUM, R. L. & DREYFUSS, G. 1993b. The protein product of the fragile X gene, FMR1, has characteristics of an RNA-binding protein. *Cell,* 74**,** 291-298.

SMART, F., ASCHRAFI, A., ATKINS, A., OWENS, G. C., PILOTTE, J., CUNNINGHAM, B. A. & VANDERKLISH, P. W. 2007a. Two isoforms of the cold-inducible mRNA-binding protein RBM3 localize to dendrites and promote translation. *J Neurochem,* 101**,** 1367-79.

SMART, F., ASCHRAFI, A., ATKINS, A., OWENS, G. C., PILOTTE, J., CUNNINGHAM, B. A. & VANDERKLISH, P. W. 2007b. Two isoforms of the cold-inducible mRNA-binding protein RBM3 localize to dendrites and promote translation. *Journal of Neurochemistry,* 101**,** 1367-1379.

SONG, C.-H., KIM, N., SOHN, S. H., LEE, S. M., NAM, R. H., NA, H. Y., LEE, D. H. & SURH, Y.-J. 2018. Effects of 17β-Estradiol on Colonic Permeability and Inflammation in an Azoxymethane/Dextran Sulfate Sodium-Induced Colitis Mouse Model. *Gut and liver,* 12**,** 682-693.

STEFL, R., SKRISOVSKA, L. & ALLAIN, F. H. T. 2005. RNA sequence- and shape-dependent recognition by proteins in the ribonucleoprotein particle. *EMBO reports,* 6**,** 33-38.

STREITNER, C., KÖSTER, T., SIMPSON, C. G., SHAW, P., DANISMAN, S., BROWN, J. W. S. & STAIGER, D. 2012. An hnRNP-like RNA-binding protein affects alternative splicing by in vivo interaction with transcripts in Arabidopsis thaliana. *Nucleic acids research,* 40**,** 11240-11255.

SUBRAMANIAM, D., RAMALINGAM, S., LINEHAN, D. C., DIECKGRAEFE, B. K., POSTIER, R. G., HOUCHEN, C. W., JENSEN, R. A. & ANANT, S. 2011. RNA binding protein CUGBP2/CELF2 mediates curcumin-induced mitotic catastrophe of pancreatic cancer cells. *PloS one,* 6**,** e16958-e16958.

SUN, J.-Y., ZHAO, Z.-W., LI, W.-M., YANG, G., JING, P.-Y., LI, P., DANG, H.-Z., CHEN, Z., ZHOU, Y.-A. & LI, X.-F. 2017a. Knockdown of MALAT1 expression inhibits HUVEC proliferation by upregulation of miR-320a and downregulation of FOXM1 expression. *Oncotarget,* 8.

SUN, X., HAIDER ALI, M. S. S. & MORAN, M. 2017b. The role of interactions of long non-coding RNAs and heterogeneous nuclear ribonucleoproteins in regulating cellular functions. *The Biochemical journal,* 474**,** 2925-2935.

SUPEK, F., BOŠNJAK, M., ŠKUNCA, N. & ŠMUC, T. 2011. REVIGO Summarizes and Visualizes Long Lists of Gene Ontology Terms. *PLOS ONE,* 6**,** e21800.

SUREBAN, S. M., RAMALINGAM, S., NATARAJAN, G., MAY, R., SUBRAMANIAM, D., BISHNUPURI, K. S., MORRISON, A. R., DIECKGRAEFE, B. K., BRACKETT, D. J., POSTIER, R. G., HOUCHEN, C. W. & ANANT, S. 2008. Translation regulatory factor RBM3 is a proto-oncogene that prevents mitotic catastrophe. *Oncogene,* 27**,** 4544-56.

SZOSTAK, E. & GEBAUER, F. 2013. Translational control by 3'-UTR-binding proteins. *Briefings in functional genomics,* 12**,** 58-65.

TAN, J., QIU, K., LI, M. & LIANG, Y. 2015. Double-negative feedback loop between long non-coding RNA TUG1 and miR-145 promotes epithelial to mesenchymal transition and radioresistance in human bladder cancer cells. *FEBS Letters,* 589**,** 3175-3181.

TANAKA, T., KOHNO, H., SUZUKI, R., YAMADA, Y., SUGIE, S. & MORI, H. 2003. A novel inflammation-related mouse colon carcinogenesis model induced by azoxymethane and dextran sodium sulfate. *Cancer Science,* 94**,** 965-973.

THAKER, A. I., SHAKER, A., RAO, M. S. & CIORBA, M. A. 2012. Modeling colitis-associated cancer with azoxymethane (AOM) and dextran sulfate sodium (DSS). *Journal of visualized experiments : JoVE***,** 4100.

THOMSON, D. W. & DINGER, M. E. 2016. Endogenous microRNA sponges: evidence and controversy. *Nat Rev Genet,* 17**,** 272-83.

TIAN, Y., XIA, S., MA, M. & ZUO, Y. 2019. LINC00096 Promotes the Proliferation and Invasion by Sponging miR-383-5p and Regulating RBM3 Expression in Triple-Negative Breast Cancer. *OncoTargets and therapy,* 12**,** 10569-10578.

TORNESELLO, M. L., FARAONIO, R., BUONAGURO, L., ANNUNZIATA, C., STARITA, N., CERASUOLO, A., PEZZUTO, F., TORNESELLO, A. L. & BUONAGURO, F. M. 2020. The Role of microRNAs, Long Non-coding RNAs, and Circular RNAs in Cervical Cancer. *Front Oncol,* 10**,** 150.

TRAN, N.-T., SU, H., KHODADADI-JAMAYRAN, A., LIN, S., ZHANG, L., ZHOU, D., PAWLIK, K. M., TOWNES, T. M., CHEN, Y., MULLOY, J. C. & ZHAO, X. 2016. The AS-RBM15 lncRNA enhances RBM15 protein translation during megakaryocyte differentiation. *EMBO reports,* 17**,** 887-900.

TRIPATHI, V., ELLIS, J. D., SHEN, Z., SONG, D. Y., PAN, Q., WATT, A. T., FREIER, S. M., BENNETT, C. F., SHARMA, A., BUBULYA, P. A., BLENCOWE, B. J., PRASANTH, S. G. & PRASANTH, K. V. 2010. The nuclear-retained noncoding RNA MALAT1 regulates alternative splicing by modulating SR splicing factor phosphorylation. *Molecular cell,* 39**,** 925-938.

VALENTE, L. & NISHIKURA, K. 2005. ADAR Gene Family and A-to-I RNA Editing: Diverse Roles in Posttranscriptional Gene Regulation. *Progress in Nucleic Acid Research and Molecular Biology.* Academic Press.

VALVERDE, R., EDWARDS, L. & REGAN, L. 2008. Structure and function of KH domains. *The FEBS Journal,* 275**,** 2712-2726.

VENUGOPAL, A., SUBRAMANIAM, D., BALMACEDA, J., ROY, B., DIXON, D. A., UMAR, S., WEIR, S. J. & ANANT, S. 2016a. RNA binding protein RBM3 increases beta-catenin signaling to increase stem cell characteristics in colorectal cancer cells. *Mol Carcinog,* 55**,** 1503-1516.

VENUGOPAL, A., SUBRAMANIAM, D., BALMACEDA, J., ROY, B., DIXON, D. A., UMAR, S., WEIR, S. J. & ANANT, S. 2016b. RNA binding protein RBM3 increases β-catenin signaling to increase stem cell characteristics in colorectal cancer cells. *Molecular carcinogenesis,* 55**,** 1503-1516.

VOLDERS, P.-J., ANCKAERT, J., VERHEGGEN, K., NUYTENS, J., MARTENS, L., MESTDAGH, P. & VANDESOMPELE, J. 2018. LNCipedia 5: towards a reference set of human long non-coding RNAs. *Nucleic Acids Research,* 47**,** D135-D139.

WALRATH, J. C., HAWES, J. J., VAN DYKE, T. & REILLY, K. M. 2010. Genetically engineered mouse models in cancer research. *Advances in cancer research,* 106**,** 113-164.

WALTHER, A., HOULSTON, R. & TOMLINSON, I. 2008. Association between chromosomal instability and prognosis in colorectal cancer: a meta-analysis. *Gut,* 57**,** 941.

WANG, K. C. & CHANG, H. Y. 2011. Molecular mechanisms of long noncoding RNAs. *Molecular cell,* 43**,** 904-914.

WANG, L., LLORENTE, C., HARTMANN, P., YANG, A.-M., CHEN, P. & SCHNABL, B. 2015a. Methods to determine intestinal permeability and bacterial translocation during liver disease. *Journal of immunological methods,* 421**,** 44-53.

WANG, Y., HE, L., DU, Y., ZHU, P., HUANG, G., LUO, J., YAN, X., YE, B., LI, C., XIA, P., ZHANG, G., TIAN, Y., CHEN, R. & FAN, Z. 2015b. The long noncoding RNA lncTCF7 promotes self-renewal of human liver cancer stem cells through activation of Wnt signaling. *Cell Stem Cell,* 16**,** 413-25.

WEIDENFELD, K. & BARKAN, D. 2018. EMT and Stemness in Tumor Dormancy and Outgrowth: Are They Intertwined Processes? *Frontiers in oncology,* 8**,** 381-381.

WELLMANN, S., BUHRER, C., MODEREGGER, E., ZELMER, A., KIRSCHNER, R., KOEHNE, P., FUJITA, J. & SEEGER, K. 2004. Oxygen-regulated expression of the RNA-binding proteins RBM3 and CIRP by a HIF-1-independent mechanism. *J Cell Sci,* 117**,** 1785-94.

WELLNER, U., SCHUBERT, J., BURK, U. C., SCHMALHOFER, O., ZHU, F., SONNTAG, A., WALDVOGEL, B., VANNIER, C., DARLING, D., HAUSEN, A. Z., BRUNTON, V. G., MORTON, J., SANSOM, O., SCHÜLER, J., STEMMLER, M. P., HERZBERGER, C., HOPT, U., KECK, T., BRABLETZ, S. & BRABLETZ, T. 2009. The EMT-activator ZEB1 promotes tumorigenicity by repressing stemness-inhibiting microRNAs. *Nature Cell Biology,* 11**,** 1487.

WELLS, S. E., HILLNER, P. E., VALE, R. D. & SACHS, A. B. 1998. Circularization of mRNA by Eukaryotic Translation Initiation Factors. *Molecular Cell,* 2**,** 135-140.

WONG, J. J. L., AU, A. Y. M., GAO, D., PINELLO, N., KWOK, C.-T., THOENG, A., LAU, K. A., GORDON, J. E. A., SCHMITZ, U., FENG, Y., NGUYEN, T. V., MIDDLETON, R., BAILEY, C. G., HOLST, J., RASKO, J. E. J. & RITCHIE, W. 2016. RBM3 regulates temperature sensitive miR-142-5p and miR-143 (thermomiRs), which target immune genes and control fever. *Nucleic acids research,* 44**,** 2888-2897.

WOTING, A. & BLAUT, M. 2018. Small Intestinal Permeability and Gut-Transit Time Determined with Low and High Molecular Weight Fluorescein Isothiocyanate-Dextrans in C3H Mice. *Nutrients,* 10**,** 685.

XU, F. & ZHANG, J. 2017. Long non-coding RNA HOTAIR functions as miRNA sponge to promote the epithelial to mesenchymal transition in esophageal cancer. *Biomedicine & Pharmacotherapy,* 90**,** 888-896.

XU, Q., DENG, F., QIN, Y., ZHAO, Z., WU, Z., XING, Z., JI, A. & WANG, Q. J. 2016. Long non-coding RNA regulation of epithelial-mesenchymal transition in cancer metastasis. *Cell death & disease,* 7**,** e2254-e2254.

XU, Y., WU, W., HAN, Q., WANG, Y., LI, C., ZHANG, P. & XU, H. 2019. New Insights into the Interplay between Non-Coding RNAs and RNA-Binding Protein HnRNPK in Regulating Cellular Functions. *Cells,* 8**,** 62.

XU, Z.-Y., YU, Q.-M., DU, Y.-A., YANG, L.-T., DONG, R.-Z., HUANG, L., YU, P.-F. & CHENG, X.-D. 2013. Knockdown of long non-coding RNA HOTAIR suppresses tumor invasion and reverses epithelial-mesenchymal transition in gastric cancer. *International journal of biological sciences,* 9**,** 587-597.

XUE, M., CHEN, L.-Y., WANG, W.-J., SU, T.-T., SHI, L.-H., WANG, L., ZHANG, W., SI, J.-M., WANG, L.-J. & CHEN, S.-J. 2018. HOTAIR induces the ubiquitination of Runx3 by interacting with Mex3b and enhances the invasion of gastric cancer cells. *Gastric Cancer,* 21**,** 756-764.

XUE, Y., JOHNSON, R., DESMET, M., SNYDER, P. W. & FLEET, J. C. 2010. Generation of a transgenic mouse for colorectal cancer research with intestinal cre expression limited to the large intestine. *Molecular cancer research : MCR,* 8**,** 1095-1104.

YAN, K. S., YAN, S., FAROOQ, A., HAN, A., ZENG, L. & ZHOU, M.-M. 2003. Structure and conserved RNA binding of the PAZ domain. *Nature,* 426**,** 469-474.

YANG, D., YU, J., LIU, H. B., YAN, X. Q., HU, J., YU, Y., GUO, J., YUAN, Y. & DU, Z. M. 2019. The long non-coding RNA TUG1-miR-9a-5p axis contributes to ischemic injuries by promoting cardiomyocyte apoptosis via targeting KLF5. *Cell Death Dis,* 10**,** 908.

YANG, F., ZHANG, H., MEI, Y. & WU, M. 2014. Reciprocal regulation of HIF-1alpha and lincRNA-p21 modulates the Warburg effect. *Mol Cell,* 53**,** 88-100.

YANG, H.-J., JU, F., GUO, X.-X., MA, S.-P., WANG, L., CHENG, B.-F., ZHUANG, R.-J., ZHANG, B.-B., SHI, X., FENG, Z.-W. & WANG, M. 2017. RNA-binding protein RBM3 prevents NO-induced apoptosis in human neuroblastoma cells by modulating p38 signaling and miR-143. *Scientific reports,* 7**,** 41738-41738.

YANG, L., LIN, C., LIU, W., ZHANG, J., OHGI, K. A., GRINSTEIN, J. D., DORRESTEIN, P. C. & ROSENFELD, M. G. 2011. ncRNA- and Pc2 methylation-dependent gene relocation between nuclear structures mediates gene activation programs. *Cell,* 147**,** 773-788.

YANG, R., WEBER, D. J. & CARRIER, F. 2006. Post-transcriptional regulation of thioredoxin by the stress inducible heterogenous ribonucleoprotein A18. *Nucleic acids research,* 34**,** 1224-1236.

YEE, N. S., IGNATENKO, N., FINNBERG, N., LEE, N. & STAIRS, D. 2015. ANIMAL MODELS OF CANCER BIOLOGY. *Cancer growth and metastasis,* 8**,** 115-118.

YEUNG, Y. T., FAN, S., LU, B., YIN, S., YANG, S., NIE, W., WANG, M., ZHOU, L., LI, T., LI, X., BODE, A. M. & DONG, Z. 2019. CELF2 suppresses non-small cell lung carcinoma growth by inhibiting the PREX2-PTEN interaction. *Carcinogenesis*.

YOON, J.-H., ABDELMOHSEN, K., SRIKANTAN, S., YANG, X., MARTINDALE, J. L., DE, S., HUARTE, M., ZHAN, M., BECKER, K. G. & GOROSPE, M. 2012. LincRNA-p21 suppresses target mRNA translation. *Molecular cell,* 47**,** 648-655.

YU, B. & WANG, S. 2018. Angio-LncRs: LncRNAs that regulate angiogenesis and vascular disease. *Theranostics,* 8**,** 3654-3675.

YU, X. & LI, Z. 2015. Long non-coding RNA HOTAIR: A novel oncogene (Review). *Mol Med Rep,* 12**,** 5611-8.

ZAMORE, P. D. & GREEN, M. R. 1991. Biochemical characterization of U2 snRNP auxiliary factor: an essential pre-mRNA splicing factor with a novel intranuclear distribution. *The EMBO Journal,* 10**,** 207-214.

ZENG, F.-C., ZENG, M.-Q., HUANG, L., LI, Y.-L., GAO, B.-M., CHEN, J.-J., XUE, R.-Z. & TANG, Z.-Y. 2016. Downregulation of VEGFA inhibits proliferation, promotes apoptosis, and suppresses migration and invasion of renal clear cell carcinoma. *OncoTargets and therapy,* 9**,** 2131-2141.

ZENG, Y., WODZENSKI, D., GAO, D., SHIRAISHI, T., TERADA, N., LI, Y., VANDER GRIEND, D. J., LUO, J., KONG, C., GETZENBERG, R. H. & KULKARNI, P. 2013. Stress-Response Protein RBM3 Attenuates the Stem-like Properties of Prostate Cancer Cells by Interfering with CD44 Variant Splicing. *Cancer Research,* 73**,** 4123.

ZHANG, H., CAI, K., WANG, J., WANG, X., CHENG, K., SHI, F., JIANG, L., ZHANG, Y. & DOU, J. 2014. MiR-7, Inhibited Indirectly by LincRNA HOTAIR, Directly Inhibits SETDB1 and Reverses the EMT of Breast Cancer Stem Cells by Downregulating the STAT3 Pathway. *STEM CELLS,* 32**,** 2858-2868.

ZHANG, H. T., ZHANG, Z. W., XUE, J. H., KONG, H. B., LIU, A. J., LI, S. C., LIU, Y. X. & XU, D. G. 2013a. Differential expression of the RNA-binding motif protein 3 in human astrocytoma. *Chin Med J (Engl),* 126**,** 1948-52.

ZHANG, J., ZHANG, P., WANG, L., PIAO, H.-L. & MA, L. 2013b. Long non-coding RNA HOTAIR in carcinogenesis and metastasis. *Acta Biochimica et Biophysica Sinica,* 46**,** 1-5.

ZHANG, L., ZHANG, D., QIN, Z. Y., LI, J. & SHEN, Z. Y. 2020. The role and possible mechanism of long noncoding RNA PVT1 in modulating 3T3-L1 preadipocyte proliferation and differentiation. *IUBMB Life*.

ZHAO, J., DU, P., CUI, P., QIN, Y., HU, C. E., WU, J., ZHOU, Z., ZHANG, W., QIN, L. & HUANG, G. 2018. LncRNA PVT1 promotes angiogenesis via activating the STAT3/VEGFA axis in gastric cancer. *Oncogene,* 37**,** 4094-4109.

ZHAO, Y., LI, H., FANG, S., KANG, Y., WU, W., HAO, Y., LI, Z., BU, D., SUN, N., ZHANG, M. Q. & CHEN, R. 2016. NONCODE 2016: an informative and valuable data source of long non-coding RNAs. *Nucleic acids research,* 44**,** D203-D208.

ZHOU, J., YANG, L., ZHONG, T., MUELLER, M., MEN, Y., ZHANG, N., XIE, J., GIANG, K., CHUNG, H., SUN, X., LU, L., CARMICHAEL, G. G., TAYLOR, H. S. & HUANG, Y. 2015. H19 lncRNA alters DNA methylation genome wide by regulating S-adenosylhomocysteine hydrolase. *Nature communications,* 6**,** 10221-10221.

ZHOU, P., LI, B., LIU, F., ZHANG, M., WANG, Q., LIU, Y., YAO, Y. & LI, D. 2017a. The epithelial to mesenchymal transition (EMT) and cancer stem cells: implication for treatment resistance in pancreatic cancer. *Molecular Cancer,* 16**,** 52.

ZHOU, R.-B., LU, X.-L., ZHANG, C.-Y. & YIN, D.-C. 2017b. RNA binding motif protein 3: a potential biomarker in cancer and therapeutic target in neuroprotection. *Oncotarget,* 8**,** 22235-22250.

ZHOU, W., YE, X. L., XU, J., CAO, M. G., FANG, Z. Y., LI, L. Y., GUAN, G. H., LIU, Q., QIAN, Y. H. & XIE, D. 2017c. The lncRNA H19 mediates breast cancer cell plasticity during EMT and MET plasticity by differentially sponging miR-200b/c and let-7b. *Sci Signal,* 10.

ZHU, H., BERKOVA, Z., MATHUR, R., SEHGAL, L., KHASHAB, T., TAO, R.-H., AO, X., FENG, L., SABICHI, A. L., BLECHACZ, B., RASHID, A. & SAMANIEGO, F. 2015a. HuR Suppresses Fas Expression and Correlates with Patient Outcome in Liver Cancer. *Molecular Cancer Research,* 13**,** 809.

ZHU, P., WANG, Y., WU, J., HUANG, G., LIU, B., YE, B., DU, Y., GAO, G., TIAN, Y., HE, L. & FAN, Z. 2016a. LncBRM initiates YAP1 signalling activation to drive self-renewal of liver cancer stem cells. *Nature Communications,* 7**,** 13608.

ZHU, X., BÜHRER, C. & WELLMANN, S. 2016b. Cold-inducible proteins CIRP and RBM3, a unique couple with activities far beyond the cold. *Cellular and molecular life sciences : CMLS,* 73**,** 3839-3859.

ZHU, X., YAN, J., BREGERE, C., ZELMER, A., GOERNE, T., KAPFHAMMER, J. P., GUZMAN, R. & WELLMANN, S. 2019. RBM3 promotes neurogenesis in a niche-dependent manner via IMP2-IGF2 signaling pathway after hypoxic-ischemic brain injury. *Nature Communications,* 10**,** 3983.

ZHU, X., ZELMER, A., KAPFHAMMER, J. P. & WELLMANN, S. 2015b. Cold-inducible RBM3 inhibits PERK phosphorylation through cooperation with NF90 to protect cells from endoplasmic reticulum stress. *The FASEB Journal,* 30**,** 624-634.

Appendices

Appendix A: Predicted Minimum Free Energy (MFE)

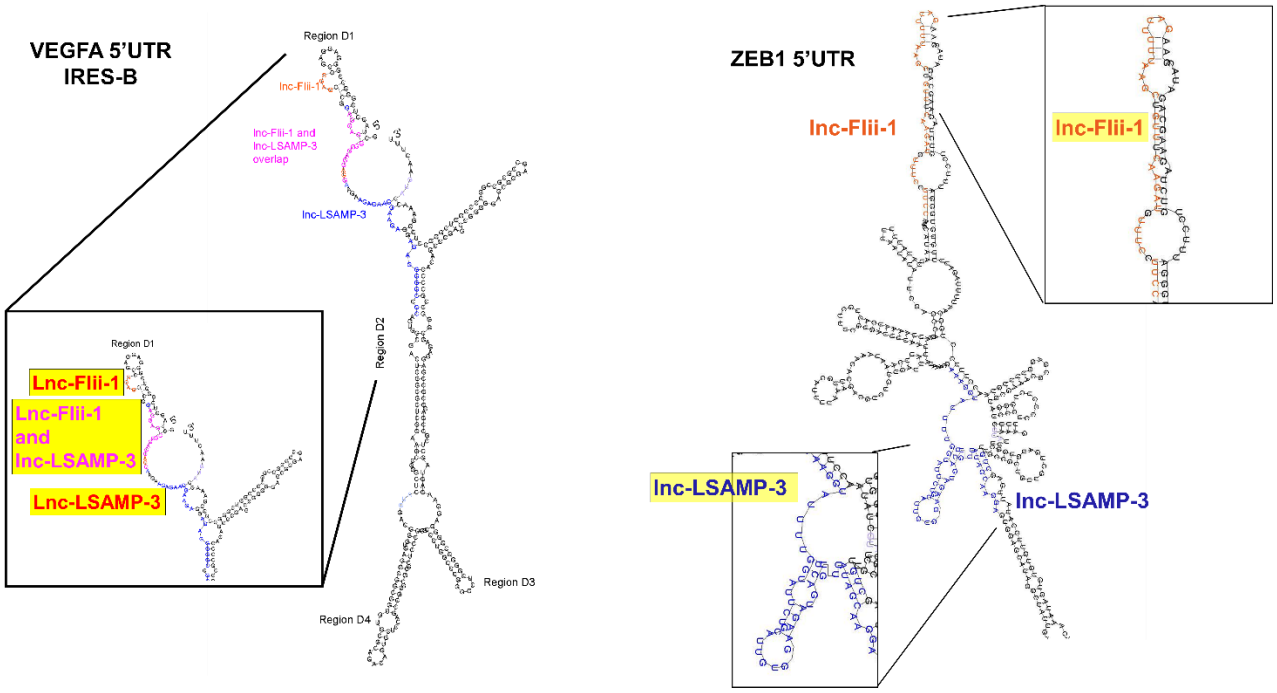

(A) Predicted Minimum Free Energy (MFE) secondary structure of VEGFA IRES-B in 5'UTR using RNAfold web server. The interactions between VEGFA IRES-B and lnc- LSAMP-3, lncFlii-1 are highlighted.

(B) Predicted Minimum Free Energy (MFE) secondary structure of ZEB1 5'UTR using RNAfold web server. The interactions between VEGFA IRES-B and lnc- LSAMP-3, lncFlii-1 are highlighted.

Appendix B: Visualization of mRNA -lncRNA interaction VEGFA 5'UTR and 3'UTR and lnc-LSAMP-3 and lnc-Flii-1

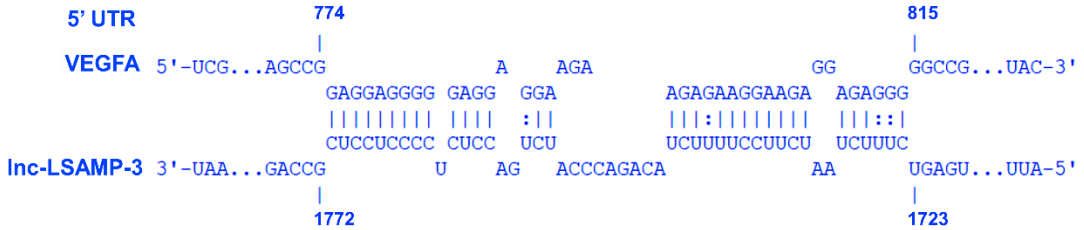

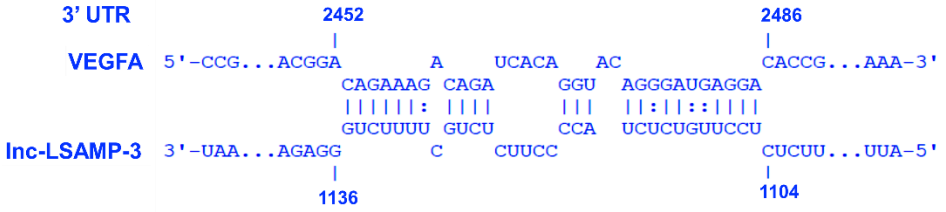

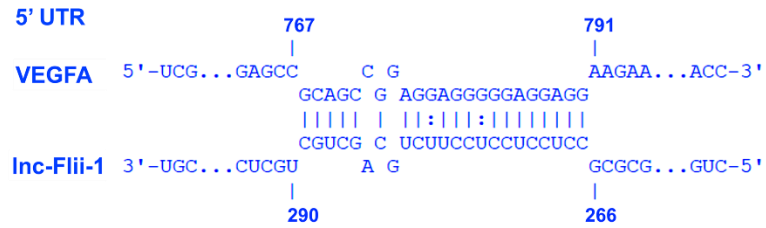

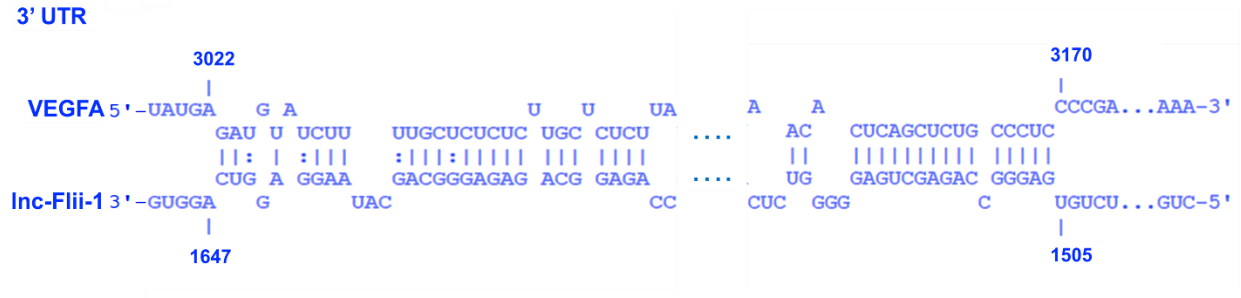

Appendix C: Visualization of mRNA -lncRNA interaction between ZEB1 5'UTR and 3'UTR and lnc-LSAMP-3 and lnc-Flii-1

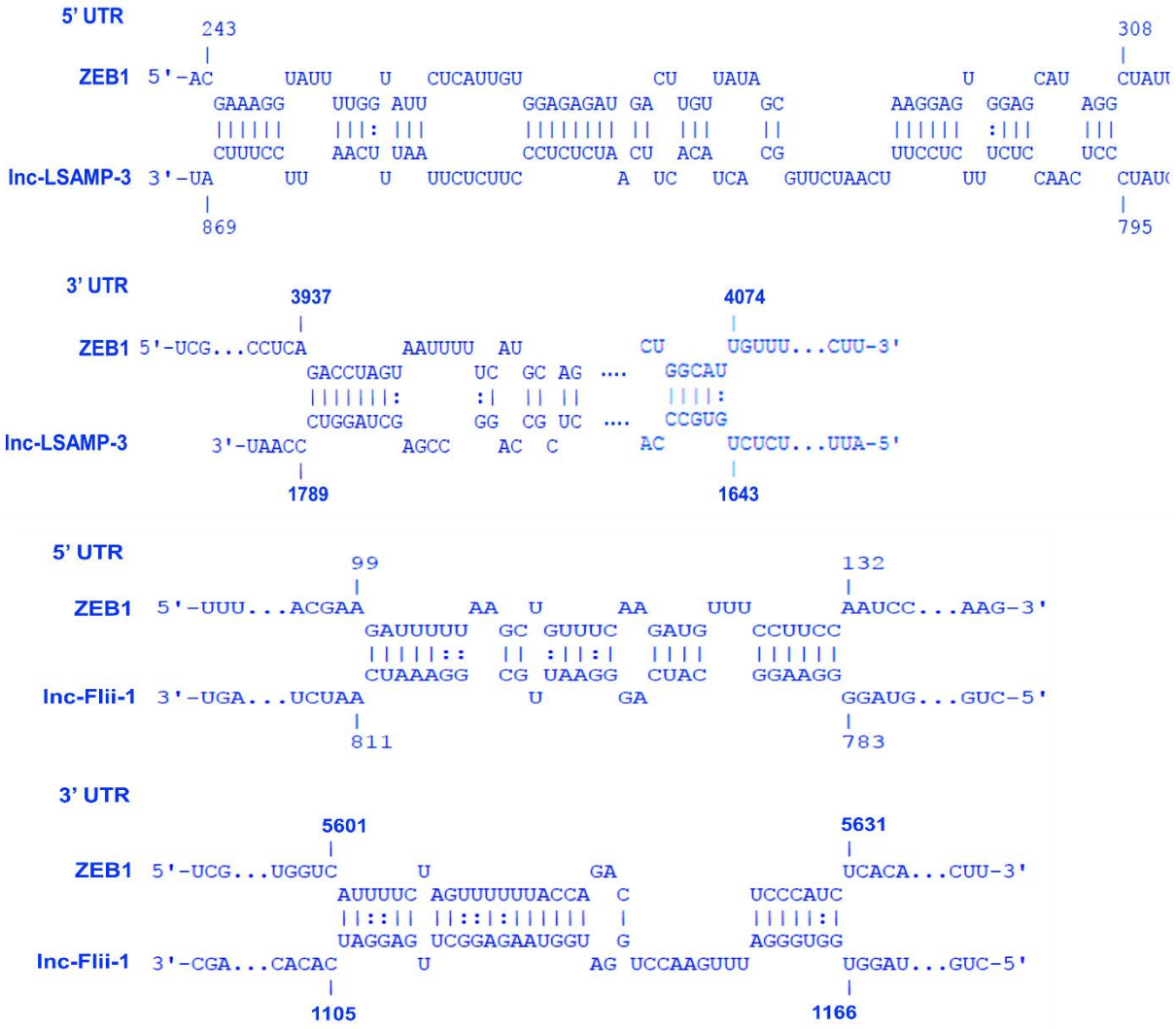

Appendix D: Visualization of mRNA -lncRNA interaction between SNAI2 5'UTR and 3'UTR and lnc-LSAMP-3 and lnc-Flii-1

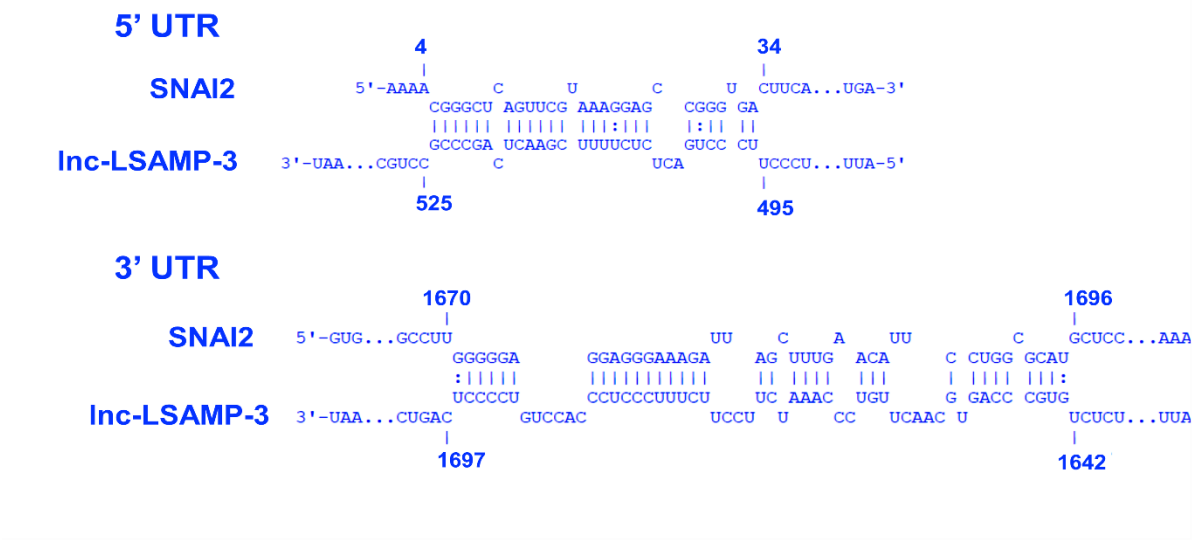

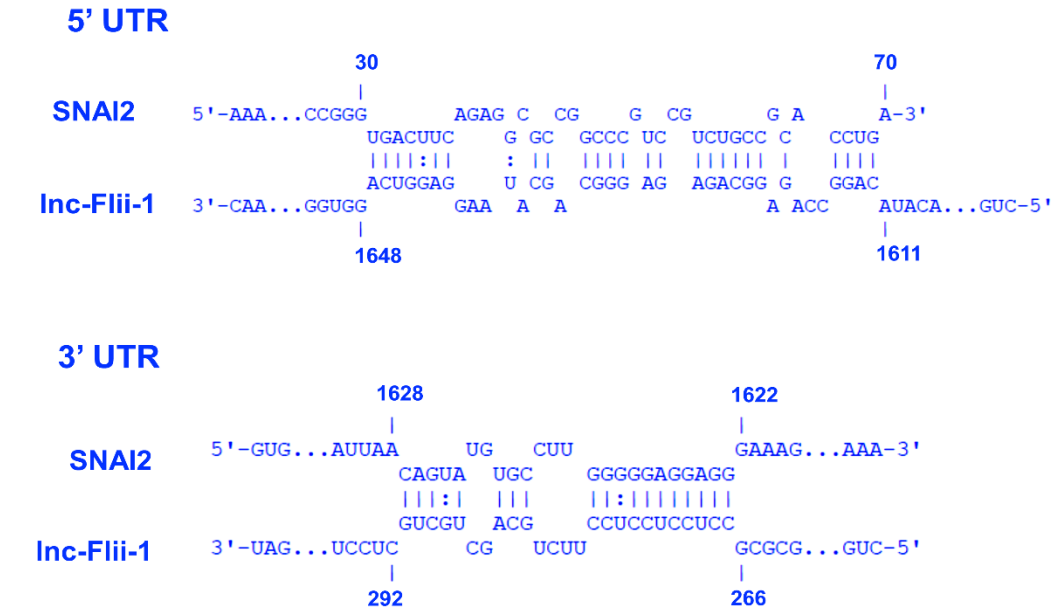

Appendix E: Visualization of mRNA -lncRNA interaction between TWIST1 5'UTR and 3'UTR and lnc-LSAMP-3 and lnc-Flii-1